Assessment of the Role of Endothelial mTORC2 in FGF2-induced Angiogenesis *in vivo*

Dissertation
zur
Erlangung der naturwissenschaftlichen Doktorwürde
(Dr. sc. nat.)

vorgelegt der
Mathematisch-naturwissenschaftlichen Fakultät
der
Universität Zürich

von

Stavroula Georgiopoulou
aus
Griechenland

Promotionskomitee
Prof. Dr. Med. Vet. Max Gassmann (Vorsitz)
Prof. Dr. Christian Grimm
Prof. Dr. Gerhard M. Christofori
Prof. Dr. med. Edouard Battegay
Dr. phil. II Rok Humar (Leitung)

Zürich, 2015

Acknowledgements

I would like to thank Prof. Battegay and Dr. Humar for giving me the opportunity to perform my research in their laboratory and for sharing during these 4 years their scientific expertise and knowledge. Additionally during my studies in their laboratory I learned valuable lessons about professionalism and ethics.

Special thanks to Prof. Max Gassmann for his scientific guidance and support during my thesis. Also I would like to thank all the members of my thesis committee for their comments and suggestions.

I would also like to thank all the laboratory members for their help and support in all these four years, and especially during the last year of my PhD. Ana and Elvira thank you for your help.

Last but most importantly I want to thank my family that always pushed my forward for the best and they made me who I am and my future husband because he stands next to me and supporting me (he even read all this thesis).

List of Contents

Summary 5
Zusammenfassung 7
List of abbreviations 9
1.INTRODUCTION 11
1.1 Blood vessels and the cardiovascular system 11
1.2. Blood vessel development 12
1.3.1. Sprouting angiogenesis 13
1.3.2. The role of Vascular Endothelial Growth Factor (VEGF**)** 14
1.3.3. Tip/stalk cell fate determination 14
1.3.4. Sprout fusion and lumen formation 17
1.3.5. Capillary and vessel maturation and stabilization. 17
1.3.6. Intussusception: an alternative mode of angiogenesis 19
1.4. Angiogenesis in health and disease 20
1.4.1. Angiogenesis as a therapeutic target for cancer and tumor growth 20
1.5. Fibroblast growth factor 2: The orchestrating angiogenic growth factor 23
1.6.mTOR signaling pathway 24
1.6.1. mTORC1 26
1.6.2. mTORC2 27
1.6.3. The implication of mTOR signaling pathway in angiogenesis 28
1.7. Aims and experimental approach 31

2. Materials and methods 33
2.1. Endothelial specific and Tamoxifen inducible Rictor$^{i\Delta ec}$ mouse 33
2.2. Determination of Rictor mRNA expression levels in aortic endothelium 33
2.2.1. Scraping of aortic endothelium 33
2.2.2. Enzymatic digestion of aortic endothelium 34
2.3. Determination of Rictor mRNA expression levels in lung endothelium 34
2.3.1. Magnetic Activated Cell Sorting (MACS) lung endothelial cells isolation 34
2.3.2. Fluorescence Activated Cell Sorting (FACS) of lung endothelial cells 35
2.4. Determination of the efficiency of endothelial cell isolation and *Rictor* knockout induction efficienc**y** 36
2.5. Rictor KO aortic endothelial cells 37
2.6. Mouse dorsal skinfold chamber and Matrigel sealing 37
2.6.1. Intravital microscopy 39
2.7. Matrigel plug assay 40

2.8. Immunohistochemical staining 41

2.9 Statistical analysis 41

2.10. Primer list 42

3. RESULTS 43

3. A. Endothelial specific Rictor knockout mouse: Assessment of the efficiency of Rictor knockout in the endothelium 43

3. A.1. Induction of *Rictor* knockout in the adult mouse endothelium 43

3. A.2. Efficiency of Rictor knockout induction in endothelial cells in aorta and lungs 45

3. A.2.1. Rictor mRNA quantification and cell marker profiling of aortic endothelial lining 46

3. A.2.2. Rictor mRNA quantification and cell marker profiling of MACS sorted lung endothelial cells 47

3. A.3. Isolation of pure endothelial cell populations from aorta and lungs: optimization and gene expression analysis. 49

3. A.3.1. Rictor mRNA quantification and cell marker profiling of enzymatically digested aortic lining 49

3. B. 3.1.1. Enzymatic digestion by trypsin 49

3. A. 3.1.2. Enzymatic digestion by Collagenase and Liberase 51

3. A.3.2. MACS endothelial cell isolation: Enrichment and purification of lung endothelial cell population and gene expression analysis 52

3. A.3.2.1. Rictor mRNA quantification and cell marker profiling of MACS-sorted murine lung endothelial cells after *in vitro* culture 54

3. A.3.3. FACS sorting of lung microvascular endothelial cell 55

3. A.3.1. Rictor mRNA quantification and cell marker profiling of directly FACS-sorted murine lung endothelial cells 56

3. A.4. Cre-ER^{T2} expression levels in MACS and FACS-sorted lung endothelial cells 58

3.B. Role of endothelial mTORC2 in angiogenesis *in vivo* 59

3.B.1. Deletion of *Rictor* in the endothelium does not affect weight gain and hematological profile of Rictor$^{i\Delta ec}$ animals 59

3. B.2. Assessment of the role of endothelial mTORC2 in angiogenesis with intravital microscopy 61

3. B.2.1. Induction of *Rictor* knockout in the endothelium does not affect the homeostasis of developed vasculatures 61

3. B.2.2. Endothelial *Rictor* knockout does not affect the response of the skin muscle vasculature in dorsal skinfold chamber implantation 62

3. B.2.3. Assessment of the role of endothelial mTOCR2 in VEGF induced angiogenesis 64

3. B.2.3.1. Matrigel-mediated VEGF delivery: The role of heparin 66

3. B.2.3.2. Intramuscular injection of VEGF expressing myoblasts for VEGF delivery in the skin muscle 68

3. B.2.4. Matrigel-mediated FGF2 stimulation of the skin muscle vasculature: Rictor$^{i\Delta ec}$ animals present different remodelling patterns 70

3. B.2.4.1. Capillary diameter distribution analysis 74

3. B.2.4.2. CD31 and Cre-ER^{T2} staining of FGF2 challenged skin muscle vasculature 76

3. B.3. Assessment of the role of endothelial mTORC2 in FGF2 induced de novo angiogenesis 77

3. B.3.1. Endothelial Rictor knockout hampers the vascularization of FGF2 loaded Matrigel plugs 78

3. B.3.2. Endothelial Rictor affects diameter of existing stromal capillaries in response to FGF2.. 80

4. DISCUSSION 81

References 90

Carriculum Vitae……...……110

Summary

Angiogenesis is a process where new capillaries are formed from pre-existing ones. It involves endothelial cell activation, extracellular matrix degradation, endothelial cell proliferation and migration and fusion with neighboring sprouts. Stabilization and lumen formation of the new capillary are the last steps of sprouting angiogenesis. Sprouting angiogenesis is one the most prominent mechanism of tumor vascularization and is a growth factor-driven process with FGF2 and VEGF being the key regulators.

The mTOR signaling pathway is a central cellular regulator and consists of two distinct complexes with individual roles and functions: mTORC1 and mTORC2. mTORC1 is a regulator of cell proliferation, protein synthesis, and growth and conveys signals from growth factors, ATP and O_2 levels. Until now mTORC2 is known to mediate growth factor signaling and regulates cell survival and cytoskeleton reorganization. In all cell types mTORC1 is sensitive to Rapamycin-based inhibition, while mTORC2 is not. However in certain cell type such as endothelial cells mTORC2 can be inhibited by prolonged Rapamycin treatment. In xenograft tumor models Rapamycin treatment reduced tumor growth and tumor vascularization. In the majority of these studies dual inhibition of both mTOR complexes results in greater inhibition of tumor growth and vascularization than mTORC1 inhibition alone, pointing to a specific role of mTORC2 in tumor vascularization. The distinct roles of mTORC1 and mTORC2 in angiogenesis have not been elucidated due to the absence of specific mTORC2 inhibitors.

In this thesis we examine the role of endothelial mTORC2 in physiologic and FGF2-induced angiogenesis. mTORC2 is a multi-protein complex composed by mTOR, Rictor and other accessory proteins. We employed an endothelial-specific and Tamoxifen-induced Rictor$^{i\Delta ec}$ mouse that ideally leads to the ceasing of mTORC2 signaling in the endothelium. We monitored FGF2 induced angiogenesis *in vivo* with intravital microscopy of the dorsal skinfold chamber and FGF2 Matrigel plug implantation. We observed that ceasing mTORC2 signaling had no impact in already developed vasculatures and in wound-

healing angiogenesis. Rictor$^{i\Delta ec}$ mice showed limited FGF2-induced capillary diameter increase, in resident skin capillaries of the skin muscle vasculature and exhibited differential remodeling architecture in the skin muscle vasculature. Impaired neo-angiogenesis in FGF2-loaded Matrigel plugs was also seen in Matrigel plugs of the Rictor$^{i\Delta ec}$ mice. Thus, we demonstrate for the first time direct evidence that endothelial mTORC2 signaling is crucial for FGF2 induced angiogenesis.

This thesis also analyses the efficiency and stability of *Rictor* knockout induction in the endothelium and the optimization of multiple endothelial cell isolation techniques, which led in the optimization of future uses of Cre-Lox based deletion techniques in the laboratory.

In conclusion the present thesis demonstrates for the first time the role of endothelial mTORC2 in FGF2-induced angiogenesis, by regulating capillary diameter, vasculature architecture and neo-angiogenesis. A mechanistic insight is further needed to reveal the molecular and cellular aspects of this regulation

Zusammenfassung

Die Angiogenese ist ein Prozess, bei welchem neue Kapillaren aus bereits bestehenden gebildet werden. Angiogenese beinhaltet unter anderem Endothelzellaktivierung, Abbau der extrazellulären Matrix, Endothelzell Proliferation und Migration und Fusion von entstehenden Kapillarspossen mit Benachbarten. Stabilisierung und Lumenbildung der neuen Kapillaren sind die letzten Schritte der sprossenden Angiogenese. Diese Art der Angiogenese ist einer der prominentesten Mechanismen der Tumorgefäßbildung. Sprießende Angiogenese ist ein Wachstumsfaktor getriebener Prozess mit FGF2 und VEGF als den wichtigsten Initiatoren.

Der mTOR-Signalweg ist ein zentraler intrazellulärer Regulierung Mechanismus und besteht aus zwei verschiedenen Komplexen mit individuellen Rollen und Funktionen: mTORC1 und mTORC2. mTORC1 ist Regulator der Zellproliferation, der Proteinsynthese und des Wachstums und prozessiert Signale von Wachstumsfaktoren, Energie und Sauerstoff Niveaus. Bis jetzt ist bekannt, dass mTORC2 durch Wachstumsfaktoren aktiviert wird, das Überleben der Zelle reguliert und das Zellskelett reorganisiert. mTORC1 ist der Komplex, welcher primär empfindlich gegenüber Hemmung durch Rapamycin ist. Besonders in Endothelzellen kann aber auch der mTOR Komplex 2 bei längerer Behandlung durch Rapamycin gehemmt werden. In Xenograft Tumormodellen reduziert Rapamycin-Behandlung das Tumorwachstum und die Neubildung der Tumorgefäße. Die Hemmung beider mTOR Komplexe mit neueren Dual-Inhibitoren führt zu einer stärkeren Inhibition des Tumorwachstums und der Gefäßneubildung. Dies deutet auf spezifische und unterschiedliche Funktionen der beiden mTOR Komplexe in der Angiogenese.

In dieser Arbeit untersuchen wir die Rolle des mTOR Komplexes 2 im Endothel während der physiologischen und FGF2 induzierten Angiogenese. mTORC2 ist ein Multiproteinkomplex von mTOR, Rictor und anderen zusätzlichen Proteinen. Zu diesem Zweck induzierten wir eine mTORC2 Defizienz in der Maus durch Tamoxifen-induzierte

Deletion des essentiellen mTORC2 Regulationsproteins Rictor im Endothel (Rictor$^{i\Delta ec}$ Maus) und überwachten und analysierten die Angiogenese *in vivo* mittels Intravitalmikroskopie der Rückenfaltenkammer und von Matrigel Plug Implantation.

Wir beobachteten, dass Defizienz von mTORC2 keine Auswirkungen in bereits entwickelten Blutgefäßen im Panniculus Carnosus hatte und keine Veränderungen in der Angiogenese zeigte, welche durch Wundheilungsprozesse initiiert wurde. Interessanterweise beobachteten wir, dass die Stimulation des Gefässbettes im Panniculus Carnosus mit einer hohen Dosis von FGF2 die induzierte Zunahme der Kapillar-Durchmesser in Rictor$^{i\Delta ec}$ Mäusen begrenzt und im Gegensatz zu Kontrollmäusen sich die Gefässarchitektur der Hautkapillaren einem geordneten Umbau oder Remodeling unterzieht. Ebenfalls wurde eine stark verminderte Neo-Angiogenese in mit FGF2 versetzten Matrigel Plugs in Rictor$^{i\Delta ec}$ Mäusen beobachtet. In dieser Arbeit beschreiben wir folglich die erste direkte Beobachtung, dass mTORC2 Signalisierung im Endothel von entscheidender Bedeutung für FGF2 induzierte Angiogenese ist. Des Weiteren wird mit dieser Doktorarbeit eine eingehende Analyse der Effizienz von Induktion des *Rictor* Knockouts im Endothel durchgeführt und mehrere Endothelzell-Isolationstechniken optimiert.

Abschließend zeigt diese Arbeit zum ersten Mal eine spezifische Funktion des Signalkomplexes mTORC2 im Endothel in FGF2 induzierter Angiogenese, charakterisiert durch Regulation des Kapillardurchmessers, Remodeling des bestehenden Gefässbettes und Effizienz von Neo-Angiogenese. Sicherlich werden zukünftige Experimente in Rictor knockout Endothelzellen und in einem verbesserten transgenen knockout approach *in vivo* dazu beitragen eine mechanistische Einsicht zu erlangen um die molekularen und zellulären Aspekte dieser mTORC2–spezifischen Rolle in der Angiogenese zu offenbaren.

List of abbreviations

1. **Ang**	Angiopoietin
2. **DLL4**	Delta Ligand 4
3. **ECM**	Extracellular matrix
4. **eIF-4E**	Eukaryotic Initiation Factor 4E
5. **eIF-4E-BP1**	Eukaryotic Initiation Factor 4E Binding Protein 1
6. **eNOS**	Endothelial nitric oxide synthase
7. **ERK1**	Extracellular signal-regulated Kinase 1
8. **FACS**	Fluorescent Activated Cell Sorting
9. **FGF**	Fibroblast Growth Factor
10.**FGF2-B**	Fibroblast Growth Factor Binding Protein
11.**FGFR1**	Fibroblast Growth Factor Receptor 1
12.**FKBP-1**	FKB Binding Protein 121
13.**HIF-1α**	Hypoxia Induced Factor-1a
14.**IA**	Intussusceptive arborisation
15.**IBR**	Intussusceptive branching remodeling
16.**IGF**	Insulin Growth Factor
17.**IGFR**	Insulin Growth Factor Receptor
18.**KO**	Knockout
19.**MACS**	Magnetic Activated Cell Sorting
20.**MCP**1	Monocyte Chemoattractant Protein 1
21.**MMP**	Matrix Metallo-Proteases
22.**mSIN1**	SAPK-interacting protein-1
23.**mTOR**	mammalian Target of Rapamycin
24.**mTORC1**	mammalian Target of Rapamycin Complex1
25.**mTORC2**	mammalian Target of Rapamycin Complex2

26.**mVEGFR1**	membrane Vascular Endothelial Growth Factor Receptor 1
27.**NO**	Nitric oxide
28.**PDGF-BB**	Platelet Derived Growth Factor BB
29.**PDGFR**	Platelet Derived Growth Factor Receptor
30.**PGE2**	Prostaglandin E2
31.**PKCα**	Protein kinase C alpha
32.**Rictor**^{iAec}	Endothelial Specific Rictor knockout
33.**SGK1**	glucocorticoid-induced kinase 1
34.**SMC**	Smooth Muscle cells
35.**sVEGFR1**	soluble Vascular Endothelial Growth Factor Receptor 1
36.**TIMP2**	Tissue Inhibitor of Metallo-proteases 2
37.**TIMP3**	Tissue Inhibitor of Metallo-proteases 3
38.**TKR**	Tyrosine Kinase Receptor
39.**TSC1**	Tuberus Sclerosis Complex1
40.**TSC2**	Tuberus Sclerosis Complex 2
41.**VCAM1**	Vascular Adhesion Molecule 1
42.**Ve-cadherin**	Vascular endothelial Cadherin
43.**VEGF**	Vascular Endothelial Growth Factor
44.**VEGFC**	Vascular Growth Factor C
45.**VEGFR1**	Vascular Endothelial Growth Factor Receptor 1
46.**VEGFR2**	Vascular Endothelial Growth Factor Receptor 2
47.**VEGFR3**	Vascular Endothelial Growth Factor Receptor 3

1. INTRODUCTION

1.1 Blood vessels and the cardiovascular system

The cardiovascular system comprises of the heart, the blood vessels and the circulating blood. The heart functions as a double pump, with a left and a right part. The right compartment of the heart collects oxygenated blood from the lungs and forwards it to the body. The left part of the heart collects the blood from the vein and returns it to the lungs to be re-oxygenated (1). The blood vessels and the capillaries network all the body so blood reaches every tissue. Vessels and capillaries have distinct structures. Capillaries consist of an endothelial monolayer, fully or partially covered by pericytes. The big vessels are composed by three layers; the tunica intima, the tunica media and the tunica adventitia. The tunica intima is the innermost layer of the artery wall and comes into contact with flowing blood. The tunica intima is composed of a monolayer of endothelial cells and is surrounded by the tunica media, which is a layer of smooth muscle cells (SMC) embedded in a rich extracellular matrix containing collagen, elastin, and proteoglycans. The outer layer is the tunica adventitia, which again is composed of a rich extracellular matrix of collagen which contains myofibroblasts. Both the tunica media and the tunica adventitia vary in their composition and thickness according to the shear stress of the blood flow (2).

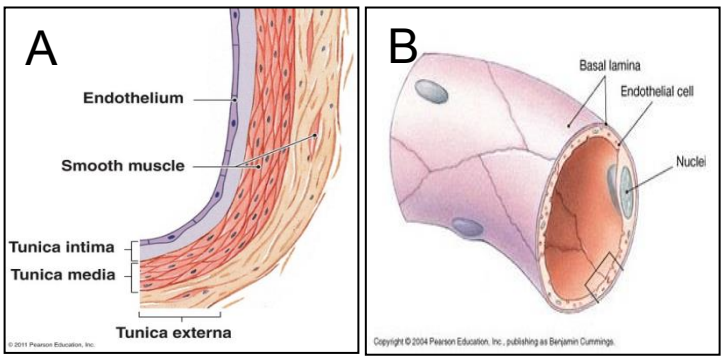

Figure 1. Structure of a typical vessel and capillary. (A) The three individual layers tunica intima, tunica media, and tunica adventitia. **(B)** Typical capillary with the endothelial monolayer and pericyte covering the basal lamina (Humans Anatomy, Pearson Education Inc. 2011).

The cardiovascular system is one of the most important systems in higher organisms, since it delivers oxygen and nutrients to the tissues, enables gas exchange, and clears the metabolic waste (3, 4). Furthermore, it has multiple functions, also in the adult body, by controlling the homeostasis, body temperature and the delivery of the immune defensive system in the positions needed (5). Accordingly, the cardiovascular system is the first to develop in a growing embryo.

1.2. Blood vessel development

In the early embryo the first vessels emerge from precursor cells, the hemangioblasts, that differentiate into endothelial cells and hematopoietic cells creating the first blood containing vascular tubes by a process called vasculogenesis (3, 6).

Oxygen and metabolic needs of the developing tissues stimulate the expansion of the initial vascular plexus by sprouting angiogenesis, a process were new capillaries and vessel emerge and develop from pre-existing vessels (3,7,8). Maturation of the new capillaries occurs by recruitment of pericytes that cover the ab-luminal surface of the endothelial cells and stabilize the capillary. Further recruitment of smooth muscle cells and subsequent vascular remodeling are the hallmarks of arteriogenesis. Regression of some new capillaries will also occur in the context of remodeling and optimization of the new capillary bed (3,4,9). Intussusceptive angiogenesis, a different mechanism than sprouting, also contributes to the expansion of the vascular plexus.

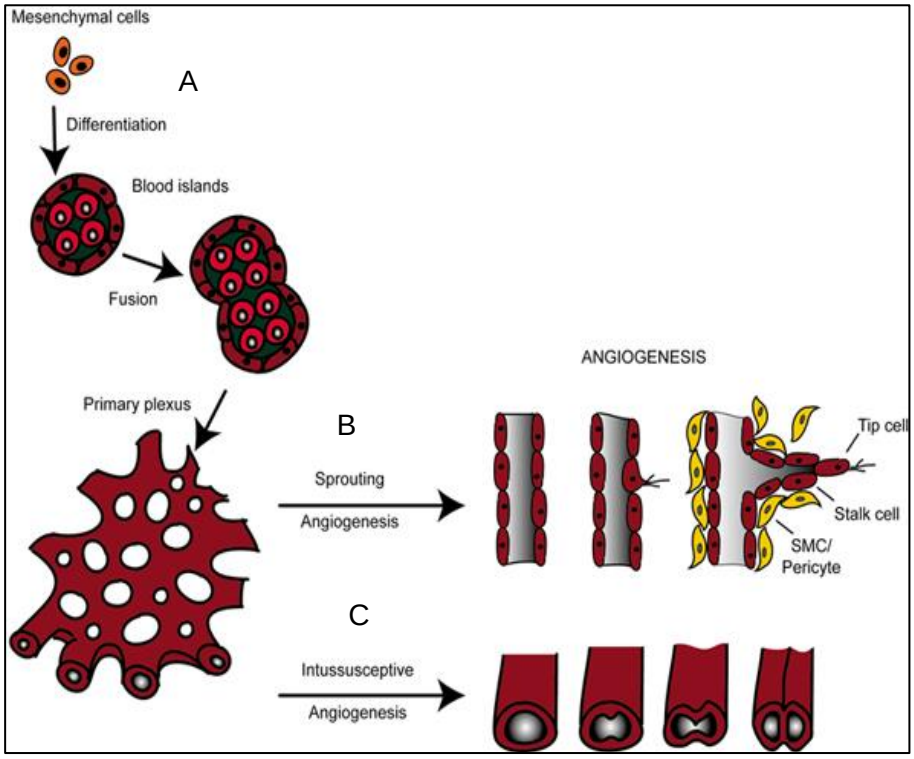

Figure 2: Schematic representation of tissue vascularization during development. (**A)** Hemangioblasts and precursor cells create the initial vascular plexus via vasculogenesis. The vascular plexus expands to meet the oxygen and metabolic demands either by sprouting angiogenesis (**B**) or intussusception (**C**) (10).

1.3. Angiogenesis

1.3.1. Sprouting angiogenesis

All blood vessels are lined with a thin layer of simple epithelium known as endothelium, that keeps blood cells inside of the blood vessels as a permeability barrier and prevents clots from forming (11). Sprouting angiogenesis is a very well described morphogenic process, tightly regulated on the cellular and molecular level (7), that begins with activation of the capillary endothelium when pro-angiogenic stimuli prevail over anti-angiogenic mediators. Activated endothelial cells initiate angiogenesis in response to hypoxia or tissue-injury ischemia by producing Nitric Oxide (NO) through endothelial Nitric Oxide Synthase (eNOS), leading to vasodilation and increased permeability of the

endothelium. NO modulates the balance of pro- and anti-angiogenic factors and increases permeability of the endothelium allowing the endothelial cells to degrade the Extracellular Matrix (ECM) and migrate, creating a new sprout (12,13).

1.3.2. The role of Vascular Endothelial Growth Factor (VEGF)

During sprouting angiogenesis endothelial cells differentiate in tip and stalk cells. The endothelial cells that are exposed to higher concentrations of VEGF can change their quiescent phenotype and transform into an activated cell with expanding philopodia called tip cells (14). The tip cells are migrating cells and drive the new sprout away from the maternal vessels. The adjutant to the tip cell, proliferating endothelial cells that elongate the new sprout are called stalk cells (14).

VEGF is the most important and endothelial-specific angiogenic growth factor that stimulates capillary growth through sprouting angiogenesis (15). The distribution of VEGF in the matrix affects the pattern of vascular branching (16). Differential affinity of VEGF for the extracellular matrix creates gradients that are essential for tip/stalk cells fate determination, a selection force for the endothelial cells that are exposed to locally different concentration of VEGF. Cells exposed to the highest concentration of the VEGF gradients are selected as tip cells (14). On the other hand, the determination of the stalk cells is not dependent on the gradients, but on the actual local concentration of VEGF (14,17). In both tip and stalk cells VEGF signals through its receptor VEGFR2 however different signaling pathways regulating the fate of the cells are translated into different cell behavior (8,18).

1.3.3. Tip/stalk cell fate determination

Investigation of the tip/stalk cell fate determination pathway in zebrafish and mouse embryonic retina revealed the essential role of Notch/Delta ligand 4(Dll4) signaling downstream of VEGF/VEGFR2 pathway (8,19,20).

The VEGF gradient induces increased signaling of VEGFR2 in a tip endothelial cell, resulting in the expression of Dll4 on the surface of this cell (21-24). The up-regulation of Dll4 in the tip cell activates Notch signaling in the adjutant stalk cell, which become less sensitive to VEGF and reduce Dll4 expression levels. The stalk cell reduces the expression of VEGFR2, however increases levels of both soluble VEGFR1 (sVEGFR1) and membrane-bound VEGFR1 (mVEGFR1). This profile of VEGF receptors makes the stalk cell less responsive to VEGF, since sVEGFR1 and the mVEGFR1 have higher affinity for VEGF and display reduced tyrosine kinase activity (25-29). The increased presence of both mVEGFR1 and sVEGFR1 sharpens the differences in local VEGF concentration and promotes the tip/stalk cell selection process (30, 31). The balance between VEGFR1 and VEGFR2 regulates the tip/stalk cell fate determination under the control of Notch/Dll4 signaling pathway (32). Endothelial cells compete for the position of the tip cells and this competition is based on the ratio of VEGR1/VEGFR2 (33).The fate of endothelial cells is not definite and the roles between the tip and the stalk cells can change due to the plasticity of the process. Thus, Notch signaling functions as control point and can reduce exaggerated tip cell formation that would otherwise lead to unsuccessful angiogenesis.

VEGF receptor 3 (VEGFR3, Flt4) is another member of the VEGF receptor family known for its role to induce lymphangiogenesis (34). The VEGFR3 is gaining attention due to its expanding importance in sprouting angiogenesis in the last years. VEGFR3 has been shown to be up-regulated in the tip cells and it can induce sprouting angiogenesis in the absence of VEGFR2/VEGFA signaling (35). This implies that tip cell formation and sprouting is not a VEGFR2-restricted process. Further studies revealed that VEGFR3/VEGFC signaling pathway promotes the conversion of tip cell to a stalk cell in areas of neighboring sprouts fusion. VEGFC is localized at the fusion areas and secreted by macrophages that localize at the leading front of the spout and sprout fusion areas (36,37).

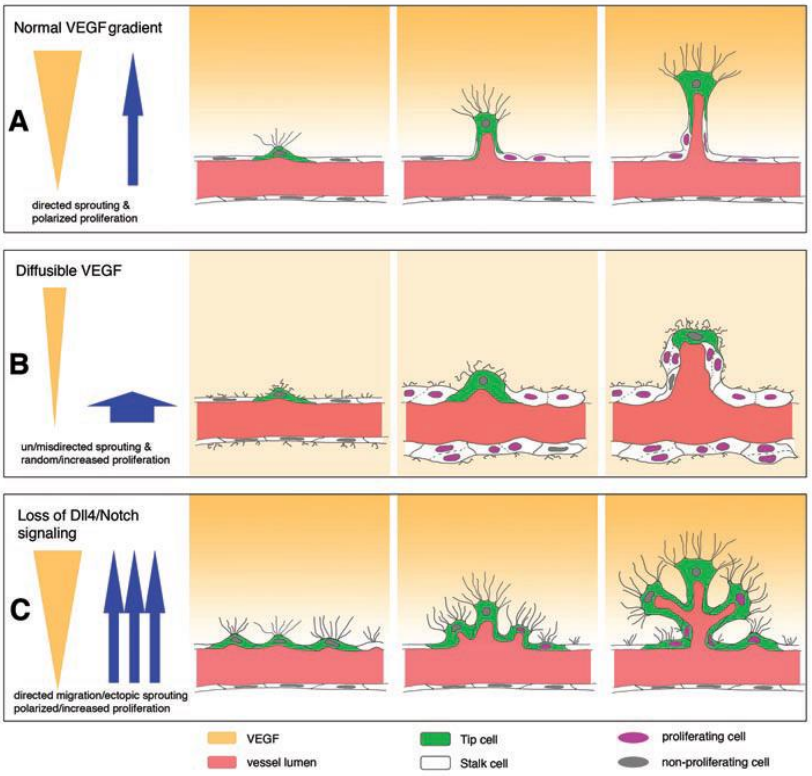

Figure 3: The importance of VEGF gradients and the crosstalk of VEGF/VEGFR2-Notch/Dll4 pathway (A) VEGF gradients promote sprouting and tip/stalk cell fate determination by the crosstalk of VEGF/VEGFR2, which up-regulates Dll4 in the tip cell. The tip cell promotes stalk cell phenotype in the adjusting cells by Notch activation via Dll4. (**B**) VEGF gradients are needed to orchestrate guidance queues. Diffused VEGF is unable to provoke sprout outgrowth. (C) Notch signaling acts as negative regulator of tip cell formation and loss of Dll4/Notch signaling leads to exaggerated sprouting but not to functional capillaries. Inhibition of Notch in the stalk cells promotes tip cell phenotype and remodeling (17) (22).

The regulation of VEGFR3 in tip and stalk cells is not yet clarified. There are opposing *in vivo* and *in vitro* data on how Notch/Dll4 signaling regulates the VEGFR3 expression pattern in the emerging sprout (35,38,39). Most recent data suggest that VEGFR3 can be also regulated by VEGFR2-VEGF and Notch/Dll4 signaling but the mechanism is not fully understood. VEGFR3 seems to be up-regulated in cells with low or absent Notch signaling and the receptor seems to be able to sustain deregulated angiogenesis even in the absence of VERGR2 signaling (38).

In the same study in conditional transgenic murine retinas and in contrast with previous knowledge, Benedito et al. demonstrated that the levels of Dll4 are not dependent only on VEGFR2 signaling and that endothelial cell fate is not only relying on the VEGFR2/VEGFA-Notch/Dll4 relation and interplay (38). Thus, angiogenic sprouting may take place without the VEGFR2, which so far has been considered as main transducer of this process.

1.3.4. Sprout fusion and lumen formation

As the tip endothelial cell migrates towards the angiogenic stimuli it still remains attached and connected to the parental vessel through the stalk cells. The stalk cells may not have migratory capacity, however exhibits increased proliferation and thereby extends the growing sprout (4,14). The reorganization of the stalk cells in the growing sprout creates a lumen, which will be perfused by the parental vessel. Finally, most of the new sprouts find each other, connect and fuse to create new capillaries. Unfused and unnecessary sprouts regress (4).

1.3.5. Capillary and vessel maturation and stabilization.

After two new neighboring sprouts fuse and merge to create one capillary, maturation increases its stability and function by the recruitment of pericytes, vascular smooth muscle cells, and the deposition of extracellular matrix to form a new basement membrane. Capillary maturation is essential for the regulation of the capillary diameter, contractility, and resistance to blood flow and shear stress (40-42).

PDGF-BB is a growth factor secreted by endothelial cells and it is one of the essential growth factors that stimulate pericyte recruitment. PDGF is mainly secreted in sites with active angiogenesis, possibly by tip endothelial cell (43-45). Secreted PDGF-BB possesses a heparin sulfate binding motif, which allows the growth factor to anchor in the extracellular matrix and form a spatial distribution in close proximity with the endothelial

cells of the newly emerged endothelial tube. Pericyte are attracted via PDGFR activation to directly cover and interact with endothelial cell and stabilize the tube (41,43,45,46).

Angiopoietin1 (Ang-1)-Tie-2 signaling pathway has a great importance in stabilization of immature vascular tubes. Ang-1 is secreted by pericytes and binds to the endothelial receptor Tie-2. Ang-1 provides a stabilizing signal to endothelial cells and promotes the coverage of the endothelial tube with pericytes. Importantly this signaling pathway hampers endothelial cells proliferation and promotes endothelial quiescence (47-52). Mechanistically Ang-1-Tie-2 signaling promotes capillary stabilization by regulation of endothelial tight junctions, the accumulation and distribution of Ve-cadherin and the rearrangement and stabilization of the endothelial cell cytoskeleton (47,53,54).

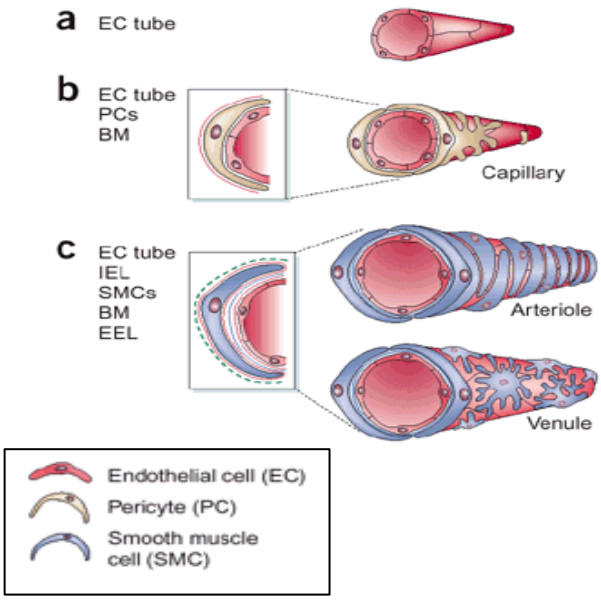

Figure 4: Capillary and vessel maturation (**A**) Nascent endothelial tube that will mature into a functional capillary or vessel. (**B**) Mature and functional capillary embedded into basement membrane and partial or fully covered with pericytes. (**C**) Arterioles and vessels have different mode of maturation. Arterioles are fully covered by SMC while venules are partially covered. Elastic lamina is present in both arterioles and venules. (40)

Maturation of the neo-vessels also includes the deposition of a new basement membrane, which offers stability, elasticity, and support in the capillaries and vessels (40, 42). *In vitro* studies revealed that the assembly and deposition of new basement membrane

after the formation of a new capillary is dependent on both endothelial cells and pericytes (55,56). Pericytes help in the maturation and the deposition of new basement membrane by inhibiting endothelial matrix metallo-proteases (MMPs), which are secreted during sprouting angiogenesis in order to create space for the migration of the new sprout. Pericyte MMP inhibitors TIMP2 and TIMP3 directly suppress the endothelial MMPs and indirectly tube formation and angiogenesis (55-60).

1.3.6. Intussusception: an alternative mode of angiogenesis

Besides spouting angiogenesis, intussusception, i.e., capillary or vessel splitting, is an additional mode of vascular expansion of an already formed vasculature without the necessity of endothelial cell proliferation and recruitment of several other cells types (61). During intussusception a pillar is created on the capillary wall, which extends inside the intraluminal space, separates and then longitudinally splits one capillary in two. (62-64). Intussusception contributes to the microvascular expansion of vascular beds and it is essential for the growth of an initial capillary plexus and the creation of a physiological vascular tree. It contributes to the hierarchical branching of vascular trees in an organ-specific way in order to meet metabolic and shear stress demands by amplifying the vascular surface and volume (61,65-67). Optimization of the flow properties of a vascular network is mediated by intussusceptive branching remodeling (IBR). This process provides the optimum geometry and architecture of a vascular bed in order to meet blood flow demands of each different tissue (61,63,67).

Sprouting angiogenesis and intussusceptive angiogenesis exist in combination in all vertebrates and they work in the direction of producing the optimal vascular bed needed for each tissue and organ. Intussusception is a plastic and energy-economic process that focuses more on the architecture and is regulated mainly by hemodynamic factors. This mechanism of vascular expansion is also implicated in tumor angiogenesis. The molecular factors that regulate intussusception are not yet clear (61,63).

1.4. Angiogenesis in health and disease

Angiogenesis is not a restricted process during embryo development and organ growth, it also occurs physiologically during tissue repair and wound healing in adults, adipose or muscle tissue expansion and in the reproductive cycle of the adult females (3) There are also pathologies that are characterized by extensive and uncontrolled angiogenesis, which is stimulated by unbalanced angiogenesis activators and inhibitors. Cancer development is one of the diseases that induces and is dependent on excessive and uncontrolled microvessel growth (7,8,68). Diabetes and rheumatoid arthritis are two more examples of diseases that promote and are worsened by excessive and uncontrolled angiogenesis (3).

1.4.1. Angiogenesis as a therapeutic target for cancer and tumor growth

In 1971 Judah Folkman recognized angiogenesis as an integral part of tumor growth and development and suggested that hampering angiogenesis in tumors could potentially lead to tumor stasis and regression (69). The understanding and the dissection of the mechanisms of physiological angiogenesis have been a valuable tool to design anti-angiogenesis drugs which have been brought to trial the past 10 years (7).

Tumor angiogenesis is triggered by hypoxia. The initial tumor cells proliferate and create a mass that can be fed and oxygenated by diffusion from the host vessels. When this tumor mass exceeds a volume of about $2mm^3$ hypoxia is occurring in the core of the tumor mass. This stimulates the expression of angiogenic molecules and growth factors leading to sprouting angiogenesis of the host vessel that invade the tumor mass and metabolically support its growth (7,70,71).

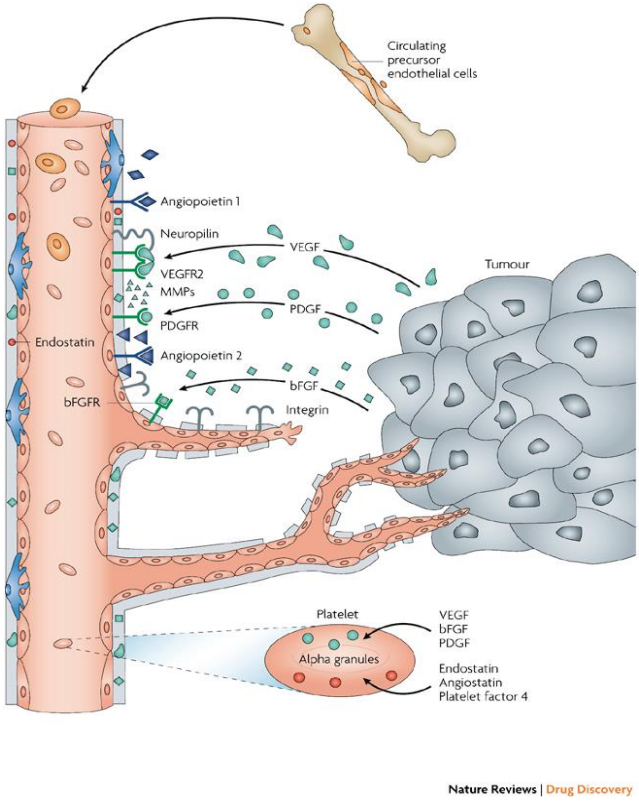

Figure 5: Tumor induced sprouting angiogenesis. Hypoxia occurring in the core of the tumor stimulates the secretion of VEGF, FGF and PDGF attracting new sprouts from the host vasculature in order to maintain their growth and survival. Endothelial and pericyte progenitor cells are also attracted to the site of active angiogenesis and contribute to tumor vascularization via vasculogenesis (7).

Sprouting angiogenesis is not the only way that a tumor can use to obtain its vascularization. Intussusceptive angiogenesis has been also observed in growing tumors were sprouting angiogenesis is hampered by chemotherapy or targeted anti-angiogenesis treatments (72).

Tumors also employ alternative means of vascularization such as host vessel co-option and vasculogenesis. Vascular co-option describes the ability of tumor cells to proliferate and migrate along host vessels, using them as survival rails which provide oxygen and nutrients (69). On the other hand the hypoxic conditions within the tumor attract endothelial and pericyte progenitor cells that can contribute to the vascularization of the tumor. Last but not least, tumor cells themselves can contribute to their own

vascularization by vascular mimicry. Tumor cells or tumor stem cells can express cancer and endothelial specific markers and can be incorporated or create vessels and capillary-like tubes and structures (7,70,73,74).

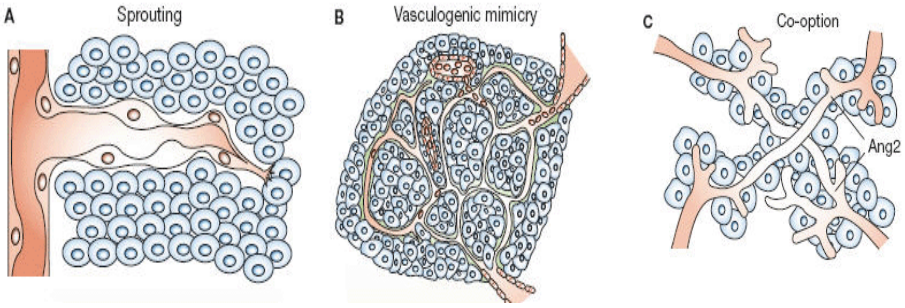

Figure 6: Different types of tumor vascularization. **(A)** Major mechanism of tumor vascularization by sprouting angiogenesis of the host vessels and capillaries invading the tumor mass. (**B**) Tumor cells or tumor stem cells mimic endothelial cells and are incorporated in tumor capillaries or create tube-like structures within the tumor. Tubular wall cells co-express endothelial or tumor surface markers. Bone marrow cells are also incorporated in the tumor capillaries via vasculogenesis. **(C)** Tumor cells migrate around host vessels via co-option using them as survival rails supporting their growth (75)

The cellular and molecular mechanisms of sprouting angiogenesis that have been revealed the last years apply also to tumor sprouting angiogenesis. This insight led to the development of targeted anti-angiogenesis treatments that focus on essential pathways such as the VEGF/VEGFR pathway, the PDGF/PDGFR pathway and the signaling via receptor tyrosine kinases (RTK) (7,74,76).

These anti-angiogenesis approaches for tumor regression showed hopeful results and some angiogenesis inhibitors are approved as treatments for specific types of cancers. However, resistance mechanisms in anti-angiogenesis treatments arise mainly due to the induction of secondary hypoxia by vessel regression, which leads to the up-regulation of alternative growth factor signaling pathways, mainly FGF2. This induces alternative

molecular mechanisms to maintain tumor vascularization and oxygen supply (7,70,73,77, 78).

1.5. Fibroblast growth factor 2: The orchestrating angiogenic growth factor

Fibroblast Growth Factor 2 (FGF2) is a very well characterized and potent angiogenic inducer first described in 1974 and is implicated in physiological, pathological and tumor angiogenesis (79,80). FGF2 possesses pleiotropic activities by regulating multiple cells types and acting synergistically with other growth factors to promote angiogenesis and vascular remodeling (80,81).

Tissues and vascular beds are exposed to FGF2 during trauma, inflammation or tumor growth; however its secretion mechanism is unclear (81). It is speculated that FGF2 is released by damaged or necrotic cells, since no specific cell-mediated secretion mechanism has been established and the only available data indicate that its secretion is independent from the Endoplasmic Reticulum-Golgi system and that the FGF2 protein lacks a secretion peptide (82,83).

FGF2 possesses high affinity for glycosaminoglycans and can bind to heparin sulfate proteoglycans in the extracellular matrix keeping the growth factor inactive (83,84). During angiogenesis, the FGF2-binding protein (FGF2-BP) interacts with the anchored FGF2 in the ECM, decreasing its affinity for the heparin sulfate proteoglycans and releasing it as an active form (84,85). FGF2 exerts its biological functions through binding to FGFR1, a tyrosine kinase receptor, causing a homodimerization of the receptor, which then signals by phosphorylating-specific tyrosine residues (81,86).

FGF2 exerts its angiogenic functions by inducing other growth factor pathways in endothelial cells and pericytes, promoting endothelial cells proliferation, resistance to apoptosis, increased cell motility and migration (80,82). FGF2 is known to induce VEGFA and VEGFR2 expression in endothelial cells, promoting endothelial and stromal cells proliferation (87-90). Several *in vivo* and *in vitro* data highlight the necessity of the cross-

talk between FGF2/VEGF signaling, suggesting that FGF2 depends on the VEGF signaling in order to induce angiogenesis. After the VEGF signaling cascade is initiated, FGF2 appears not to be required to drive endothelial cell proliferation and angiogenesis (91-94). This crosstalk between the two growth factors does not necessarily translate in regulation of the same genes involved in angiogenic processes. VEGF and FGF2 both regulate genes that modulate cell adhesion, cell growth, DNA damage repair, apoptosis and activity of transcription factors, i.e., Tie-2 precursor, Tie-1, VEGFC, VEGFR1, MCP1, and ERK1. On the other hand there are genes differentially regulated by these growth factors such as VCAM-1, β-CATENIN, E-Cadherin, IGFR2, MAP2K3, phospholipase C, IGF, ERK3/MAPK4 (95).

FGF2 and VEGFA induce different patterns of neo-vasculatures in Matrigel plugs: FGF2-induced angiogenesis creates endothelial tubes which are partially covered by pericytes and actively perfused. On the other hand VEGFA alone failed to induce the generation of functional capillaries in Matrigel plugs and only the combination of both growth factors resulted in a functional, not leaky and mature neo-vasculature (96). Similarly, in a corneal angiogenesis assay FGF2 induced the formation of well-structured and functional capillaries that were well fused. On the other hand VEGF resulted in pseudo-hemorrhagic phenotype and irregular fusion patterns (97). These finding may be explained by the fact that FGF2 acts also on the PDGF-BB/PDGFR system and on the Ang-1/2-Tie-2 system that are involved in vessel maturation (96,98-100).

1.6. mTOR signaling pathway

Cell proliferation and growth are regulated through different signaling pathways, of which the mammalian target of Rapamycin (mTOR) signaling pathway is central and of major importance (101).

Two distinct multi-protein complexes lie at the core of the mTOR signaling pathway, mTOR complex 1 (mTORC1) and mTOR complex 2 (mTORC2). mTORC1 and mTORC2 sense and respond to different extracellular stimuli, have different regulatory mechanisms and distinct substrates that at the end regulate different cellular actions and processes (102, 103). They have the same core protein mTOR, which is a highly conserved serine/threonine kinase. The two complexes share accessory proteins, mLST8 and DEPTOR (104-106). Additionally, mTORC1 contains regulatory binding proteins Raptor and PRAS40 (107-110). mTORC2 besides the common protein scaffold contains the regulatory binding proteins Rictor, mSIN1, and PRR5/Protor (104, 111-114). Rictor in collaboration with mSIN1 promotes the structural stability of the full complex (111,115-117).

Rictor, mSIN1, and Raptor are essential parts of the two mTOR complexes and have distinct sensitivity in Rapamycin treatment. Once Rapamycin enters the cell it binds to FKBP-12 forming a complex that interacts and inhibits mTORC1 through allosteric conformational changes of the kinase domain or by changing the structural integrity of the full complex (118-121). In the majority of cell types mTORC2 is not sensitive to Rapamycin-based inhibition. However, and most evidently in endothelial cells, long term or high dose of Rapamycin treatment induces mitigation of mTORC2 signaling. It is unclear why this distinction in certain cell types exists. Mechanistically, the inhibition of mTORC2 signaling by Rapamycin relies on the reduced bioavailability of mTOR; mTORC2 assembly is hindered since the Rapamycin-FKBP12 binds most of the available free mTOR in mTORC1 (104,112,122,123)

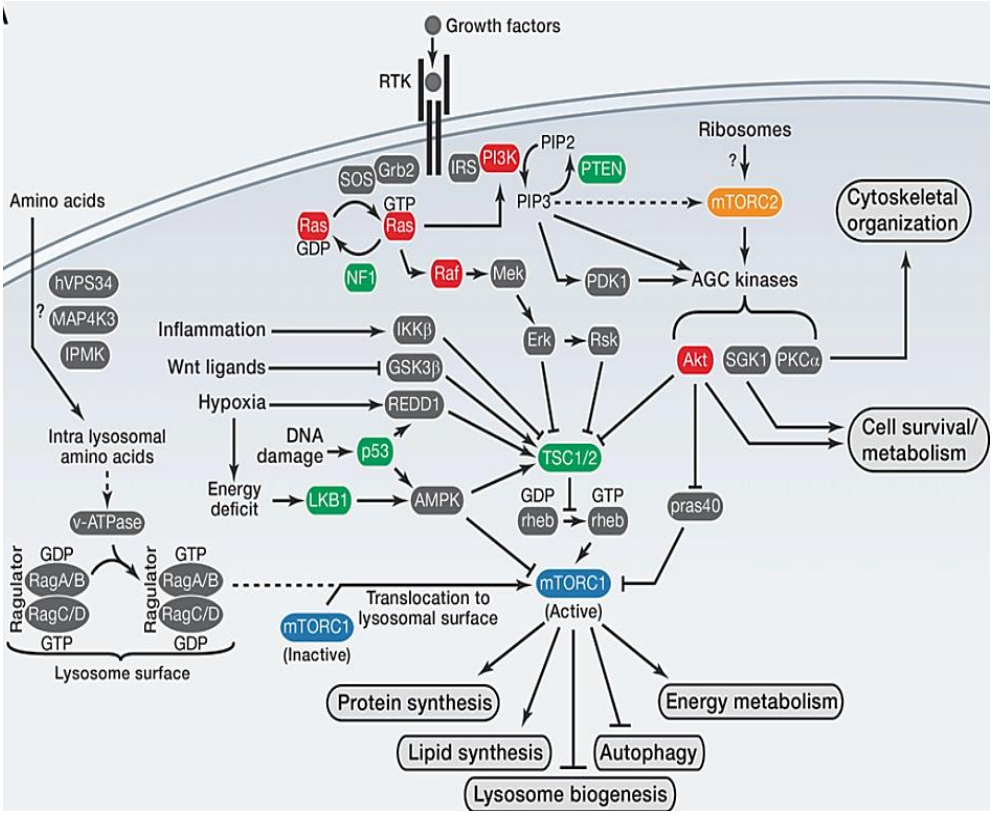

Figure 7. The mTOR signaling pathway (102)

1.6.1. mTORC1

mTORC1 has been shown to regulate anabolic processes such as protein synthesis, lipid synthesis, and metabolism. These are cellular functions that are central for survival. mTORC1 conveys signals from growth factors, stress, O_2 levels, ATP, and amino acids, which induce anabolic or katabolic pathways (101,102). The major upstream regulator of mTORC1 activity when stimulated by growth factors is the heterodimer tuberous sclerosis complex 1 and 2 (TSC1/TSC2 complex). Binding of a growth factor to its surface receptor activates the signaling cascade of the PI3K/Ras pathway that leads to the phosphorylation of TSC1/2 by Akt and ERK1/2 pathway. This phosphorylation inactivates TSC1/2 leading to the activation of mTORC1 via GTP-Rheb protein (124-129). Inflammatory cytokines,

ATP, and O_2 levels also activate mTORC1 via TSC1/2 - however there is also an Akt activating path that is independent from TSC1/2 (110,130,131)

The major activity mTORC1 signaling is activation of cell growth by protein synthesis. The effectors downstream of mTORC1 are well established. mTORC1 has a kinase activity that phosphorylates eIF-4E-BP1 (eukaryotic initiation factor E4 binding protein). eIF-4E is an initiation factor for mRNA translation. Phosphorylation via S6K of eIF-4E-BP binding protein does not allow the binding with eIF-4E, which now can actively participate in protein translation (132-134). S6K1 kinase is the direct target of mTORC1, which is also regulating mRNA synthesis and translation (102). mTORC1 also positively regulates the synthesis of lipids and ATP production in hypoxic conditions by up-regulating glycolysis. All these processes boost cell proliferation and survival (101,102).

1.6.2. mTORC2

So far, it has been established that mTORC2 is activated only by growth factor signals and not by nutrient and energy levels, or O_2 saturation (103). mTORC2's major and initially described substrate is Akt, a kinase with central activity for almost all cellular functions. Phosphorylation of Akt by mTORC2 at Serine 473 induces its translocation to cellular membranes in association with mTORC2 (135, 136). This activity of mTORC2 provides the maximal and optimal activation of Akt, which in turn phosphorylates its targets FoxO1/3a (111,117,137). Several researchers suggested that the activation of FoxO1/3a is specifically dependent on mTORC2 mediated Akt Ser473 phosphorylation. mTORC2 also phosphorylates Akt in Ser450, which is not a constitutive reaction but is needed when nascent Akt exits the ribosome as a polypeptide. This phosphorylation induces conformational changes, enhancing Akt stability (135,138,139).

mTORC2 also acts as a specific kinase of Protein Kinase C alpha (PKCα) and Serum and Glucocorticoid-induced Kinase 1 (SGK1). PKCα is phosphorylated by mTORC2 and promotes its maturation, folding and stability by recruiting Hsp90 chaperon (103,140,141). SGK1 is also phosphorylated by mTORC2, which allows its optimal activation, resulting in FoxO1/3a phosphorylation and activation (142,143). The activation of mTORC2 is associated with cytoskeleton and actin rearrangement, and cell migration. The molecular mechanism of mTORC2 regulation of the cytoskeleton still remains to be elucidated (104, 112). The association of mTORC2 with the ribosomes may suggest a direct regulatory role in protein synthesis (144,145). Indirectly, the full activation of Akt by mTORC2 can interfere with TSC1/2 activation via Akt and, by consequence, with mTORC1 signaling, which regulates protein synthesis and other metabolic processes. While mTORC1 is very well studied regarding upstream regulators and downstream effectors, mTORC2 is less studied and little is known about its contribution on important physiological and pathological processes.

1.6.3. The implication of mTOR signaling pathway in angiogenesis

The investigation and characterization of the mTOR signaling pathway has revealed its role in fundamental cellular processes including cell survival, proliferation, and apoptosis by conveying signals from the extracellular environment. The discovery of Rapamycin and its known function in mTORC1 and occasional mTORC2 inhibition prompted the scientist to investigate the effects of Rapamycin, mTORC1, and mTORC2 in tumor growth and development.

A series of *in vivo* experiments have highlighted the effect of mTOR inhibition not only on tumor growth, but also on tumor vascularization. Temsirolimus (commercial name for Rapamycin) successfully inhibited tumor growth and vascularization in a xenograft model of Matrigel plugs containing Human Epidermal Growth factor Receptor (HER)-

dependent breast cancer cells. mTORC1 silencing by siRNA interference confirmed the involvement of this signaling pathway. Similarly, Rapamycin and analogues exerted analogous inhibitory effects on the growth of Kaposi sarcoma and vascular tumors in *in vivo* models (146-148). Furthermore, the anti-angiogenic effect of mTOR inhibition was linked to inhibition of VEGF expression and translation (149-151).

While these effects were initially attributed to specific inhibition of mTORC1, later studies also implicated Akt and mTORC2 to be part of anti-angiogenic response by Rapamycin and analogues (150,152). Development of new mTOR inhibitors that specifically inhibit both mTORC1 and mTORC2 underscored the anti-tumor and anti-angiogenic potential of the mTOR signaling pathway: Dual inhibition resulted in more pronounced decrease in tumor growth, tumor vascularization, and VEGF production from tumor cells in a spontaneous pancreatic islet tumor model in comparison with Rapamycin alone, revealing an important role for mTORC2 in tumor growth and angiogenesis. Possibly the dual inhibition of the two mTOR complexes abolishes any negative feedback loop that would activate mTORC2 signaling (153-156).

Besides vascular regression, targeting mTOR may also normalize aberrant tumor vasculature: The concept of vascular normalization aims at increasing the functionality of improperly formed tumor vasculature. Fokas et al. have shown that dual inhibition of mTOR pathway and PI3K pathway resulted in improved vascular structure and better tumor oxygenation, which in turn sensitizes the tumor for radiotherapy (157,158).

In vitro experiments are expected to shed some light on the mechanism by which mTOR regulates tumor growth and – more interestingly for the purposes of this thesis - tumor vascularization. Initially it was shown that Rapamycin can inhibit the accumulation of HIF-1α in prostate and breast cancer cells. Decreased HIF-1α ultimately resulted in lower VEGFA levels in normoxic and hypoxic conditions, clearly suggesting a role for mTORC1 in VEGFA production and stimulation of sprouting initiation (134,146,159). Recent work revealed that mTORC1 regulates VEGFA production in a HIF-1α-dependent but also -

independent manner (160). HIF-1α is shown to be directly regulated by mTORC1 and recent data showed that Rictor specifically regulates the expression of HIF-2α and the stabilization of this hypoxia induced factor (161)

The fact that mTOR inhibitors affect tumor vascularization *in vivo* draws attention to mTOR signaling in endothelial cells, since endothelial cells are the drivers of angiogenesis. It has been demonstrated that mTOR signaling is required for endothelial cell proliferation and *in vitro* angiogenesis. Under hypoxic conditions, which are usually found in tumors, both mTORC1 and mTORC2 are needed for endothelial cell proliferation (162). Inhibition of both complexes with Rapamycin inhibited sprouting of endothelial cells from rat aortic rings specifically under hypoxia (162,163). Temsirolimus not only inhibited endothelial cell proliferation and migration, it also decreased VEGF and PDGF secretion in a model of retinal vascularization (164). The functional significance of Akt/mTOR signaling was highlighted when inhibition of these pathways in endothelial cells decreased survival and proliferation of endothelial cells due to FoxO1/3a activation (165).

In most of the above mentioned experiments Rapamycin or Rapamycin-based inhibitors have been used to assess the role of mTOR in angiogenesis. However, it is not clear to which mTOR complex the observed effects can be attributed. A few recent studies showed that PGE2-induced endothelial survival and migration is directly regulated by mTORC2 and that the PI3K/mTORC2 signaling axis is central for VEGF-mediated endothelial cell survival via FoxO1/3a (166,167).

1.7. Aims and experimental approach

In vivo experiments with dual inhibition of mTOR complexes indirectly suggest a specific and distinct role for mTORC2 in tumor vascularization. However the nature of the existing mTOR inhibitors does not allow the discrimination between the individual functions of mTORC1 and mTORC2 in angiogenesis. It is evident that the specific roles of mTORC2 in angiogenesis are not yet defined. Specifically, the role of mTORC2 in the biology of the endothelium as the initiating tissue during sprouting angiogenesis remains to be elucidated. VEGF and FGF2, abundantly found in growing tumors are the most important and orchestrating growth factors in both physiologic and pathological angiogenesis that will be used as stimulus for angiogenesis *in vivo*.

Aims of this thesis

Assessment of the role of endothelial mTORC2

- in vascular homeostasis
- in existing vascular beds challenged by high doses of VEGF and FGF2
- in neo-vascularization in response to a high dose of VEGF and FGF2

Experimental approach

Ceasing mTORC2 signaling in the endothelium is induced by the deletion of Rictor, an mTORC2 specific accessory protein. Endothelium-specific and Tamoxifen inducible *Rictor* knockout mice were used in order to study the role of endothelial mTORC2 in angiogenesis *in vivo*. The experimental approach includes:

- Validation and assessment of *Rictor* knockout in the endothelium from these transgene mice

- Monitoring and assessment of the health status of control and knockout mice during adolescence
- Monitoring existing vascular beds of control and knockout mice using the dorsal skinfold chamber and fluorescent intravital microscopy
- Modification of the dorsal skinfold chamber for FGF2-stimulation of the skin muscle vasculature and monitoring of vascular changes
- Assessment of neo-angiogenesis in FGF2-loaded Matrigel plugs

2. Materials and methods

2.1. Endothelial specific and Tamoxifen inducible Rictor$^{i\Delta ec}$ mouse

Mice with floxed *Rictor* exons 3 and 4 (168, 169) were crossed with mice that express Tamoxifen (Tx)-inducible Cre-ER^{T2} recombinase under the transcriptional control of the endothelium-specific VE-cadherin promoter (VECad-Cre-ER^{T2}) (170) (kind gift of Dr. Iruela-Arispe, Department of Molecular, Cell & Developmental Biology, UCLA, USA), both on a congenic C57Bl/6J background. Offspring were genotyped for Cre-recombinase, Rictor ^{floxed} and Rictor^{wt} alleles using qPCR. Briefly, DNA was isolated from ear biopsies and amplified by qPCR with the following primer pairs (5'-3'): Forward: GCG GTC TGG CAG TAA AAA CTA TC; Reverse: GTG AAA CAG CAT TGC TGT CAC TT. The mice were bred, housed and handled according to the local animal ethics committee (license 77/2009 and 179/2012, Kantonales Veterinäramt Zürich).

2.2. Determination of Rictor mRNA expression levels in aortic endothelium

2.2.1. Scraping of aortic endothelium

Rictor deletion was induced in VECad-Cre-ER$^{T2\ +/+}$; Rictor $^{floxed/floxed}$ mice at an age of four weeks with five consecutive intraperitoneal Tamoxifen (Tx) injections (2 mg Tx /ml dissolved in corn oil at a concentration of 80 mg/kg bodyweight, T5648, Sigma-Aldrich). Littermate control mice were injected with vehicle corn oil alone. Aortae were excised from 2 or 6 month old Tx-injected (Rictor $^{i\Delta ec}$) and control mice (Ctrl), cleaned from adhering tissue and opened longitudinally. Endothelial cells were carefully scraped directly in RLT buffer (Qiagen) and RNA was extracted using the RNAeasy micro kit (Qiagen) according to the recommendations of the manufacturer. Equal amounts of RNA were transcribed to cDNA by WT (Whole Transcript)-Ovation™ Pico RNA Amplification System (NuGEN).

Quantitative real-time PCR was performed using a SYBR green-based standard protocol. Tubulin, GAPDH, and β-actin were used as housekeeping control. The specificity of the primers was tested by melt curve and agarose gel analysis and sequencing. Relative expression levels were calculated using the comparative ΔΔCt method (171).

2.2.2. Enzymatic digestion of aortic endothelium

Two month old mice were sacrificed and thoracic aorta was excised and transferred in petri dish. A pediatric catheter was inserted in one edge of the aorta and was stabilized with a hemostatic clamp. The aorta was washed with ice cold PBS through the catheter. Then the other opening of the aorta was sealed with a hemostatic clamp. Trypsin 0.25%/EDTA (Gibco), Collagenase D or Liberase (172) were administered in the clamped aorta through the catheter. Aortic walls were incubated with the enzymes for 7-10 minutes. After enzymatic digestion, the detached cells were flushed with Vasculife endothelial specific medium (Lifeline Cell technology) in a collection tube for total RNA isolation. A piece of the denudated aorta was kept as a negative control.

2.3. Determination of Rictor mRNA expression levels in lung endothelium

2.3.1. Magnetic Activated Cell Sorting (MACS) lung endothelial cells isolation

Lungs were excised from 2 month old Tx-injected (Rictor $^{i\Delta ec}$) and control mice (Ctrl), and stored in Vasculife endothelial specific media (on ice). When lungs from all mice were removed, samples were transferred under sterile laminar flow. Lungs were washed with ice cold PBS and minced with parallel scalpels and scissors. Minced lung tissue from every mouse was incubated in Collagenase D (1mg/ml, Roche) for 1 hour at 37^{O}C. Every 5 minutes the collagenase-lung suspension was re-suspended with a 5 or 10ml serological pipette. Collagenase activity was blocked with 5ml bovine serum and the cell

suspension was washed with MACS buffer (1% BSA in PBS). Cell suspension was passed through a 70μm nylon mesh. Cells that passed through the mesh were washed 2 times with MACS buffer and then passed through a 30μm Pre-Separation filter (MACS, Miltenyi Biotec). Cells were incubated with 2% mouse serum at 4 ^{O}C for 30 minutes. Cells were washed with MACS buffer and incubated 4^{O}C for 30 minutes with rat anti-mouse CD31, rat anti-mouse CD105 (BD Pharmigen) and biotinylated Isolectin B4 (Vector laboratories). Cells were labeled with secondary goat anti-rat IgG microbeads (MACS, Miltenyi Biotec), which are magnet conjugated antibodies and magnet conjugated Streptavidin (MACS, Miltenyi Biotec). Cell suspension was passed through MACS magnetic LS separation column (MACS, Miltenyi Biotec). The positive and negative selected cells were directly subjected to total RNA isolation with Qiagen RNAeasy mini kit.

Enrichment of the MACS sorted endothelial cells was achieved with the culture of the $CD31^{+}/CD105^{+}/IB4^{+}$ positive selected cells. The positive selected population was plated in a 2% collagen (Carl Roth GmbH 4274.1) coated 3 cm petri dish and cells were cultured at 37^{o}C and 5% O_2 in Vasculife endothelial specific medium for 7 to 10 days until 60% confluence and then total RNA was extracted.

2.3.2. Fluorescence Activated Cell Sorting (FACS) of lung endothelial cells

Lungs were excised from 2 month old Tx-injected (Rictor $^{i\Delta ec}$) and control mice (Ctrl), and stored in Vasculife endothelial specific media on ice. When lungs from all mice were removed, samples were transferred under sterile laminar flow. Lungs were washed with ice cold PBS and minced with parallel scalpels and scissors. Minced lung tissue from every mouse was incubated in Collagenase D (1mg/ml, Roche) for 1 hour at 37^{O}C. Every 5 minutes the collagenase-lung suspension was re-suspended with a 5 or 10ml serological pipette. Collagenase activity was blocked with 5ml Vasculife endothelial specific medium and the minced tissue was passed through a 100μm nylon mesh. Cells were washed in ice

cold FACS buffer (1%BSA in PBS), counted and passed through a 30μm Pre-Separation Filters (MACS, Miltenyi Biotec). Cell suspension was incubated with FACS buffer for 30 minutes in ice and then incubated with rat anti-mouse APC-CD31 and rat anti-mouse PE-Cy7-CD45 antibody (BD Pharmigen) for 30 minutes in dark. Live/dead staining with aqua fluorescent Live/Dead Fixable Cell Stain kit (Invitrogen) was made 30 minutes before FACS analysis and sorting Final samples were reconstituted in 400μL volume of FACS buffer and FACS sorting was conducted with FACSAria III sorter (Flow cytometry facility, University of Zurich, Irchel Campus). Single cells were gated and live/dead cells were distinguished. $CD31^{+}/CD45^{-}$ cells of the gated cell population represent the endothelial cells. Positive and negative populations were flushed in Vasculife endothelial medium or directly in RLT buffer for total RNA isolation.

2.4. Determination of the efficiency of endothelial cell isolation and *Rictor* knockout induction efficiency

Endothelial cell isolation was attempted with the above mentioned techniques, i.e. aorta scraping, aorta enzymatic digestion, lung endothelial cells isolation with MACS and enrichment with culturing and FACS sorting of lung endothelial cells. Total RNA isolation was conducted with either RNeasy-mini or RNeasy-micro kit (Qiagen) depending on the amount of isolated cell populations. Equal amounts of RNA were transcribed with iScript kit (Biorad). When the amount of total RNA that was isolated was below 20ng/μL transcription and cDNA amplification was conducted with WT (Whole Transcript)-Ovation™ Pico RNA Amplification System (NuGEN). The presence of endothelial cells in the isolated cell populations and the efficiency of the isolation technique were assessed with qRT-PCR using a SYBR green-based standard protocol for CD31, Ve-Cadherin, CD45, and SPA when the isolation was performed from lung tissue. SMA was assessed when the isolation was performed from aortic tissue. *Rictor* deletion and Cre-ER^{T2} expression in the

endothelium was assessed in the same tissues with real-time PCR. All primer sequences are at the end of the Material and Methods section.

2.5. *Rictor* KO aortic endothelial cells

Mouse aortic endothelial cells (MAECs) were isolated from aortae of 8-10-week-old *Rictor* floxed male mice as described earlier (173),(163). Rictor KO cells were generated by adenoviral transfection of Cre-Recombinase. $8x10^5$ Rictor floxed MAECs were seeded on a 10 cm culture dish. The next day, the media was removed and a virus (100 MOI) that contained either Ade-CRE-GFP (Vector Biolabs 1045) or Ade-CMV-GFP (Vector Biolabs 1060) was added in 3 ml of growth media to the cells. After 6 hours, the media was removed, replaced by 10 ml of normal growth media, and incubated at 37°C. Endothelial cells expressed GFP the following day. Down-regulation of *Rictor* and disruption of mTORC2 signaling was assessed by using qRT-PCR. *Rictor* knockout and control MAECS were used as control samples for the detection of *Rictor* qRT- PCR in the lung or aortic isolated endothelial cells.

For all experiments using MAECs, cell culture dishes were coated with 0.1% gelatin gold (Carl Roth GmbH 4274.1) for 20 minutes at 37°C. MAECs were maintained in DMEM (Biochrom FG435), complemented with 10% or 1% (complete or starvation medium), FCS (Biochrom S0615), 1% sodium pyruvate (GIBCO 15140), 1% non-essential amino acids (GIBCO 11140), and 1% penicillin-streptomycin (GIBCO 15140). Stimulation with growth factors always included addition of heparin at a fixed ratio (1 IU heparin per 1, 5 µg/ml GF).

2.6. Mouse dorsal skinfold chamber and Matrigel sealing

To study the capillary remodeling and angiogenesis *in vivo* we used the dorsal skin fold chamber as described previously (174) with a novel modification in order to deliver growth factors via Matrigel to the tissue. Figure 8 shows the steps for the surgical

implantation of the dorsal skinfold chamber. Briefly for chamber implantation, two symmetrical titanium frames were mounted on the dorsal skin fold of the animal. One skin layer as well as the underlying fat were then completely removed in a circular area of 15 mm in diameter, and the remaining layers (consisting of striated skin muscle, subcutaneous tissue and skin) were covered with NaCl 0.9% and a glass cover slip incorporated into one of the titanium frames. The animals were allowed to recover for two days. The baseline vasculature was recorded with intravital microscopy (see below) and then, skin from the remaining layer was carefully detached from the underlying muscle and removed in a circular area of 7 mm in diameter from the back of the chamber. Growth factor reduced Matrigel (BD Biosciences) was thawed on ice and mixed with either FGF2 (1,5 mg/ml) or VEGF (1,5mg/ml) (R&D Systems) and Heparin (5 IU units B.Braun) or Heparin alone. The defect on the back of the chamber was sealed with 200µl of the Matrigel mixtures that were allowed to gel for 5 min, and covered with NaCl 0.9% and a glass cover slip incorporated into the other titanium frame.

An alternative modification for VEGF delivery in the dorsal skin was the intramuscular injection of primary myoblasts isolated from C57BL/6 mice and transduced to express the β-galactosidase marker gene (lacZ) from a retroviral promoter (175). They were further infected at high efficiency (176) with retroviruses carrying the cDNA for murine $VEGF_{164}$ (176). Myoblast clones were isolated using a FacStar cell sorter (Becton Dickinson) and single cell isolation was confirmed visually. The stability of the VEGF secretion was assessed periodically by ELISA. All myoblast populations were cultured in 5% CO_2 on collagen-coated dishes as previously described (kind donation from Dr. Roberto Gianni Barrera, University Hospital Basel Institute for Surgical Research and Hospital Management Cell and Gene Therapy Group) (176). Figure 8 below all the steps of the surgical implantation of dorsal skinfold chamber.

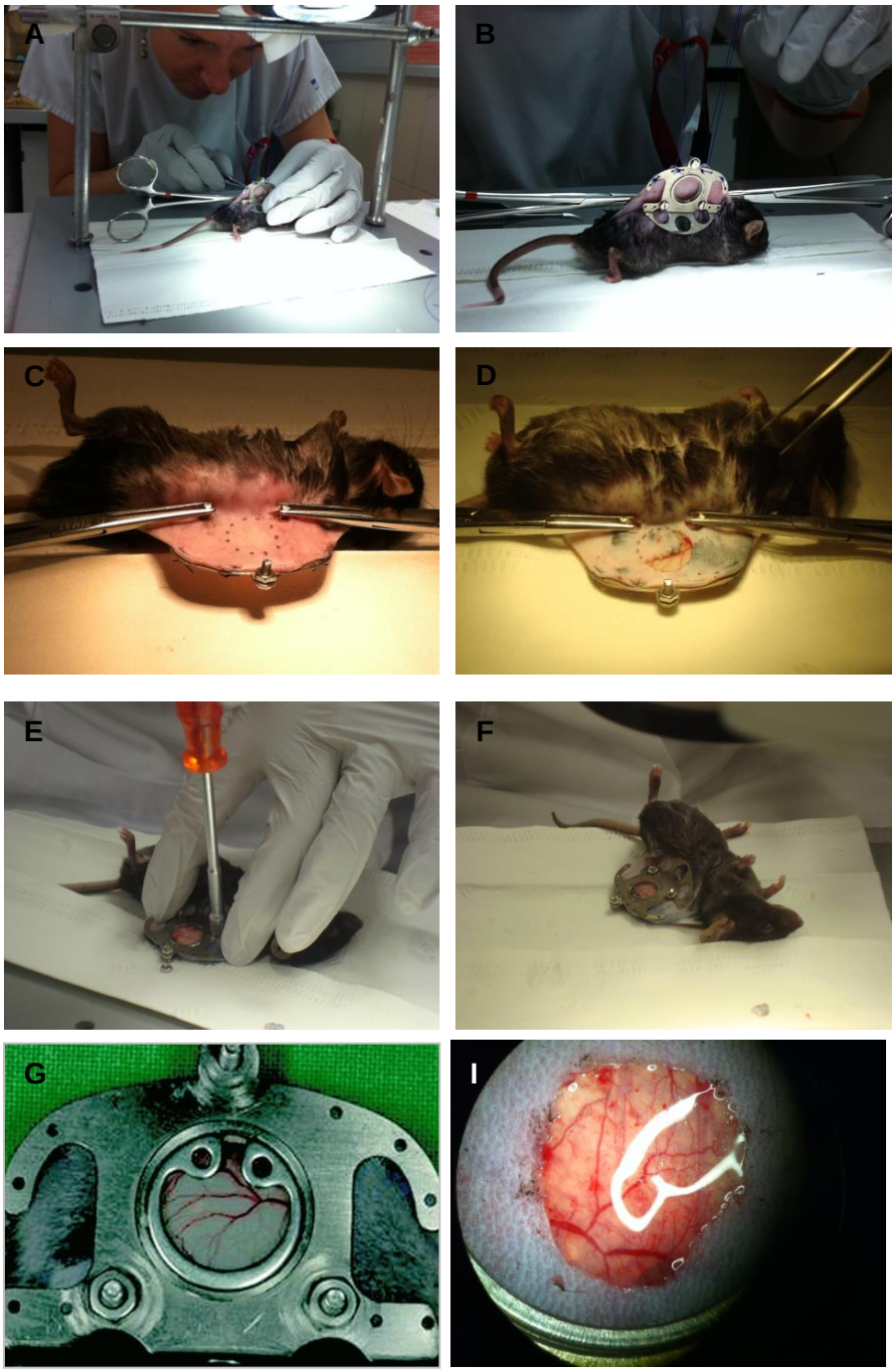

Figure 8. Overview of the implantation of the dorsal skinfold chamber. Surgical procedure for the dorsal skinfold chamber implantation **(A-F).** The skin muscle vasculature through the observation window of the skinfold chamber **(G).** Modification of the dorsal skinfold chamber for growth factor delivery. Skin defect on the opposite site of the observation window sealed with Matrigel to deliver growth factors (**I**).

2.6.1. Intravital microscopy

Repetitive intravital microscopic analyses of skin microvasculature were carried out daily over a time period of 7 days. Microscopic images were taken at 8 different areas

within the center and the periphery of the wound. After intravenous injection of 0.2 ml FITC-labeled dextran (2%; MW 70000, Sigma-Aldrich, Munich, Germany) the microcirculation was visualized by intravital fluorescence microscopy (Leica DM/LM; Leica Microsystems, Wetzlar, Germany). Microscopic images were captured by a CCD television camera (Kappa Messtechnik, Gleichen, Germany) and recorded on video (50 Hz; Panasonic AG-7350-SVHS, Tokyo, Japan) for subsequent offline analysis. Using × 10 (N-Plan × 10/0.25 LD, Leica), × 20 (HCX Apo × 20/0.50 W, Leica) objectives blood flow was monitored in capillaries of the superficial and deep dermal plexus of the skin muscle. The epi-illumination setup included a mercury lamp with a blue filter (450–490 nm/>520 nm excitation/emission wavelength) and a green filter (530–560 nm/>580 nm). Quantification of vascular parameters was done with CapImage version 8.6.3 software (Created by Dr. Zeintl).

2.7. Matrigel plug assay

The Matrigel plug assay was performed as previously described (177). In brief, 8-week-old male C57BL/6 mice were injected subcutaneously with 0.20 ml of Matrigel containing 1.5μg/ml FGF2 with 1μl (5 IU) Heparin. The injected Matrigel rapidly formed a single, solid gel plug. After 7 days the mice were euthanized and the skin was pulled back to expose the Matrigel plug. The Matrigel plug was removed, photographed, fixed in formalin, and paraffin embedded. Hemoglobin content was roughly estimated by measuring the magenta channel in CMKY converted images by NIH Image J program. Sections were made and infiltrating ECs were identified with rabbit polyclonal anti-mouse CD-31(1:10, Lifespan Biosciences) immunohistochemical staining according to the manufacturer's protocol.

2.8. Immunohistochemical staining

On day 7 of intravital microscopy experiment was terminated and skin muscle was removed, washed and fixed in 2% paraphormaldehyde overnight. The next day tissue was paraffin-embedded and then sectioned. Similar procedures were followed for the Matrigel plugs after experiment termination. Capillaries and vessels were immuno-labeled with CD31 peroxidase staining. Briefly, sections were deparaffinized and rehydrated in xylene and in decreasing concentrations of ethanol. Antigen retrieval was done by boiling in Trisodium Citrate (Tri.Na.Citrat) (ph6.4). Tissue sections were blocked with 10% goat serum in 1% BSA / 0.1% TritonX-100 in PBS. Rabbit polyclonal anti-mouse CD31 antibody (1:10) (Lifespan Biosciences) was added and detection was made with Peroxidase rabbit IgG Vectastain ABC kit (Vector Laboratories), following manufacturer's instructions. Nuclei were stained with Hematoxylene and sections were dehydrated in increasing concentrations of ethanol and xylene. The cover slip was mounted with permanent VectaMount mounting medium (Vector Laboratories).

Cre-ER^{T2} was visualized by immuno-fluorescent staining of Estrogen Receptor α (ER^{T2}). Briefly, sections were deparaffinized and rehydrated in xylene and decreasing concentrations of isopropanol and antigen retrieval was done with boiling in Trisodium Citrate (Tri.Na.Citrat). (ph6.4). Tissue sections were blocked with 10% goat serum in 1% BSA / 0.1% TritonX-100 in PBS. Primary rabbit polyclonal anti-mouse anti-Estrogen Receptor α antibody (1:400/Millipore) was added and detection was made with secondary goat anti-rabbit Alexa-Fluo 555 (1:200/Invitrogen). Nuclei were stained with Hoechst 33342 (1:200/Invitrogen) and the cover slip was mounted with Fluosave (Calbiochem).

2.9 Statistical analysis

Statistical tests were performed by using GraphPad Prism 5.04 for Windows® (GraphPad software, San Diego, CA, USA). We have used unpaired t-test to evaluate

differences between two groups. If there were more than two groups, we used one-way ANOVA, followed by a Bonferroni post-test. $P<0.05$ was considered significant.

2.10. Primer list

Gene	Forward Primer	Reverse Primer
β-actin	CGT GCG TGA CAT CAA AGA GA	CCC AAG AAG GAA GGC TGG A
β-Tubulin	TCA CTG TGC CTG AAC TTA CC	GGA ACA TAG CCG TAA ACT GC
CD31	AGG CTT GCA TAG AGC TCC AG	TTC TTG GTT TCC AGC TAT GG
CD45	GAA CAT GCT GCC AAT GGT TCT	TGT CCC ACA TGA CTC CTT TCC
Cre	CGT ACT GAC GGT GGG AGA AT	CCC GGC AAA ACA GGT AGT TA
GAPDH	AAA TGG TGA AGG TCG GTG TG-	GTT GAA TTT GCC GTG AGT GG
Rictor	TGC GAT ATT GGC CAT AGT GA	ACC CGG CTG CTC TTA CTT CT
SMA	GCG GCC TTT AAA CCC CTC ACC C	GAG GCA GAG AAG GCT TGG TCG T-
SPA	AGG CAG ACA TCC ACA CAG CTT	ACT TGA TGC CAG CAA CAA CAG T
Ve-Cadherin	GCT GAC CAG CCT CCA ACG GG	TGC TCT CAA GTG AAA CCG GGC T

3. RESULTS

3. A. Endothelial specific *Rictor* knockout mouse: Assessment of the efficiency of *Rictor* knockout in the endothelium

3. A.1. Induction of *Rictor* knockout in the adult mouse endothelium

Investigation of the role of endothelial mTORC2 in angiogenesis *in vivo* was conducted by using an endothelial specific and inducible *Rictor* knockout mouse, as Rictor is a specific component of mTORC2. This mouse was generated by crossing a mouse with loxed exons 4 and 5 of the *Rictor* gene (168, 169) with a mouse expressing Cre-ER^{T2} under the transcriptional control of Ve-Cadherin promoter (170). Tamoxifen injections of Cre-ER$^{T2\ +/+}$ mice at the age of 4 weeks allowed Cre-ER^{T2} recombinase translocation into the nucleus of endothelial cells and the excision of exon 4 and 5 of *Rictor*. As control Cre-ER$^{\mathbf{T2+/+}}$ mice were injected with corn oil (170).

Figure 1 shows the efficiency of *Rictor* knockout induction in the aortic endothelium of adult mice (February 2011). These mice were used in this project in order to assess the role of endothelial mTORC2 in angiogenesis *in vivo*. The efficiency of *Rictor* knockout was assessed in the aortic endothelium of 28-week-old mice. Aortas of corn oil or Tamoxifen injected mice were removed, washed, and cut in a flap mount. The aortic endothelium was treated with RLT buffer for total RNA isolation and smoothly scraped with a scalpel.

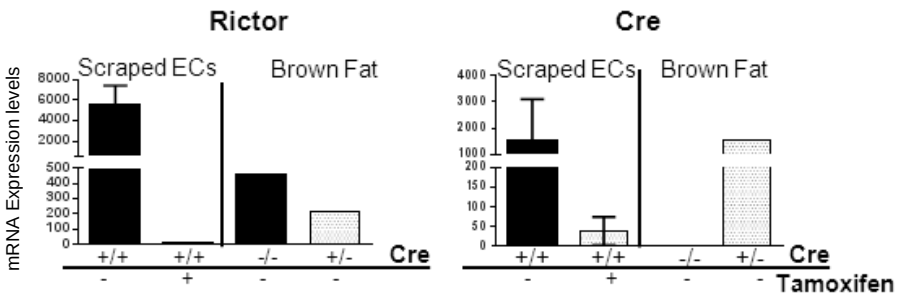

Figure 1: mRNA levels of Rictor and Cre-ER^{T2} recombinase in scraped aortic endothelium. Rictor mRNA levels show almost complete ablation of *Rictor* expression in Tamoxifen-treated Rictor$^{i\Delta ec}$ mice (Control n=3/Rictor$^{i\Delta ec}$ n=2). Cre-ER^{T2} was expressed in Cre^{+} animals and was absent in Cre- animals. Brown fat from a constitutive Rictor knockout model in the adipose tissue was used as a control for *Rictor* knockout efficiency and Cre expression.

Detection of Rictor mRNA levels of scraped endothelium of control versus Rictor$^{i\Delta ec}$ mice showed complete depletion of *Rictor* expression and high efficiency of *Rictor* knockout induction with this Tamoxifen injection regimen (**Figure 1**). Adipose tissue from an adipose specific and constitutive *Rictor* knockout mouse was used as a control for Cre-mediated expression and *Rictor* deletion (179). The adipose tissue of these mice exhibited an established significant reduction of Rictor mRNA expression levels of about 50% (**Figure 1**). The levels of Cre-ER^{T2} recombinase mRNA varied in different Cre^{+} animals and were absent in Cre^{-} adipose specific *Rictor* knockout animals (**Figure 1**).

The presence of endothelial cells in the scraped tissue was confirmed by Real-Time PCR. CD31 and Ve-Cadherin were used as markers for endothelial cells while CD45 as a marker for blood cells (178) and Smooth Muscle Actin (SMA) as a marker for smooth muscle cells. Figure 2 shows the mRNA expression profile of the scraped aortic endothelium.

High levels of CD31 mRNA confirmed endothelial cell abundance in the scraped tissues. Ve-Cadherin showed variable mRNA expression levels among the samples. CD45 mRNA was detected in the scraped tissue of the corn oil injected animals. CD45m RNA represent hematological cells that also co-express CD31 and these cells can contribute to some extend in the CD31 mRNA levels observed (178). However, smooth muscle actin mRNA levels were low in the scraped endothelium of both animal groups compared to the levels from the whole aorta (**Figure 2**).

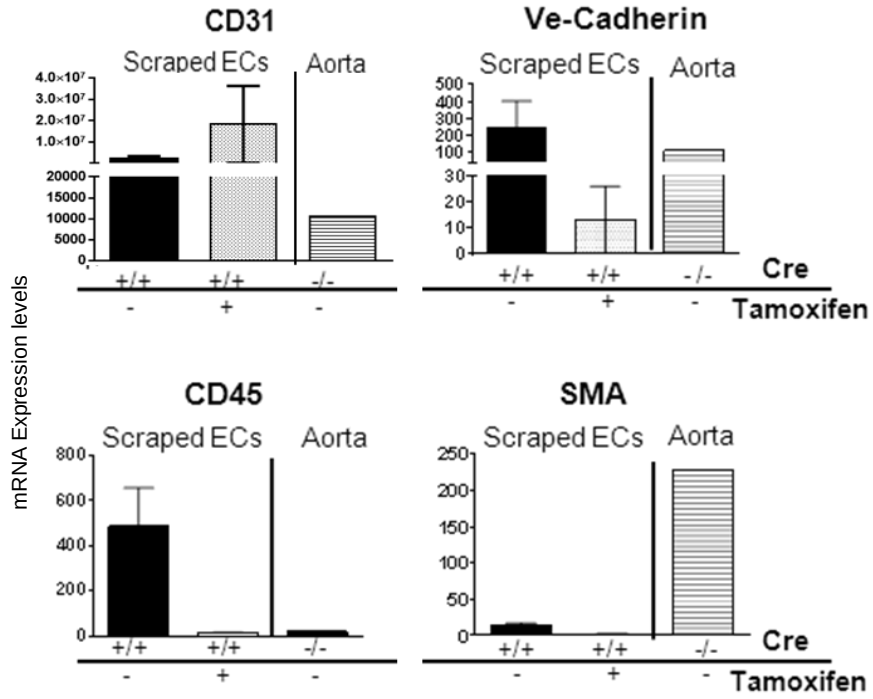

Figure 2: mRNA levels of endothelial, hematologic and smooth muscle markers of scraped aortic endothelium and full aorta. CD31 and Ve-Cadherin mRNA levels are used as endothelial positive markers. CD45 and SMA are used as hematological cell and smooth muscle cells markers respectively. The scraped endothelium of Control ($Cre^{+/+}$, Tamoxifen $^{-}$) and $Rictor^{i\Delta ec}$ ($Cre^{+/+}$, $Tamoxifen^{+}$) showed abundant presence of CD31 positive cells and presence of Ve-Cadherin mRNA. CD45 mRNA was not equally distributed between the sample and the smooth muscle cells were not present in the scraped endothelium. (**Control n=3/$Rictor^{i\Delta ec}$ n=2**)

3. A.2. Efficiency of *Rictor* knockout induction in endothelial cells in aorta and lungs

At the end of the second year of the project (September 2013) and after acquiring the *in vivo* data presented in this thesis (**Results Part B**) the question about the *Rictor* knockout induction efficiency in tissues that are subjects of investigation (muscle, retina, and tumors) was raised.

The designed experimental approach was based on optimization of endothelial cell isolation with Magnetic Activated Cell Sorting (MACS) from the lungs, the most vascularized tissue in the body (180). After the optimization of the technique, endothelial cells from skin muscle, retina and melanoma tumors would be isolated in order to assess the efficiency of *Rictor* knockout. The efficiency of *Rictor* knockout in the aortic endothelial lining as observed in the beginning of the project, would be considered as an internal

control for the efficiency of *Rictor* knockout induction in the lung endothelial cells and the mRNA levels of aortic endothelial Rictor would be assessed side by side with mRNA arriving from lung endothelial cells or cells from other tissues.

Thoracic aorta and lungs from 3 control and 3 Rictor$^{i\Delta ec}$ mice were dissected in order to isolate the aortic endothelial lining and the lung endothelial cells. The lungs of the 3 control and 3 Rictor$^{i\Delta ec}$ mice were pooled together in order to increase the number of endothelial cells that would arrive from the MACS isolation. The scraping of aortic endothelium has been previously conducted; one aorta can provide enough endothelial material in order to conduct gene expression analysis (**Figure 1**).

3. A.2.1. Rictor mRNA quantification and cell marker profiling of aortic endothelial lining

The presence of endothelial cells in the scraped lining was assessed as previously described in Figure 1. Established cultures from our laboratory, of control and Rictor KO MAECS were used as samples of pure endothelial cells and as a control of Rictor mRNA depletion.

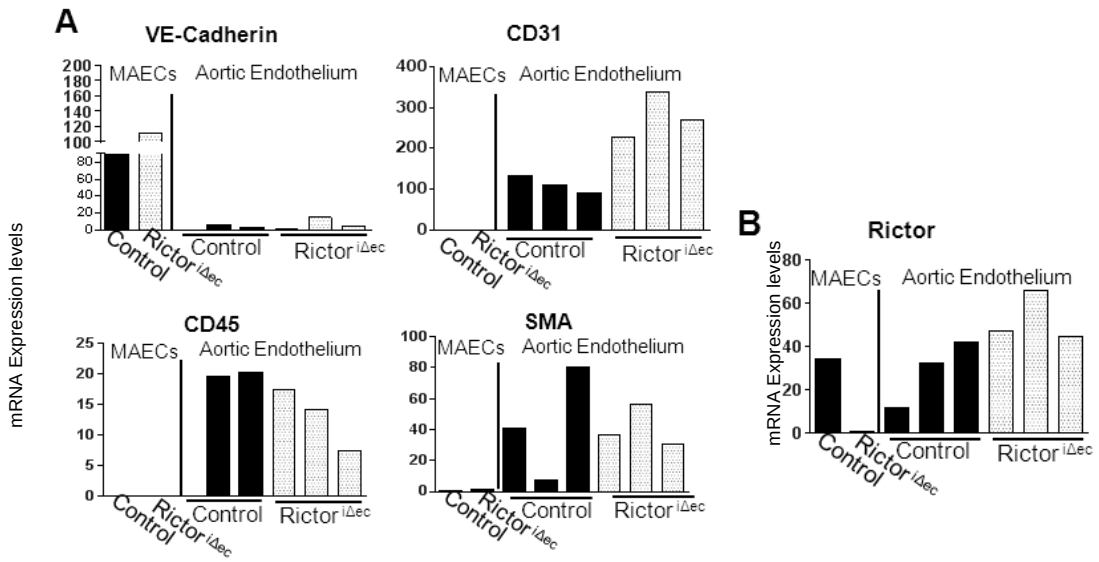

Figure 3: mRNA levels of endothelial, hematologic and smooth muscle cell markers in cultured endothelial cells and scraped aortic endothelium. Each column of the aortic endothelium represents one animal. **(A)** Expression levels of Ve-Cadherin and CD31 mRNA as endothelial specific markers and CD45 and SMA mRNA levels as controls for the presence of blood cells and smooth muscle cells respectively. **(B)** Variable Rictor mRNA levels showing no induction of the *Rictor* knockout in scraped aortic endothelium **(n=3).**

The scraped endothelial lining was positive for CD31 mRNA. However Ve-Cadherin was very low expressed. The cultured MAECs show a reverse mRNA profile of CD31 and Ve-Cadherin (**Figure 3A**). There is a low presence of CD45 positive blood cells and a sporadic presence of smooth muscle cells. (**Figure3A)**. In the scraped endothelium of the three individual Rictor$^{i\Delta ec}$ animals the Rictor mRNA levels showed that there is no knockout induction and that the levels of Rictor mRNA in the Rictor$^{i\Delta ec}$ animals were even higher than in control mice (**Figure 3B)**. Based on the Rictor mRNA levels, the fact that Ve-Cadherin mRNA was not detectable in the scraped endothelium and the results from the respective experiment on 2011 (**Figures 1-2**) doubts concerning the efficacy of *Rictor* knockout induction and the and the efficiency of the aortic scraping as a technique was raised.

3. A.2.2. Rictor mRNA quantification and cell marker profiling of MACS sorted lung endothelial cells

The lungs of the above three control and Rictor$^{i\Delta ec}$ mice were subjected to collagenase digestion and endothelial cells were sorted with MACS based on the presence of CD31, CD105 cell surface markers and Isolectin B4, which specifically binds to endothelial cells (181). Total RNA was isolated from the $CD31^{+}/CD105^{+}/IB4^{+}$ cell suspension and from the flow-through of the magnetic separation that should contain all the non-endothelial lung cells.

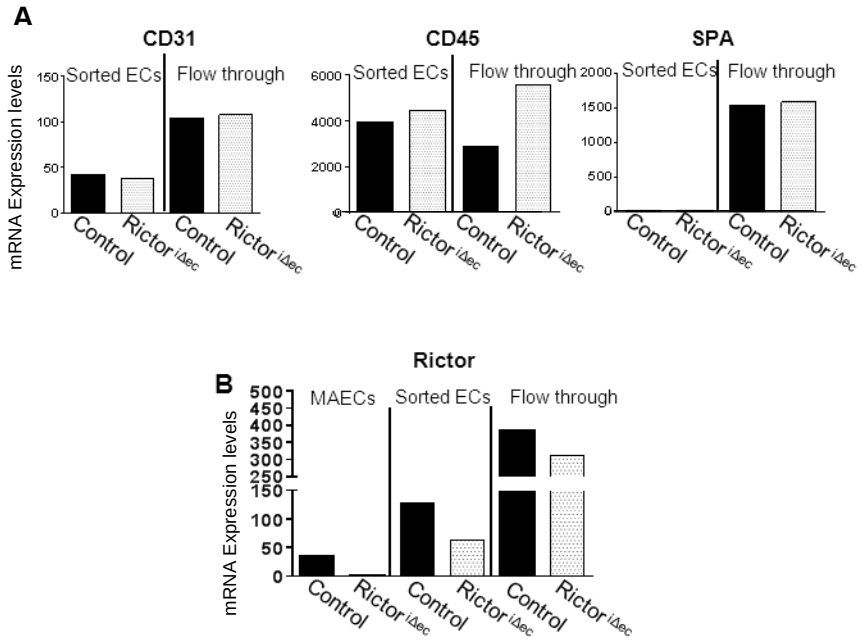

Figure 4 Quantification of Rictor mRNA of directly MACS-sorted murine lung endothelial cells. Lungs from three mice per group were pooled together. Every sample represents three mice. (**A**) mRNA levels of endothelial CD31 was equal in two animal groups. mRNA of Ve-Cadherin was not present. High rate of CD45 positive cells was observed. Lung epithelial cells were removed during the isolation process since SPA mRNA was absent the sorted ECs sample but highly present in the flow-through. (**B**) Rictor$^{i\Delta ec}$ mice show reduced mRNA levels, but Rictor mRNA levels from the aortic endothelium of the same animals **(Figure 3**) show no *Rictor* knockout induction (**n=3).**

The positively CD31^{+}/CD105^{+}/IB4^{+} selected cells present no mRNA of Ve-Cadherin and the amount of CD31 mRNA was equal in both control and Rictor$^{i\Delta ec}$ mice. On the other hand there is a very high presence of CD45^{+} blood cells. The efficiency of the magnetic separation was adequate in order to discard the lung epithelium from the sorted cells since SPA mRNA was not detected (**Figure 4A**). The levels of Rictor mRNA in the CD31^{+}/CD105^{+}/IB4^{+} samples arriving from the 3 Rictor$^{i\Delta ec}$ mice were about 50% lower than in the samples arriving from the control mice. The negative selected cells also present similar levels of CD31 mRNA and the same trend of Rictor mRNA.

In combination with the results from the aortic endothelium scraping the data suggest that either the techniques used are not adequate to demonstrate the efficiency or *Rictor* knockout induction, or that the knockout *of Rictor* in the endothelium is not induced (**Figure 3/Figure 4**).

3. A.3. Isolation of pure endothelial cell populations from aorta and lungs: optimization and gene expression analysis.

As the above data could not proof the induction of *Rictor* knockout in the aortic endothelium, we invested on other techniques for isolation of enriched and pure endothelial cell populations for gene expression analysis to monitor *Rictor* knockout efficiency. Optimization of aortic endothelial cells isolation was attempted with enzymatic digestion of the aortic wall. Isolation of lung endothelial cells was approached simultaneously with two different techniques: MACS sorting and culturing the isolated cells and FACS sorting. The first part of the following results describes the isolation of aortic endothelial cells with enzymatic digestion of the aortic wall. The second part presents the MACS isolation and optimization and FACS sorting of lung endothelial cells.

3. A.3.1. Rictor mRNA quantification and cell marker profiling of enzymatically digested aortic lining

Techniques of enzymatic digestion of the aortic endothelium to isolate pure populations of aortic endothelial cells were used. Digestion of the endothelium was attempted with Trypsin, Collagenase and Liberase.

3. A. 3.1.1. Enzymatic digestion by trypsin

The aortas of two control and one Rictor$^{i\Delta ec}$ mice were removed from the thorax and cannulated *ex vivo* from one side and clamped from the other. Trypsin 0,25%+EDTA was flushed through the cannula in the aorta and the enzyme was allowed to detach endothelial cells from the aortic wall for 7 minutes. The cells were flushed in a tube with endothelial specific medium and were subjected to total RNA isolation. The denudated

piece of aorta was kept and RNA was isolated from them as a negative control of the isolated endothelium.

As shown in Figure 5A there is no Ve-Cadherin mRNA and the levels of CD31 mRNA were very variable from high in the isolated aortic cell suspension to undetectable. The mRNA levels of CD45 follow a similar trend with CD31 mRNA (**Figure 5A**).

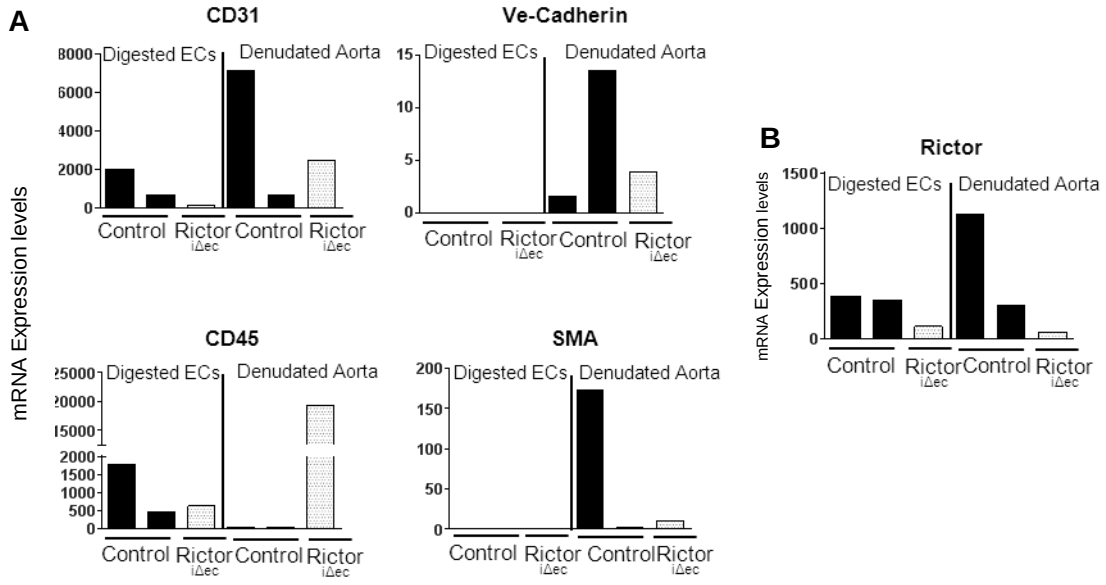

Figure 5: mRNA levels of endothelial, hematologic, and smooth muscle markers and Rictor in trypsin digested aortic endothelium lining. (**A)** mRNA levels of CD31 and Ve-Cadherin serve as endothelial cell marker while CD45 and SMA are indicators of the presence of blood cells and smooth muscle cells from the aorta respectively**.** Pieces of denudated aortas were used for negative controls of endothelial cells and positive controls for smooth muscle cells. (**B**) Rictor mRNA levels are lower in the digested endothelial lining but the denudated aorta also present very low levels o*f Rictor* expression (**Control n=2, Rictor$^{i\Delta ec}$ n=1**).

The reduced levels of Rictor mRNA of the Rictor$^{i\Delta ec}$ animal cannot be representative of the efficiency of the induction of the knockout due to the questionable amount of endothelial cells that were isolated on one hand. On the other hand the denudated aorta of the Rictor$^{i\Delta ec}$ animal presents equally low levels of Rictor mRNA (**Figure 5B**). The denudated aorta of Rictor$^{i\Delta ec}$ mice consists of cells that express normally *Rictor*, so it is not expected to present so low levels of Rictor mRNA.

3. A. 3.1.2. Enzymatic digestion by Collagenase and Liberase

A variation of the enzymatic digestion of the aortic endothelium with trypsin was followed using enzymes with higher enzymatic activity. Collagenase 1% and Liberase 1% (172) were used to detach the endothelial cells from the aortic wall. The same protocol as for the trypsin digestion was followed and cells were collected for total RNA isolation.

Collagenase digestion resulted in similar findings with trypsin (**Figures 5/6**). CD31, CD 45 and Rictor mRNA follow the same expression trend in the Rictor$^{i\Delta ec}$ mice, showing higher levels of expression than digested aortic tissue of control animals. VE-Cadherin and SMA mRNA were completely absent (**Figure 6A**). The Rictor mRNA levels were vice versa from the expected results with, control animals presenting lower lever of *Rictor* expression than the Rictor$^{i\Delta ec}$ mice.

Liberase enzymatic digestion detached endothelial cells from the aorta that were positive for Ve-cadherin and CD31 mRNA. However there were smooth muscle cells and some CD45 positive blood cells in the digested aortic cell suspension. Thus Liberase also removed part of smooth muscle cells.

Both techniques show weakness in isolating aortic endothelial cells and more optimization would be necessary to stabilize the yield of isolated endothelial cells. Thus, we aimed for another technique to define us if knockout of *Rictor* occurred or not.

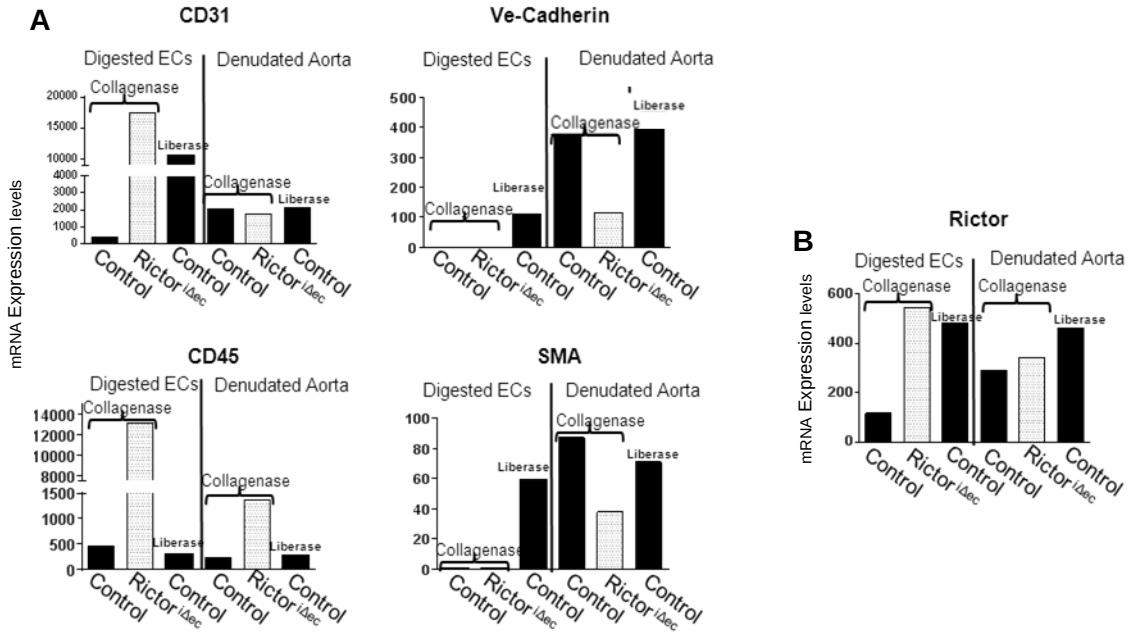

Figure 6: mRNA levels of endothelial, hematologic and smooth muscle markers in enzymatically treated aortic endothelial lining. **(A)** mRNA levels of the endothelial markers CD31 and Ve-Cadherin show variable amount of endothelial cells from the Collagenase aortic wall. There are also variable but high amounts of CD45 mRNA. Liberace treatment detached more endothelial cells but also hematological cells and smooth muscle cells were present in the sample. (**B**) mRNA levels of *Rictor* show no induction of knockout in Rictor $^{i\Delta ec}$ animals (Control n=2, Rictor$^{i\Delta ec}$ n=1).

3. A.3.2. MACS endothelial cell isolation: Enrichment and purification of lung endothelial cell population and gene expression analysis.

The MACS isolation of lung endothelial cells is an adequate technique to remove the lung epithelial cells, but it was evident that it could not separate CD45 positive blood cells from the endothelial population (**Figure 4**). MACS sorted cells were plated and the non-adherent cells were washed away the following day. The attached endothelial cells were cultured until the desirable amount. The following day microscopic observation of the petri dish showed that 10-30 cells were attached. The cells were cultured with growth factor enriched endothelial specific media under moderate hypoxia (5% O_2). During 7 days of culturing, the cells proliferated, exhibited an endothelial phenotype with typical philopodia, and formed monolayers with endothelial cobblestone morphology at confluence. When a 3

cm dish was about 60% confluent with endothelial cells, total RNA was extracted and the purity of the growing endothelial cells was assessed with real time PCR. The expression levels of the endothelial markers were compared with directly sorted cells and their flow through (**Figure 7**).

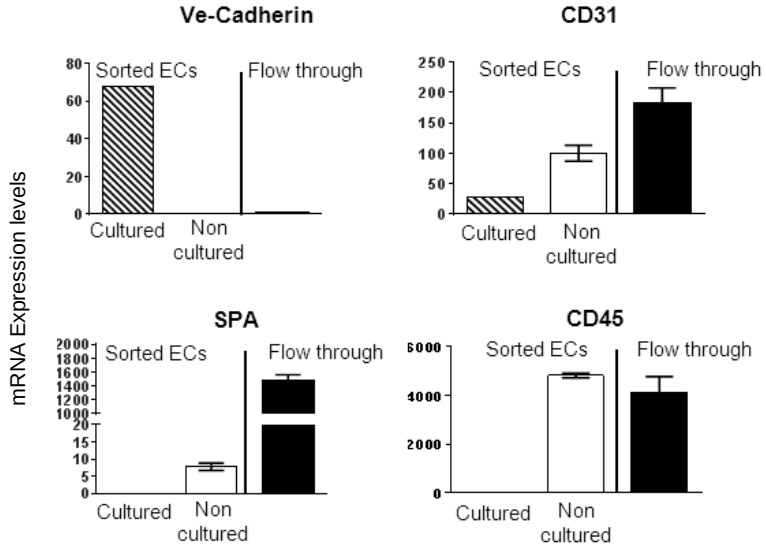

Figure 7: Enrichment of the endothelial cell population by plating CD31/CD105/IB4 positive selected cells with MACS sorting. Each sample represents cells from one animal. mRNA levels of endothelial markers show reversed expression profile in cultured CD31/CD105/IB4 positive selected cells after MACS sorting in relation to MACS sorted/non cultured CD31/CD105/IB4 positive population. Blood cells and lung epithelial cells are cleared from the MACS positive selected cells. The cultured population represents endothelial cells as seen also microscopically.

The $CD31^+/CD105^+/IB4^+$ sorted cells after culturing showed Ve-Cadherin and CD31 expression. These data are similar with expression levels of established cultured MAECs that are isolated and used in our laboratory (**Figure 3**). Directly sorted $CD31^+/CD105^+/IB4^+$ cells and sorted/plated $CD31^+/CD105^+/IB4^+$ cells show a reverse pattern of Ve-Cadherin and CD31 mRNA expression. The phenotype of these cultured cells under the microscope and the levels of mRNA of all the examined markers suggest that are pure endothelial cells in abundance.

3. A.3.2.1. Rictor mRNA quantification and cell marker profiling of MACS-sorted murine lung endothelial cells after *in vitro* culture

Lungs were removed from 2 control and 2 Rictor$^{i\Delta ec}$ mice. Lungs were enzymatically digested and the MACS sorted CD31^{+}/CD105^{+}/IB4^{+} fraction was plated separately for each individual mouse. Cells presented typical endothelial philopodia and created cobblestone monolayers. After 7 days of culturing total RNA was isolated.

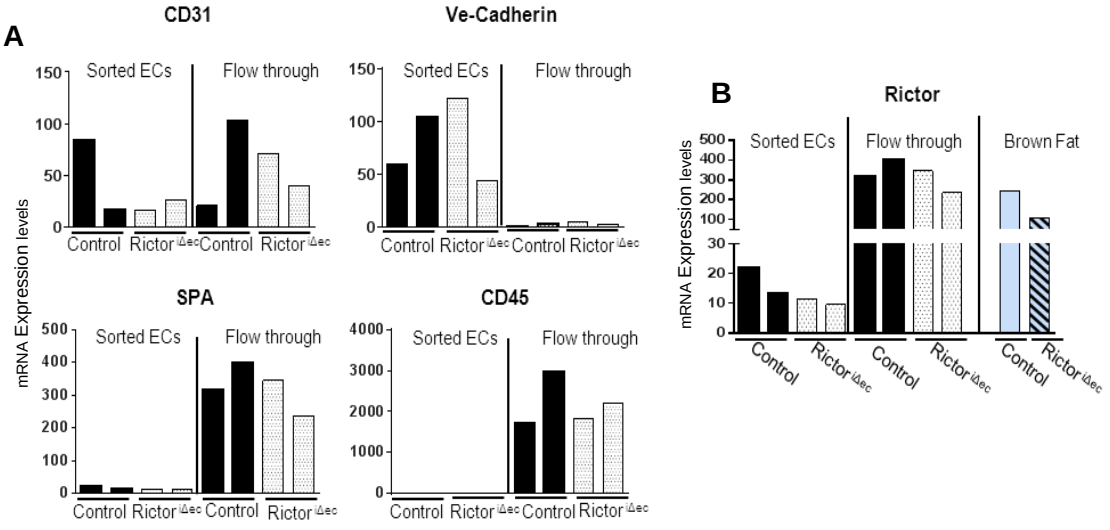

Figure 8: Enrichment and purification of MACS sorted endothelial cells and quantification of Rictor mRNA levels. Each sample represents one animal. **(A)** *In vitro* culture of MACS sorted CD31/CD105/IB4 positive cells resulted into a pure CD31 and Ve-Cadherin positive endothelial cell population. Hematological cells (CD45) and lung epithelial cells (SPA) are absent in the sorted endothelial cells. **(B)** mRNA levels of Rictor in MACS sorted, cultured endothelial cells show no induction of *Rictor* knockout in lung endothelial cells. Constitutive *Rictor* knockout adipocytes were used as an internal control. *Rictor* knockout adipocytes have an established reduction in Rictor mRNA of 50-60%.

Even though the population of endothelial cells was adequately pure there were no significant differences in Rictor mRNA levels between control and Rictor$^{i\Delta ec}$ mice (**Figure 8**). Control and *Rictor* knockout samples from an established constitutive adipose specific *Rictor* knockout mouse were used as internal control for the experiment (179). The result of this experiment showed that Cre-ER^{T2} recombinase did not excise the exons 4 and 5 of

Rictor in Rictor$^{i\Delta ec}$ mice and that the gene is actively transcribed as in the control animal group.

3. A.3.3. FACS sorting of lung microvascular endothelial cell

While the process for optimizing the isolation of the $CD31^+/CD105^+/IB4^+$ endothelial cells with MACS sorting, an effort to acquire pure endothelial cell populations from lungs was attempted also with FACS sorting. Due to the importance of these experiments, which would indicate the current situation of the efficiency of *Rictor* knockout induction *in vivo*, the optimization of the MACS and FACS sorting was conducted simultaneously and the results from both techniques arrived within the same week.

FACS sorting of endothelial lung cells was designed to target endothelial cells which are $CD31^+/CD45^-$. This combination was designed in order to exclude blood cells that express CD31. The initial step in the sorting was to distinguish dead and live cells (Gate P1) and exclude the debris of the sample (Gate P2). Single cells were distinguished from multicellular clusters (Gate P3). $CD31^+/CD45^-$ positive endothelial cells were selected (Gate P4) against the red blood cells (Gate P5) and $CD45^+/CD31^-$ hematological cells (Gate P6) (**Figure 9**).

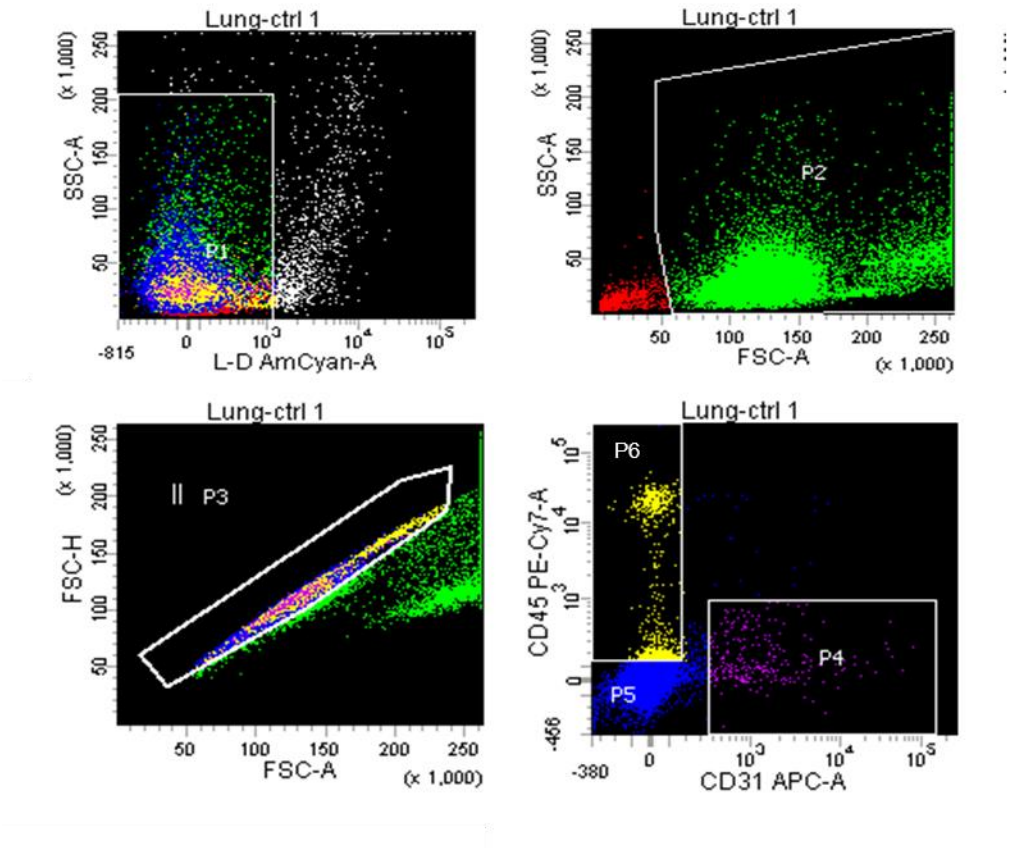

Figure 9: Isolation of lung endothelial cell with FACS sorting. Representative FACS sorting analysis of one control mouse. Gate **P1** represents all the live cells after lung collagenase digestion and FACS antibody staining protocol**.** The aqua L-D negative cells are selected for further analysis and sorting. Gate **P2** distinguishes between the cells and the debris that in the cell suspension. Gate **P3** selects all the live single cells. All the duplets or bigger cell clusters are negative selected. Gate **P4** represent the $CD31^{+}/CD45^{-}$ endothelial cells. Gate **P5** represents the erythrocytes and gate **P6** contained $C31^{-}/CD45^{+}$ blood cells.

A pure $CD31^{+}/CD45^{-}$ population that corresponds to endothelial cells and which was about 2% of the total lung cells population was isolated. Cells were flushed directly to RLT buffer for total RNA isolation, transcription and Real-time PCR.

3. A.3.1. Rictor mRNA quantification and cell marker profiling of directly FACS-sorted murine lung endothelial cells

Two control and two $Rictor^{i\Delta ec}$ mice were used for FACS sorting of lung endothelial cells. As observed previously with the MACS endothelial cell sorting of directly isolated endothelial cells, they present very low or even undetectable Ve-Cadherin mRNA while

CD31 mRNA is present. Purity of the population was confirmed by the absence of CD45 and SPA mRNAs in the samples (**Figure 10**).

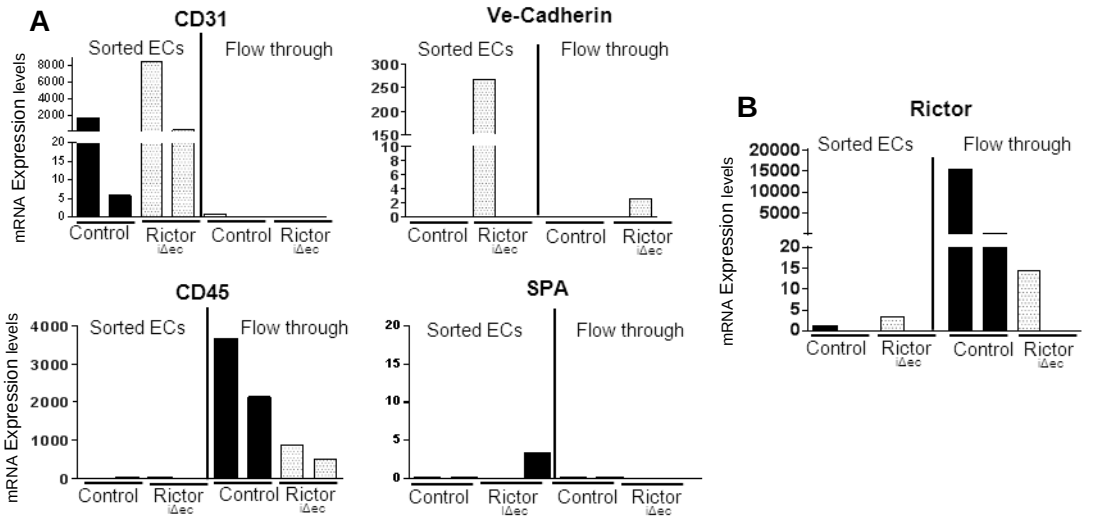

Figure 10. mRNA quantification of FACS sorted endothelial cells for endothelial specific markers, lung and blood cells and Rictor. Each sample represents one animal. **(A)** mRNA levels of CD31 and CD45 indicated the good technical quality of the FACS sorting CD31 $^{+}$/CD45^{-} endothelial cells. There are variable levels of CD31 mRNA in the sorted endothelial population and Ve-Cadherin is mostly low expressed as observed in MACS directly sorted cells**.** Blood cells and lung epithelial cells are negatively selected. **(B)** Rictor mRNA levels do not indicate that the induction of *Rictor* knockout took place in the endothelium of Rictor$^{i\Delta ec}$ animals.

The result of MACS sorted/cultured endothelial cells was confirmed. No evident and significant differences were detected on Rictor mRNA between the two animal groups (**Figure 10**).

In summary, all the isolation techniques employed and the gene analysis of the isolated cells point to the conclusion that exons 4 and 5 of *Rictor* are not excised anymore and the gene encoding *Rictor* is transcribed normally.

3. A.4. Cre-ER^{T2} expression levels in MACS and FACS-sorted lung endothelial cells

The excision of exons 4 and 5 of *Rictor* is mediated by Cre-ER^{T2} recombinase, which is expressed in the endothelial cells. The above experiments showed that the Cre-ER^{T2} –mediated *Rictor* excision is not occurring. Thus, we investigated the expression pattern of Cre-ER^{T2} in the MACS-sorted isolated endothelial cells. Cre-ER^{T2} recombinase is under the transcriptional control of an inserted VE-Cadherin promoter. The endogenous Ve-Cadherin promoter is shown to normally transcribe Ve-Cadherin in these cells (**Figure 8**). The levels of Cre-ER^{T2} mRNA were assessed in cultured MACS-isolated endothelial cells.

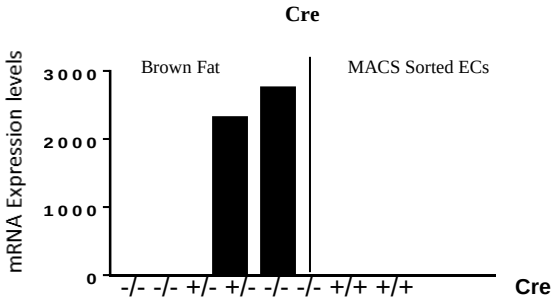

Figure 11. Quantification of Cre recombinase mRNA in cultured,-MACS sorted endothelial cells. The endothelial cells were sorted from mice positive-homozygous for Cre. These cells show no expression of Cre-ER^{T2} recombinase. Brown fat from a constitutively Cre expressing mouse was used as a control. Adipose specific *Rictor* knockout, heterozygous mice for Cre display very high amounts of Cre mRNA while the control mice for brown fat *Rictor* knockout mice exhibit no Cre expression.

As shown in Figure 11 the MACS sorted endothelial cells do not transcribe *Cre-ER^{T2}*. Cre-ER^{T2} mRNA was also absent from FACS directly sorted endothelial cells. Brown fat from constitutive adipose *Rictor* knockout mice was used as a control to for positive *Cre* expression (179). These data suggest that the inserted Ve-Cadherin promoter is not driving expression of the Cre transgene (**Figure 7**).

3. B. Role of endothelial mTORC2 in angiogenesis *in vivo*

The assessment of the role of endothelial mTORC2 in angiogenesis *in vivo* was conducted in endothelial specific and inducible *Rictor* knockout mice. The efficiency of *Rictor* knockout induction, as described in figure 1 (February 2011) and the immunohistological staining of Cre-ER^{T2} in the tissue from these mice (**Figure 28, data shown below**) suggest that the animals included in the present study were knockout for *Rictor* and expressing Cre-ER^{T2} recombinase in the endothelium. The following experiments presented in this thesis were conducted with the functioning transgene animals and the significant differences that were observed between control and Rictor$^{i\Delta ec}$ animals enforce this statement.

3. B.1. Deletion of *Rictor* in the endothelium does not affect weight gain and hematological profile of Rictor$^{i\Delta ec}$ animals

After demonstrating the induction of *Rictor* knockout in the endothelium in February 2011 (**Figure 1**) the first study we followed was a weight gain and health status of male and female mice up to an age of 28 weeks. No significant differences in body weight or lethality were observed between control and Rictor$^{i\Delta ec}$ mice in both genders after monitoring for six months (n=10) (**Figure 12**). As VE-Cadherin-promoted Cre-recombination may also affect hematopoietic development (182) we assessed hematological profiles in 8 weeks old control and Rictor$^{i\Delta ec}$ mice and found similar physiological values in both groups that were in the range of healthy C57/Bl6 mice (**Figure 13**)

These experiments indicate that ablation of endothelial *Rictor* does not cause obvious general health problems as supported by normal weight gain, viability and hematological profiles.

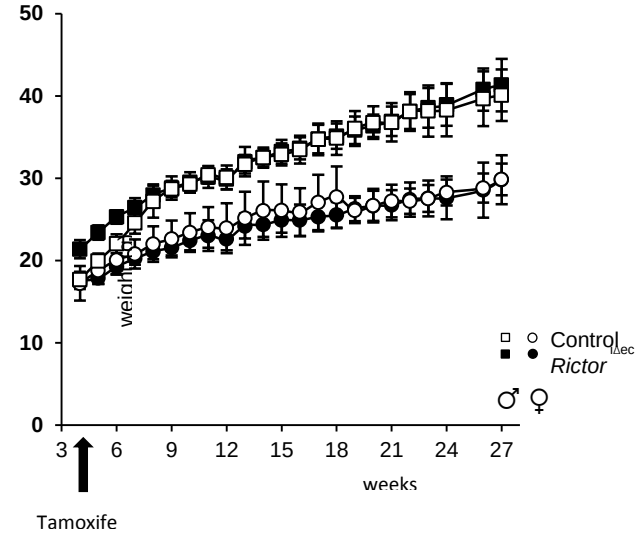

Figure 12: Rictor^{iΔec} induction does not affect weight gain. Cre-ER$^{T2+/+}$ mice were injected with Tamoxifen and corn oil respectively. Weight gain was normal for male and female for both control and Tamoxifen injected mice after 27 weeks of monitoring (**n=10**).

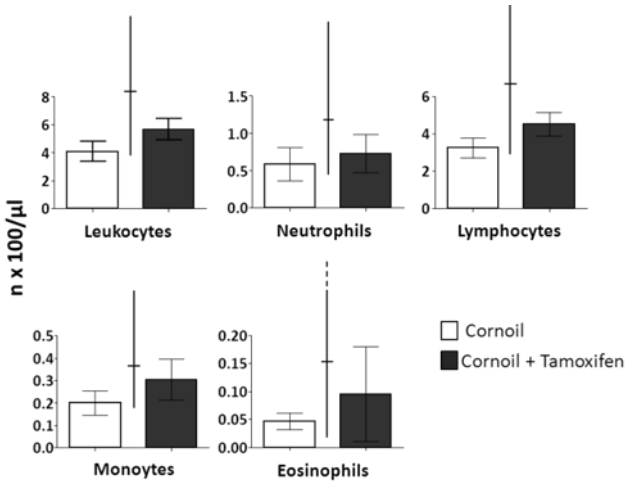

Figure 13: Endothelial *Rictor* knockout does not affect hematological profile. Hematological profile (Count of leukocytes, neutrophils, lymphocytes, monocytes and eosinophils) was assessed on 10-week-old corn oil and Tamoxifen injected male Cre$^{+/+}$/Rictor$^{lox/lox}$ mice. Line between bars indicates normal range of parameters for C57/Bl6 mice (**Control n=3/Rictor^{iΔec} n=7)**.

3. B.2. Assessment of the role of endothelial mTORC2 in angiogenesis with intravital microscopy

One of the main goals of this project was the assessment of the potential microscopic alterations of capillary morphology in the skin muscle vasculature in the absence of endothelial *Rictor* and observation of the angiogenic capacity of Rictor$^{i\Delta ec}$ mice during VEGF and FGF2 stimulation of the skin vasculature. To do so, a dorsal skinfold chamber was surgically mounted into 8-week-old control and Rictor$^{i\Delta ec}$ mice and the existing vascular bed was observed by intravital fluorescent microscopy.

3. B.2.1. Induction of *Rictor* knockout in the endothelium does not affect the homeostasis of developed vasculatures

The skin muscle vasculature was observed three days after the implantation of the skinfold chamber (observation day 0, baseline). The capillary bed showed no apparent differences in control and Rictor$^{i\Delta ec}$ mice (**Figure 14A**). In both experimental groups the wound bed consisting of the panniculus carnosus with its capillary structures organized in typical parallel orientation and the subcutaneous layer with draining arterioles and venules exhibited the typical perfusion pattern as observed in previous studies of the dorsal skinfold chamber (174). Quantification of vascular parameters such as capillary number, capillary diameter, and number of branching points confirmed the similarity of the vasculature of the two animal groups (**Figure 14B**).

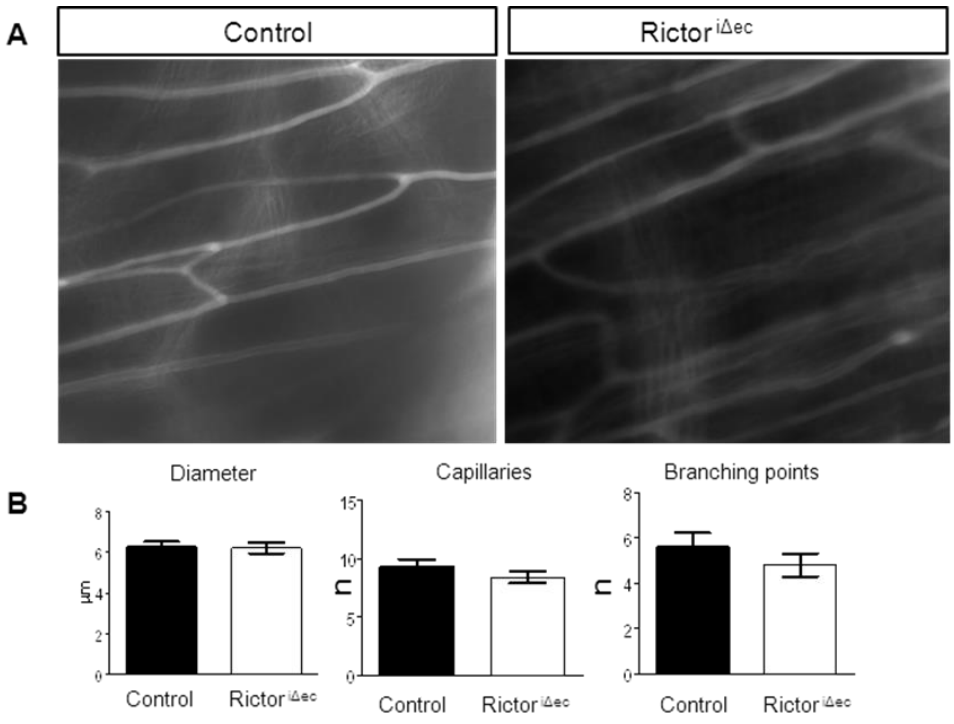

Figure 14: Endothelial *Rictor* knockout does not affect already developed skin muscle vasculature:
Stacked frames of representative videos of the capillary vasculature recorded through the dorsal skinfold chamber by intravital fluorescence microscopy. (**A**) The baseline vasculature for both animal groups is identical 3 days after the implantation of the dorsal skinfold chamber. (**B**) Quantification of vascular density (Capillary and branching point number) and capillary diameter show that the baseline vasculature of control and Rictor$^{i\Delta ec}$ are identical.

3. B.2.2. Endothelial *Rictor* knockout does not affect the response of the skin muscle vasculature in dorsal skinfold chamber implantation

The dorsal skin fold chamber was modified by additionally removing cutis and subcutis on the opposite side of the observation window. This defect was sealed by growth factor-reduced Matrigel. The response of the vasculature into the dorsal skinfold chamber implantation and the presence of Matrigel on the skin defect was assessed on a daily basis by intravital fluorescent microscopy up to 7 days after Matrigel sealing. Both animal groups exhibited similar baseline vasculature architecture. Three days later, both animal groups showed similar response to the chamber implantation by increasing the capillary diameter. In the bigger arterioles and venules local vessel wall enlargements were observed (**Figure**

15A). After seven days of observation both Rictor$^{i\Delta ec}$ and control animals showed similar patterns of vascular remodeling in the skin muscle wound bed.

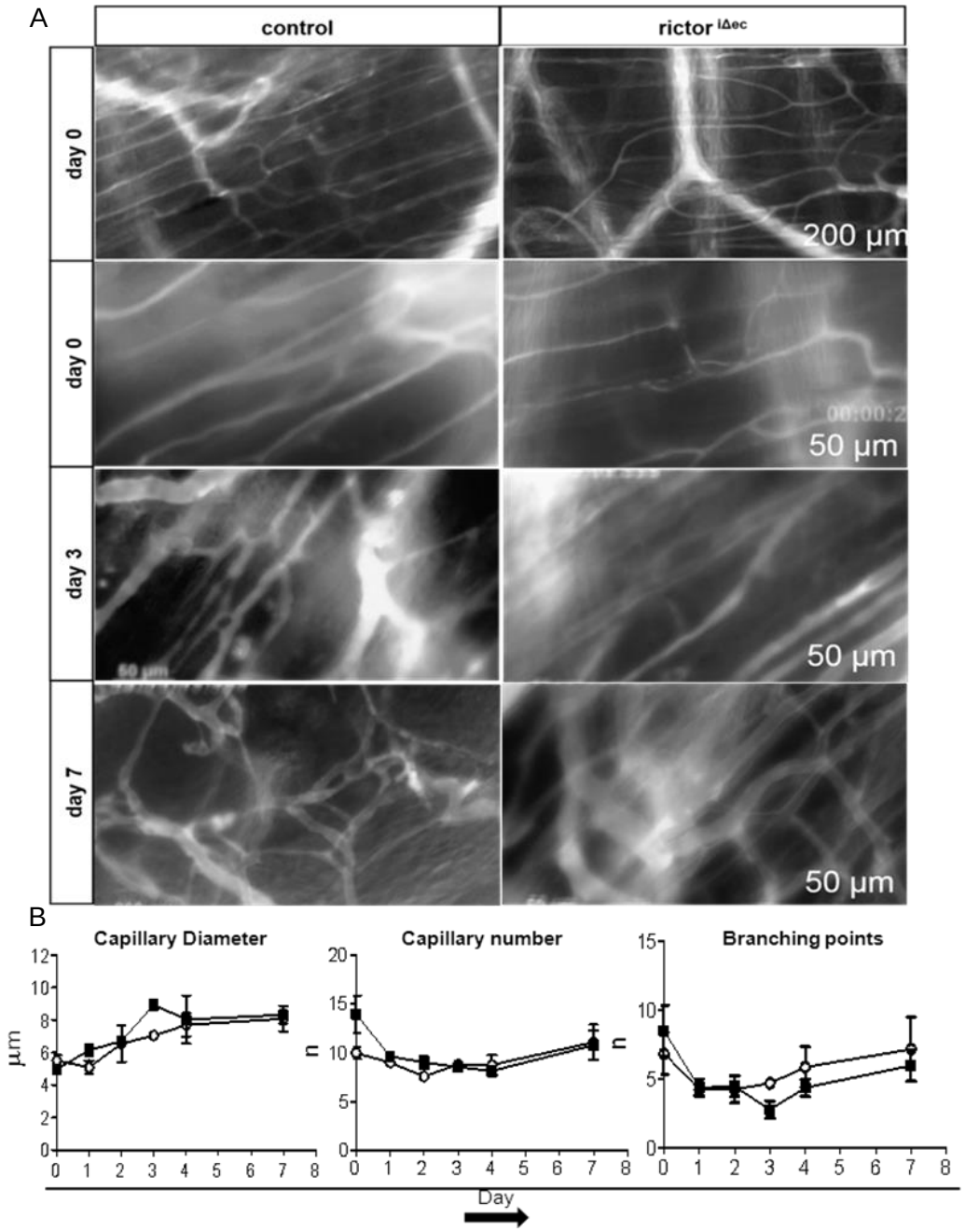

Figure 15: Control and Rictor$^{i\Delta ec}$ mice respond similarly to the dorsal skinfold chamber implantation:
Stacked frames of representative videos of the capillary vasculature recorded through the dorsal skinfold chamber by intravital fluorescence microscopy are shown. **(A)** Skin muscle capillary structure from day 0 (baseline, 10x and 20X magnification), day 3 (after wound sealing with heparin-loaded Matrigel, 20x magnification) and day 7 (20x magnification) in control (left micrographs) and Rictor$^{i\Delta ec}$ mice (right micrographs). **(B)** Quantification (lower graphs) of capillary diameter demonstrates increase in capillary diameters with no significant differences in both animal groups. Similarly, no significant changes are detected in capillary number and number of branching point between control and Rictor$^{i\Delta ec}$ mice (**Control n=4/Rictor$^{i\Delta ec}$ n=4**)

The quantification of vascular parameters (**Figure 15B**) demonstrated an increase in capillary diameters, but not an increase in microvessel densities (segments between branching points) or branching points (n=4). Of note, the changes in capillary diameters were mainly due to remodeling of larger sized capillaries that were connected with draining arterioles and venules. Importantly, dermal microvasculature responded similarly to the wound, the chamber implantation, and Matrigel sealing in control and Rictor$^{i\Delta ec}$ mice. During the seven day period of monitoring vascular changes we observed an inflammatory response likely caused by the presence of an open wound on the skin. In some animal the inflammatory response was obvious macroscopically by the presence of edema and fluid in the area of the chamber and in some cases there was accumulation of mucous material in the wound. However, the similar responses of vascular beds in control and Rictor$^{i\Delta ec}$ mice in the dorsal skinfold implantation provided an appropriate baseline for further studies.

3. B.2.3. Assessment of the role of endothelial mTORC2 in VEGF induced angiogenesis

VEGF is considered one the key growth factors implicated in sprouting angiogenesis. It exerts its functions on endothelial cells, stimulating endothelial cell fate determination pathways and sprout formation (17). The investigation of the role of VEGF in relation to endothelial mTORC2 in angiogenesis was conducted with intravital microscopy of modified dorsal skinfold chamber for VEGF delivery through Matrigel. The skin muscle vasculature was stimulated with a high dose of VEGF (1.5μg/ml) and the vasculature was observed for 7 consequent days. The results of the intravital microscopy are shown in **Figure 16A**.

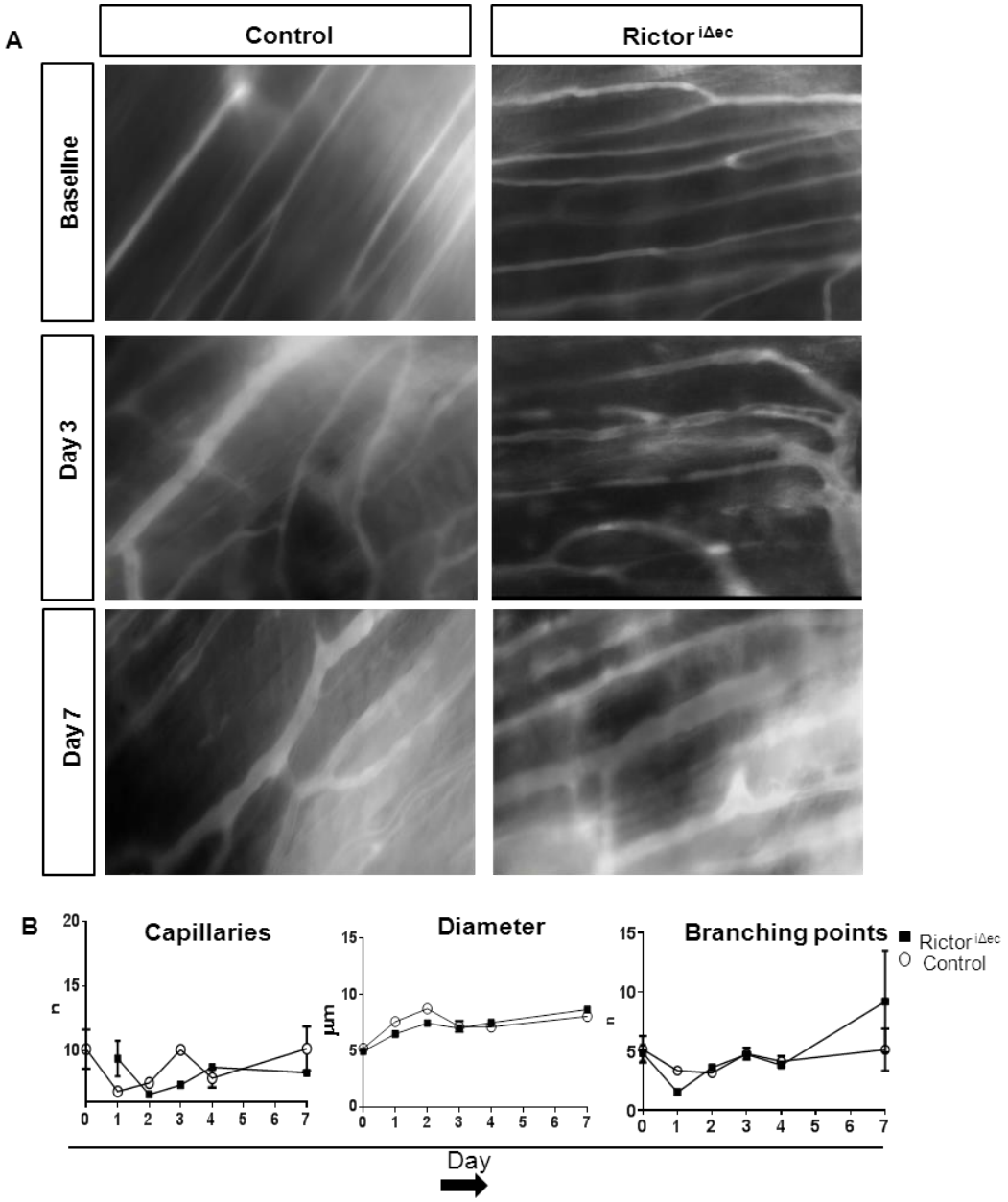

Figure 16: Control and Rictor $^{i\Delta ec}$ mice response upon high dose of VEGF stimulation.
Stacked frames of representative videos of the capillary vasculature recorded through the dorsal skinfold chamber by intravital fluorescence microscopy are shown. **(A)** Skin muscle capillary structure from day 0 (baseline, 20x magnification), day 3 (after wound sealing with heparin-VEGF loaded Matrigel, 20x magnification) and day 7 (20x magnification) in control and Rictor $^{i\Delta ec}$ mice. **(B)** Quantification of capillary diameter demonstrates increase in capillary diameters with no significant differences in both groups. Similarly, no significant changes are detected in capillary number and number of branching points between control and Rictor $^{i\Delta ec}$ mice (**n=3**).

Both control and Rictor$^{i\Delta ec}$ animals presented almost identical baseline vasculature as that already observed in the previous intravital microscopy experiments. 3 days after high dose VEGF stimulation both animal groups present almost equally dilated capillaries and retained their parallel orientation. No significant differences were observed even after 7 days of continuous VEGF stimulation, with both animal groups presenting dilated capillaries and some extent of vascular remodeling. The appearance of the VEGF stimulated vasculature was similar to vasculature that was examined for the effect of the chamber implantation itself (**Figure 15**). Quantification of the microvascular density and capillary diameter confirmed the microscopic observations, i.e. no significant differences between the two animal groups and similar behavior as an un-stimulated vasculature (**Figure 16B**).

3. B.2.3.1. Matrigel-mediated VEGF delivery: The role of heparin

Due to the therapeutic importance VEGF its delivery in *in vivo* systems has been intensively studied. This growth factor in its free form has a half-life of 90 minutes (11) and it needs heparin and a scaffold mimicking the extracellular matrix to exert it biological function (10). Heparin is a glycosaminoglycan that naturally binds to growth factors like VEGF and FGF, stabilizing them, increasing their half-life and their bioavailability in *in vivo* delivery systems. FGF2 is known to be used in a mixture with heparin and scaffold material like Matrigel and hydrogels (75). The intravital microscopy of VEGF challenged vasculature showed no difference between the two animal groups. In order to exclude insufficient delivery of VEGF into the vasculature, we increased the amount of heparin into the VEGF-Matrigel mixture to optimize the half-life and the bioavailability of VEGF.

A dose response experiment was set up with 10 fold higher heparin concentration than the initially used in the VEGF-Matrigel mixture. The skin muscle vasculature was stimulated with these mixtures and intravital microscopy was conducted. The skin muscle

vasculature of both control and Rictor$^{i\Delta ec}$ mice exhibited similar behavior when stimulated with VEGF+10X heparin. Both animal groups resulted after 7 days of stimulation with dilated capillaries without losing their parallel orientation and the vasculature retained its initial architecture and basic structure (**Figure 17**).

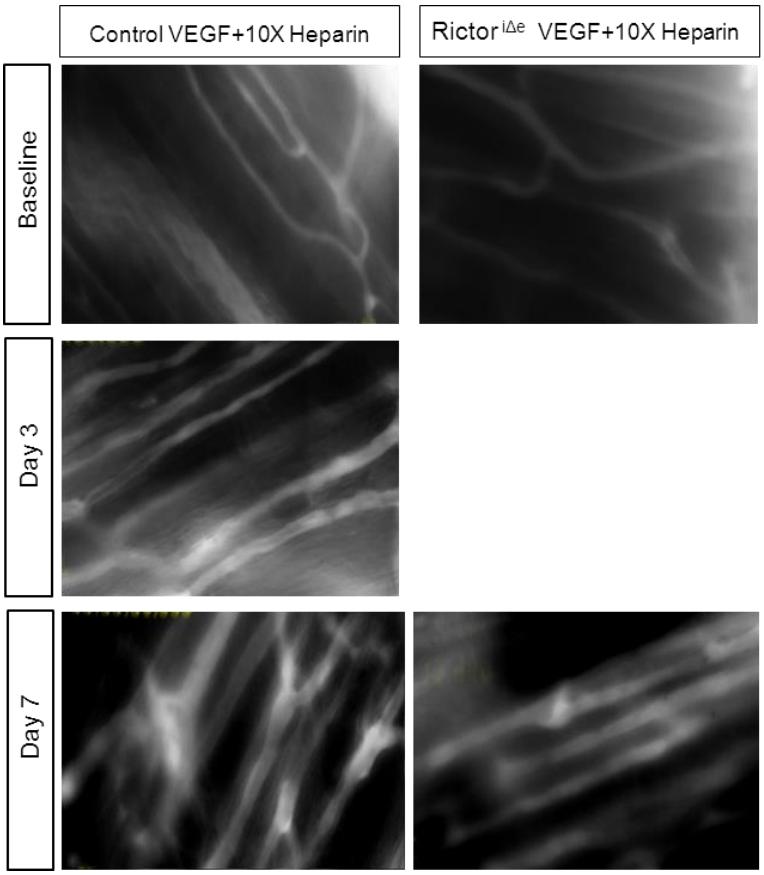

Figure 17: High doses of heparin do not influence the stimulatory effect of VEGF.
Stacked frames of representative videos of the capillary vasculature recorded through the dorsal skinfold chamber by intravital fluorescence microscopy are shown. Control and Rictor$^{i\Delta ec}$ mice respond similarly in low and high doses of heparin (low: Fig.15). The high amount of heparin does not change the effect of VEGF. Rictor$^{i\Delta ec}$ on day 3 visibility was not appropriate to produce a stacked image (video available).

There are data supporting the fact that heparin has a vasodilating effect on blood vessels (183). In the experiments for VEGF delivery in the skin muscle vasculature through Matrigel seal, high doses of heparin were used and significant capillary diameter increase

was observed. To exclude the effect of heparin in the diameter increase that was observed, the skin muscle vasculature of both animal groups was stimulated with 10 fold higher heparin concentration through Matrigel seal. After 7 days of high dose of heparin stimulation the capillaries of the skin muscle vasculature presented increased capillary diameter in both animal groups and in comparable levels to when stimulated with VEGF+10X heparin (**Figure 18**). This experiment suggests that there is inefficient stimulation of VEGF through Matrigel in the dorsal skinfold chamber and the observed dilation is caused by high amount of heparin.

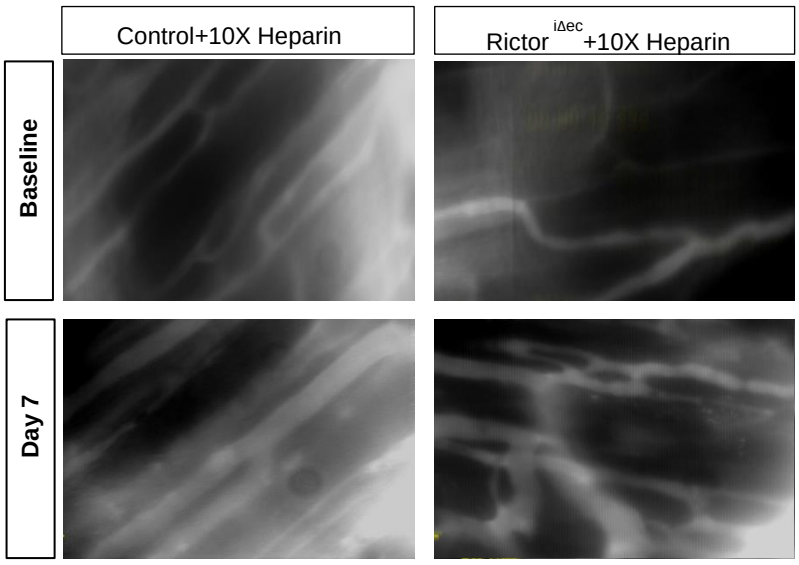

Figure 18: High dose of heparin acts as a vasodilator in the skin muscle vasculature. Intravital microscopy shows high doses of heparin increasing the capillary diameter in both animal groups.

3. B.2.3.2. Intramuscular injection of VEGF expressing myoblasts for VEGF delivery in the skin muscle

An alternative approach for VEGF delivery into the skin muscle vasculature was attempted by injecting modified murine VEGF expressing myoblasts. Primary myoblasts

isolated from C57BL/6 mice and transduced to express the β-galactosidase marker gene (*lacZ*) from a retroviral promoter (175) were further infected at high efficiency (176) with retroviruses carrying the cDNA for murine $VEGF_{164}$ (184). An intramuscular injection of VEGF expressing myoblasts was made on the dorsal skin after the skinfold chamber was implanted and vasculature was monitored with intravital microscopy. Only one control animal was used as a pilot experiment in order to assess if this approach is technically possible (**Figure 19**).

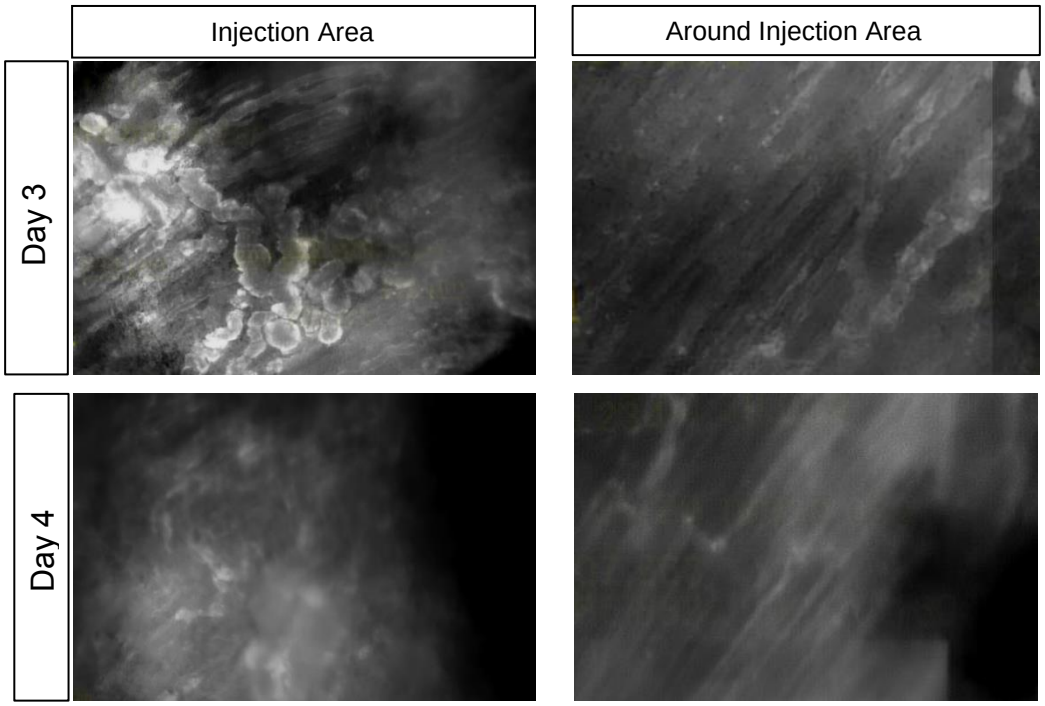

Figure 19. Injection of murine VEGF secreting myoblast induces exaggerated capillary diameter and severe inflammation. Pilot experiment of one control animal. Intravital microscopy of the intramuscular injection area and the surrounding area. Microscopy was possible until day 3. Extensive inflammation influences visibility after this time frame.

3 days post injection the myoblasts were visualized due to their red fluorescent color. The capillaries were visualized with FITC dextran, so there was no overlap between the signals. The myoblasts were not rejected at this time point by the immune system of the mouse. In the injection area an exaggerated angiogenic reaction was observed with extreme

capillary and vessel dilation with many and big protuberances in the capillary and vessel walls. The area around the injection was characterized by capillaries with increased diameter. However from day 4 and on microscopy of the area was not possible due to extensive edema and mucus **(Figure 19).**

The observations on day 3 suggest that myoblast can deliver VEGF and that the secreted growth factor stimulates angiogenesis. However the inflammation due to the presence of the myoblast and the trauma from the intramuscular injection is considerable and substantial. Furthermore visibility during microscopy was restricted after day 3. Indeed, myoblasts are derived from a BL6N sub-strain which may have a different immunogenic background than our mice with a BL6J background. Therefore, we did not further consider the application of this type of VEGF delivery.

3. B.2.4. Matrigel-mediated FGF2 stimulation of the skin muscle vasculature: Rictor$^{i\Delta ec}$ animals present different remodeling patterns

FGF2 is a potent angiogenic factor with an established function in vascular development and angiogenesis. This growth factor affects multiple cell types related to angiogenesis and it exerts its angiogenic function in endothelial cells by regulating VEGF2 and VEGFR2 expression among others (80). Since FGF2 is acting up-stream from VEGF and it is known to orchestrate the angiogenic response (80) we then proceeded to assess the potential role of endothelial mTORC2 in vascular morphologic changes in response to FGF2.

The skin muscle vasculature was stimulated with a high dose of FGF2 (1.5 μg/ml) that was delivered as already described with Matrigel. Morphologic changes were monitored with intravital fluorescent microscopy. The effective pro-angiogenic concentration of FGF2 was determined in pilot experiments using Matrigel plugs injected s.c. at the ventral flank of the mice (Data not shown).

Intravital recordings through the dorsal skinfold chamber revealed a strong angiogenic response of the skin muscle vascular bed to FGF2 in control mice, evident on and from day 3 after stimulation (**Figure 20A**). Vessel diameters increased markedly in small parallel-oriented capillaries and also displayed diameter variability (local dilation and narrowing) within the same vessel segment. In contrast, these changes in FGF2-stimulated vasculature were more restricted in Rictor$^{i\Delta ec}$ mice (**Figure 20A**).

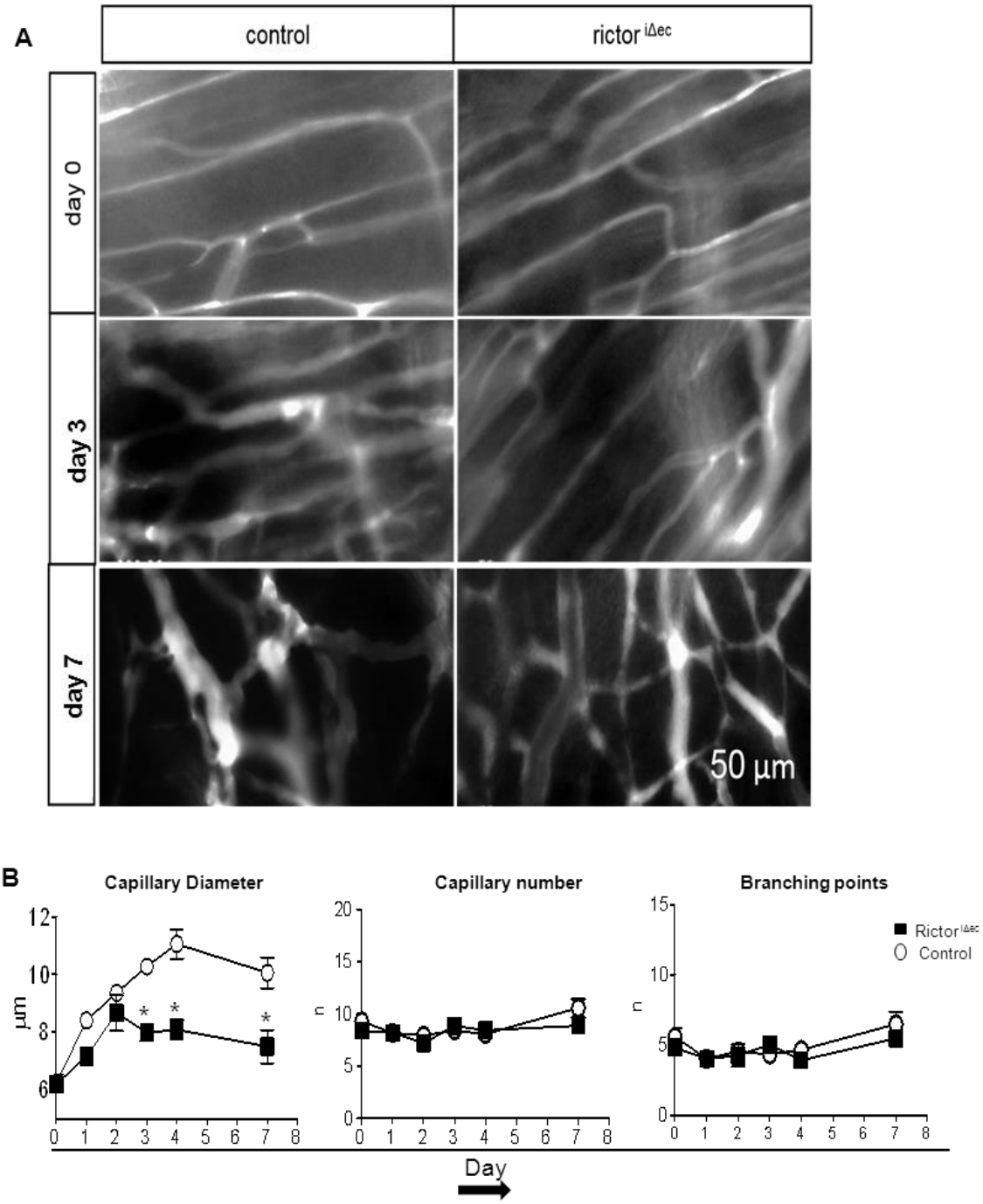

Figure 20: Rictor $^{i\Delta ec}$ impedes extensive capillary remodeling and limits the increase in capillary diameters in response to FGF2. Stacked frames of representative videos of the capillary vasculature recorded through the dorsal skinfold chamber by intravital fluorescence microscopy are shown. **(A)** Skin muscle capillary structure from day 0 (baseline, 20x magnification), day 3 (after wound sealing with FGF2/heparin-loaded Matrigel, 20x magnification), day 7 (20x) in control (left micrographs) and Rictor $^{i\Delta ec}$ mice (right micrographs). After 7 days of FGF2-stimulation, control mice exhibit an extensively remodeled vascular bed, with rather tortuous and heterogeneous capillary structure. In Rictor $^{i\Delta ec}$ mice, FGF2-induced remodeling is more subtle and retained parallel oriented vessels. (**B**) Quantification of capillary diameter demonstrates marked and significant limitation of capillary diameter increase from day 3 until end of observation period on day 7 in Rictor $^{i\Delta ec}$ compared to control mice. No differences were detected in capillary number and number of branching point between control and Rictor $^{i\Delta ec}$ mice (**Control n=8, Rictor $^{i\Delta ec}$ =9**).

From day 3 on, the vascular bed of control mice displayed extensive remodeling in response to FGF2, i.e., further enlargement of capillary diameters and development of tortuous and bulbous vascular structures that were observed also on levels above the capillary bed in draining arterioles and venules (**Figure 20A** day 7). In Rictor$^{i\Delta ec}$ mice the vascular bed showed a more restrained and different mode of remodeling. Capillary diameters stopped to increase after day 2 of FGF2-stimulation. Interestingly thin connecting anastomoses emerged between capillaries and draining arterioles in Rictor$^{i\Delta ec}$ mice. These interconnections formed a lumen as evidenced by the presence of FITC-dextran. However the anastomoses seemed not to be part of the circulation as no flow was observed (**Figure 20A,** day 7). Lower magnification (x10) micrographs display the different vascular remodeling patterns between control and Rictor$^{i\Delta ec}$ mice after 7 days of FGF2 stimulation (**Figure 21**).

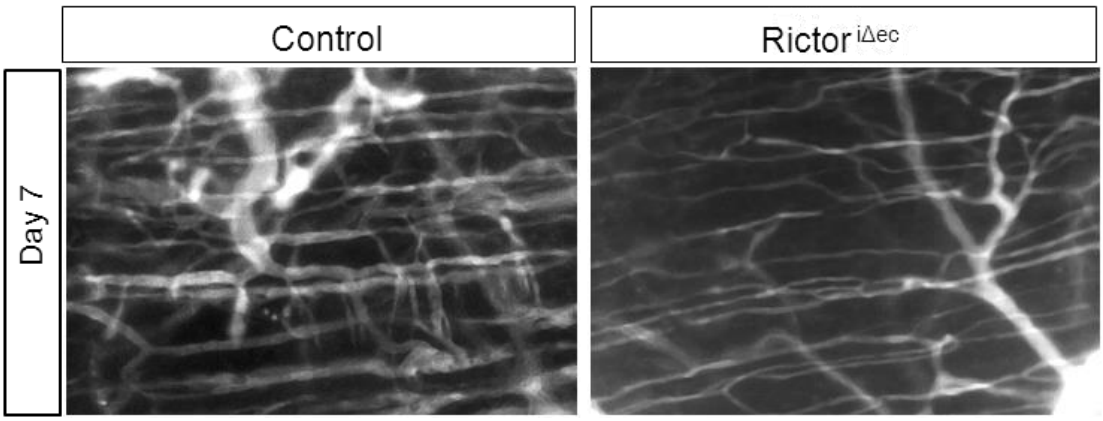

Figure 21: Overview of FGF2-stimulated capillary bed. Stacked frames of representative videos of the capillary vasculature recorded through the dorsal skinfold chamber by intravital fluorescence microscopy (10 x magnifications). Control animals exhibit a more heterogeneous and aberrant vasculature with dilated vessels and capillaries, while the Rictor$^{i\Delta ec}$ mice present a more physiologic appearance with most capillaries retaining their parallel orientation and small increases in capillary diameters

Vascular morphological parameters were quantified taking only perfused vessels into the account. Vessel diameters ranged from 4 to 16 μm, thus representing typical capillary microvasculature (**Figure 20B**). We observed that capillary numbers and branching points increased slightly in both experimental groups. Importantly, quantification displayed a steady increase of capillary diameters in control mice peaking on day 4, while capillary dilation in Rictor$^{i\Delta ec}$ mice reached its upper limit on day 2 of FGF2 stimulation. From day 3 until the end of the observation period on day 7, capillary diameters were significantly smaller (ca. 3 μm) in Rictor$^{i\Delta ec}$ mice compared to control mice (n=9; P>0.05).

3. B.2.4.1. Capillary diameter distribution analysis

Analysis of the distribution of capillary diameters showed that control animals react to FGF2 stimulation with a significant increase in the capillary diameter from day 4 until day 7 of stimulation compared to un-stimulated control mice on the corresponding days. Thus, vascular changes were FGF2-specific. Furthermore, when compared to un-stimulated controls, the FGF2 response generated a wide spread of capillary diameter sizes ranging from approximately 5 to 20 μm (**Figures 22/23).** Deletion of endothelial *Rictor* appeared to completely suppress FGF2-induced changes when compared to un-stimulated controls on day 4 and 7. Thus, FGF2-stimulated vasculature in Rictor$^{i\Delta ec}$ mice is similar and statistically not different to the un-stimulated vasculature in control mice. Furthermore capillary diameter distribution remained as narrow as in controls with the peak only slightly moving towards larger capillary diameters. Thus capillary diameter range was confined approximately between 4 and 12 μm in Rictor$^{i\Delta ec}$ mice (**Figures 22/23).** We therefore conclude that FGF2 induced capillary diameter increase crucially requires endothelial mTORC2.

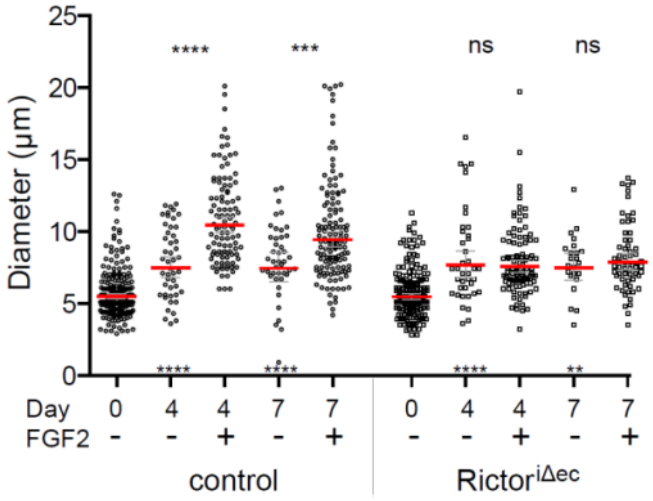

Figure 22. Un-stimulated and FGF2 stimulated vascular bed of Rictor$^{i\Delta ec}$ mice exhibit the same behavior in capillary diameter increase. Distribution of all capillary diameter values describes the more heterogeneous vasculature of control animal and the significant increase when stimulated with FGF2. The Rictor$^{i\Delta ec}$ mice present a less spread capillary diameter distribution and equal average capillary diameter between un-stimulated and FGF2 stimulated vascular beds on day 4 and 7.

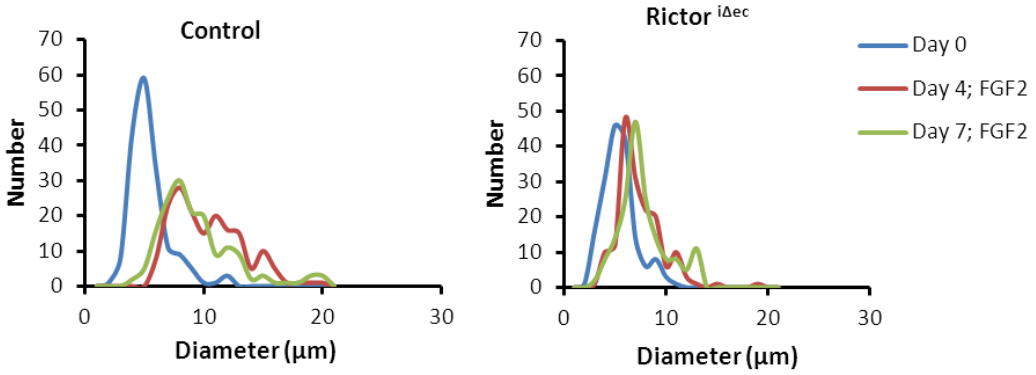

Figure 23: Capillary diameter distribution comparing the changes in capillary diameter in each animal group. Control mice show a shift in capillary diameter when stimulated with FGF2 and the include capillaries with wide range of different diameters. Rictor$^{i\Delta ec}$ mice show identical behavior in capillary diameter distribution regardless the presence of the stimulus.

3. B.2.4.2. CD31 and Cre-ER^{T2} staining of FGF2 challenged skin muscle vasculature

Intravital microscopy is limited when focusing on different depths of the vasculature due to visibility issues. We therefore performed histological sections from the skin muscle at the end of intravital microscopy on day 7. The previously analyzed skin muscle tissue was removed, paraffin embedded, cut vertically and stained with the endothelial specific marker CD31. The peroxidase CD31 staining confirmed the data of the intravital microscopy with the control animals present capillaries around skin muscle with wider lumina in comparison to the Rictor$^{i\Delta ec}$ mice (**Figure 24**).

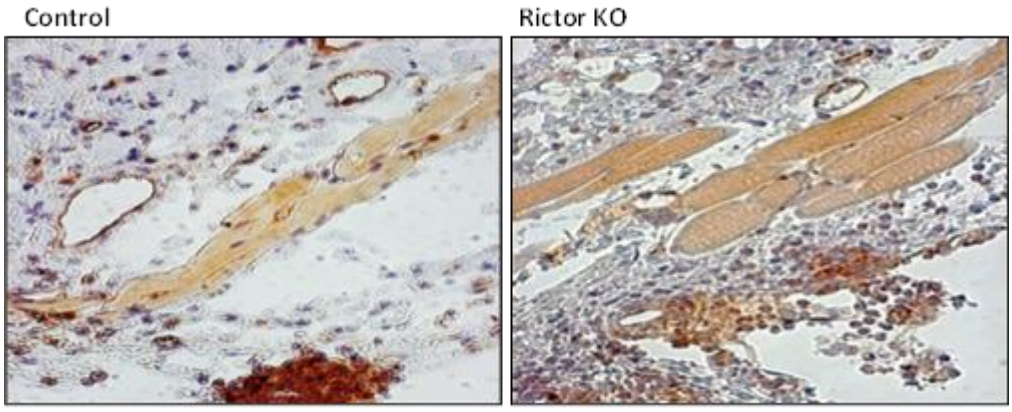

Figure 24: CD31 immunohistological staining of skin muscle capillaries. Vertical sections of paraffin embedded skin muscle after 7 days of FGF2 stimulation. Control animals have capillaries and vessels around the skin muscle with wider lumen than the Rictor$^{i\Delta EC}$.

Vertical sections of the skin muscle from Cre^{+}; *Rictor* lox mice were stained for the Estrogen Receptor α. Cre-ER^{T2} that is expressed in these mice and drives the excision of *Rictor* exons is a fused Cre recombinase with the Estrogen Receptor α. A positive staining of the Estrogen Receptor α is an indirect proof of Cre recombinase presence and expression (185-187). The presence of Cre-ER^{T2} in animals is an additional measure and confirmation of the *Rictor* knockout efficiency. Figure 25 is a representative example of Estrogen

Receptor α staining that is located and restricted to the vasculature. The skin muscle displays auto-fluorescence (**Figure 25**) (188).

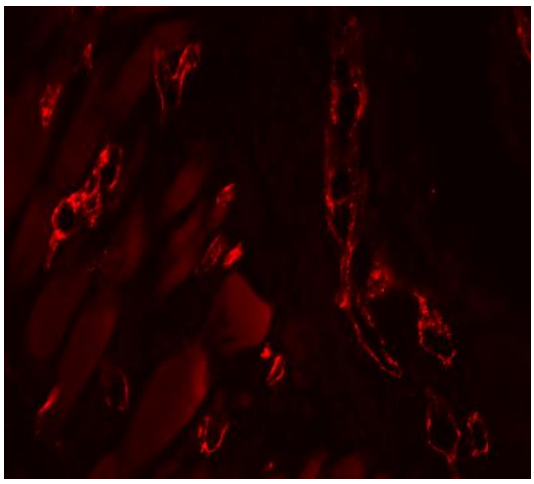

Figure 25: Cre-ER^{T2} positive expression in the skin muscle vasculature. Vertical section of FGF2 stimulated skin muscle vasculature positively stained for Estrogen receptor α (ER^{T2}) which is conjugated with Cre recombinase. Positive staining is localized in the capillaries.

3. B.3. Assessment of the role of endothelial mTORC2 in FGF2 induced de novo angiogenesis

The effect of endothelial mTORC2 deficiency in FGF2-induced neovascularization *in vivo* was assessed using the Matrigel plug angiogenesis assay. Matrigel was injected subcutaneously in the mouse flank with 1, 5 μg/ml FGF2/heparin or diluent (heparin). 7 days post injection mice were sacrificed and Matrigel plugs were removed (**Figure 26**).

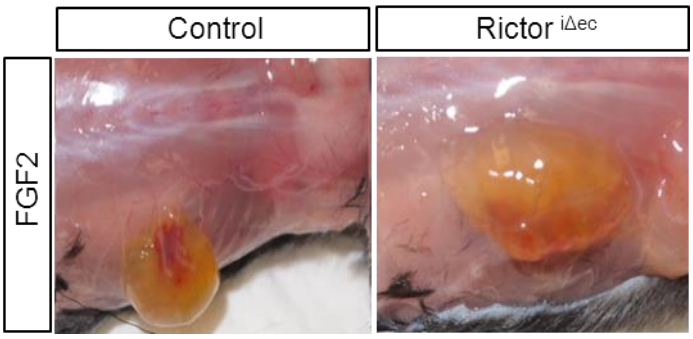

Figure 26: Matrigel plug assay. Ice cold liquid Matrigel is subcutaneously injected and solidifies creating a plug attached to the host tissue. Host vasculature and stroma grows on and into the FGF2-loaded Matrigel plug in both animal groups.

The diluent plugs were used as control for a potential effect of the host animal to Matrigel itself which contains a reduced amount of growth factors. As can be seen in Figure 27 the diluent plugs from both control and Rictor$^{i\Delta ec}$ animals were transparent with no obvious vascularization or tissue growth. Absence of vascularization was confirmed by histological analysis of Hematoxylene and CD31 immunological staining (data not shown). Blood containing microvessels and signs of hemorrhage were macroscopically evident in plugs containing FGF2 from control mice compared to rather homogenous, unobtrusive vascularization in plugs from Rictor $^{i\Delta ec}$ mice (**Figure 27**).

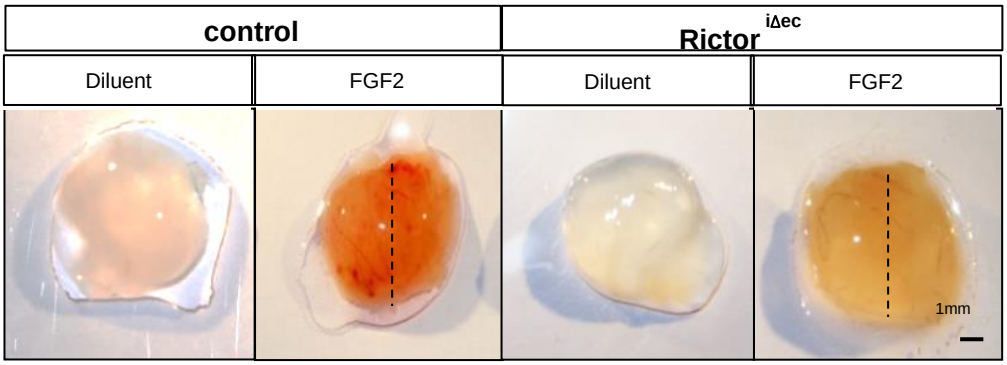

Figure 27 Neovascularization of FGF2 containing Matrigel plugs is reduced in Rictor$^{i\Delta ec}$ mice.
Matrigel containing heparin (diluent) or 1.5µg/ml FGF2 with heparin (FGF2) was injected subcutaneously into the ventral flank of 8-week-old male control and Rictor$^{i\Delta ec}$ mice. The plugs were removed 7 days later and analyzed. Representative macro-photographs (scale bar = 1mm) of Matrigel plugs from control (left panels) and Rictor $^{i\Delta ec}$ mice (right panels) are displayed.

3. B.3.1. Endothelial *Rictor* knockout hampers the vascularization of FGF2 loaded Matrigel plugs

Histological sections and CD31 immunohistochemical staining of the capillaries revealed the growth and the invasion pattern of the host capillaries into the FGF2-containing plugs. The histological analysis showed that capillaries invade on average to about 800 µm from the surface of the plug into the center, whereas microvessels from

Rictor$^{i\Delta ec}$ mice invaded plugs only to about 300 µm (P<0.05; n=4/7) (**Figure 28,** upper micrographs and quantification to the right).

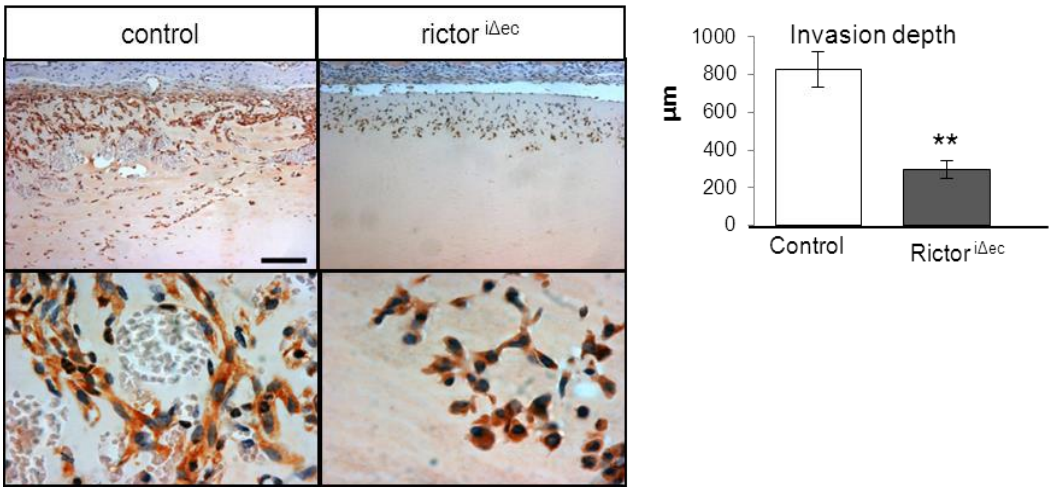

Figure28: Rictor^{iAec} hampers the invasion of host capillaries and the vascularization of FGF2 containing Matrigel plugs (A) Paraffin-embedded FGF2 containing plugs were sectioned horizontally (see dashed lines in Fig. 12) and immune-stained for CD31 (brown) and Hematoxylene (blue/nuclei). Upper representative micrographs show 10x magnification (scale bar = 200 µm) and display the invasion depth of newly ingrown microvessels from the surface towards center of the Matrigel plug. Lower micrographs show 40x magnification (scale bar = 50 µm) displaying heterogeneity of vessel structure and local hemorrhage in plugs from control mice. (**B**) Quantification displays significant reduction of ingrowth (in µm) of neovessels into plugs from Rictor^{iAec} compared to control mice (P<0.05, n=4/7).

In control plugs, the CD31 positive microvessel structure was heterogeneous with large microvascular structures at the periphery of the plug, and smaller capillaries towards the center. Erythrocytes containing compartments in the plug indicated leaky vasculature and local hemorrhage (**Figure 28**). In contrast, the microvasculature in FGF2-containing plugs from Rictor$^{i\Delta ec}$ mice was composed of homogenously small capillaries with no evident hemorrhage (**Figure 28**)

3. B.3.2. Endothelial *Rictor* affects diameter of existing stromal capillaries in response to FGF2

During the 7 days of FGF2 exposure, the Matrigel plug was encapsulated by a thin layer of stromal tissue that also contained arterioles and venules. Quantification of these vessels showed similar vessel density in plugs from both experimental groups (data not shown). However, the luminal area was significantly smaller in vessels of the stromal capsule from Rictor$^{i\Delta ec}$ mice compared to control (**Figure 29** P<0.05; n=3). Thus, larger stromal vessels were observed in the stromal area of Control FGF2 plug in comparison to Rictor$^{i\Delta ec}$ mice as already seen by intravital microscopy in remodeling of the preexisting dermal microvasculature.

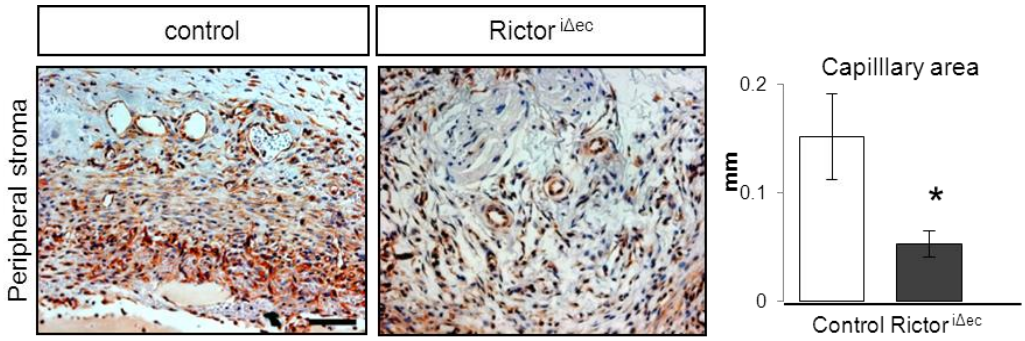

Figure29: Rictor$^{i\Delta ec}$ hampers dilation of the FGF2 Matrigel plug surrounding stromal capillaries Representative micrographs of peripheral stroma covering FGF2-containing Matrigel plugs from control and Rictor$^{i\Delta ec}$ mice. The area and number of identifiable microvessel lumina were measured. Whereas vessel number did not vary (data not shown), a significant reduction of the inner luminal area in stromal vessels from Rictor$^{i\Delta ec}$ compared to control mice was detected (**P<0.5, n=4**).

4. DISCUSSION

Angiogenesis is a process where new capillaries are formed from pre-existing ones. Endothelial cells are the drivers of sprouting angiogenesis since it requires their activation when pro-angiogenic stimuli prevail over anti-angiogenic mediators (12, 13). Physiological angiogenesis is a process which aims in the appropriate vascularization of a tissue in order to meet its metabolic demands or in the revascularization of an injured tissue (70). Pathological angiogenesis occurs mainly in proliferative diseases like cancer and vascular malformations and is characterized by unbalanced angiogenic growth factor secretion (70).

The mTOR signaling pathway is a central regulator of cell growth and survival and consists of mTORC1 and mTORC2. It has been demonstrated that the dual inhibition of both of these complexes has anti-tumor and anti-angiogenic properties, however due to the lack of specific mTORC2 inhibitors the contribution of each complex in angiogenesis has not been clarified yet (153,157,158). Since the endothelial cell is the driving force of sprouting angiogenesis, in this thesis we aim to investigate the role of endothelial mTORC2 in physiological and growth factor induced angiogenesis using an endothelial specific *Rictor* knockout mouse. Rictor is a specific accessory protein of mTORC2 and its depletion will cease mTORC2 signaling.

The efficiency of the induction of *Rictor* knockout was demonstrated in the scraped aortic endothelium (**Figure 1, Results Part A**) just before the initiation of the dorsal skinfold chamber experiments. The immunohistological staining of Cre-ER^{T2} in the dorsal skin muscle from animals included in the study and the significant phenotype observed in Rictor$^{i\Delta ec}$ animals with intravital microscopy enforce the statement that the animals included in this study were indeed endothelial specific *Rictor* knockout mice. The problem regarding Cre-ER^{T2} expression was detected 1.5 year after the completion of these *in viv*o experiments described in this thesis.

Intravital microscopy of the skin muscle vasculature showed that the deletion of *Rictor* does not affect the homeostasis of unchallenged vasculature (**Figure 14**). Rictor$^{i\Delta ec}$ mice present the typical vascularization of the panniculus carnosus with parallel capillaries and typical perfusion (**Figure 14A**) and microvessel density (**Figure 14B**).

Unlike adult Rictor$^{i\Delta ec}$ mice, data in our laboratory suggest that endothelial *Rictor* knockout embryos present increased lethality and growth retardation when the knockout is induced between E9.5 until E11.5 (Data generated by Dr. Kalus). These results were acquired using the inducible knockout model in 2011. The results regarding lethality of Rictor$^{i\Delta ec}$ embryos were confirmed by a constitutive model of *Rictor* deletion in the endothelium available in our research group (182) (Data generated by Dr. Humar). During embryo development there is a different microenvironment that promotes differentiation of hemangioblasts to endothelial and blood cells (189). Different ratio and distribution of angiogenic factors (190) could be causing the different response of *Rictor* knockout endothelial cells in the embryo and in wound healing of young adult mice. We could speculate that mTORC2 affects angiogenesis when it is stimulated by specific growth factor ratio or above a threshold of growth factor concentrations. Given that mTORC2 is known to convey signals from growth factors (103) it could be possible that mTORC2 does not affect the vasculature in late stages of physiologic development.

Stimulation with high dose of FGF2 induced a differential response in adult Rictor$^{i\Delta ec}$ mice showing a limited increase in capillary diameter, without changes in the microvessel density (**Figure 20A**). Distribution analysis of the capillary diameters demonstrate that Rictor$^{i\Delta ec}$ mice behave similarly when stimulated or not with high dose of FGF2 (**Figure 22/23**). A similar effect of mTORC2 was seen in the diameter of existing capillaries of the stroma surrounding the FGF2 loaded Matrigel plugs of the Rictor$^{i\Delta ec}$ mice (**Figure 29**).

Further investigation is required in order to understand by which mechanism endothelial mTORC2 regulates capillary diameter. Nitric oxide synthase (eNOS) expression

and function (13) and by consequence NO production and bioavailability (12) are major determinants of capillary diameter. The majority of the studies associate these cellular parameters with mTORC1. Though it has been demonstrated *in vitro* that mTORC2 inhibition in endothelial cells hampers the transcription of eNOS and the production of NO a regulator of vasodilation/vasoconstriction (191,192).

Important elements in regulation of capillary diameter are the pericyte coverage and the structure and the amount of ECM covering a capillary (42). A direct relationship between pericyte coverage and mTOR signaling has not been established yet. However a study on vascular injury showed that Rapamycin treatment hampers SMC proliferation and ECM deposition (193).

Intravital microscopy of FGF2 stimulated vasculature also revealed different remodeling architecture in Rictor$^{i\Delta ec}$ mice (**Figure 20/21**). High dose of FGF2 in the vasculature of control animals resulted in an aberrant vasculature that lacks the typical architecture of panniculus carnosus, with signs of intussusception and capillaries with high diameter variability within the same segment (local bulges and stenosis). On the other hand Rictor$^{i\Delta ec}$ mice present capillaries with more homogenous diameter distribution within the same segment (**Figure 20A/21**). Interestingly the FGF2 challenged vasculature of Rictor$^{i\Delta ec}$ mice show capillary-like structures with a lumen but with no functional perfusion (**Figure 20A**).

A similar phenotype was observed in the endothelial Notch knockout mouse (194). These mice present enhanced sprouting angiogenesis and tip cell formation leading to excessive but not functional vascularization. Additional experiments in our laboratory have shown that FGF2 induced endothelial network formation on Matrigel *in vitro* is disabled by *Rictor* knockout endothelial cells, however, can be rescued by VEGFA stimulation (Data generated by Rok Humar and Fabienne Lehner). Interestingly, disabled FGF2-dependent network formation was accomplished by an excessive sprouting in all directions without establishing connected segments.

Deletion or silencing of the Dll4 in embryos and adult mice resulted in decreased vascular maturation, reduced pericyte recruitment/coverage and defective basement membrane deposition (25,195). Additionally these studies show that Dll4 deletion promotes endothelial cell proliferation and migration resulting in increased vascular density but with defective lumen formation (25,196). A recent study by Skuli et al. in 2012 showed that HIF2 down-regulates the expression of Dll4 in *HIF2* knockout endothelial cells (196). In this study it was also shown that HIF2 regulates endothelial cell proliferation, migration and morphogenic event which are translated *in vivo* to increased vessel formation with poor perfusion and functionality (196). Possibly the reduced signaling of Dll4/Notch pathway leads to excessive tip cell formation generating multiple sprouts with defective lumens. A connection between the above studies with our results comes from the fact that HIFa and HIF2 are differentially regulated by mTORC1/2 and mTORC2 respectively (197). An investigation regarding of the relationship of mTORC2 signaling with Dll4/Notch and HIF2 would be very interesting since there are not many available data.

On a transcriptional level FoxO1and FoxO3a influence and regulate angiogenesis. These two transcription factors which are abundantly expressed in endothelial cells regulate endothelial cell migration, proliferation and tube formation (199). Increased activation of FoxO1/3a hampers all the above cellular functions and suppresses eNOS expression (198). mTORC2 is an integral component of the Akt-FoxO signaling pathway (117). We can speculate that part of our *in vivo* phenotype can be attributed to differential activation of the FoxO transcription factors due to mTORC2 silencing (117). Akt phosphorylation that is mediated by mTORC2 leads to the phosphorylation and inactivation of FoxO1/3a which in turn activates angiogenic processes (Data generated by Fabio Aimi. Manuscript in preparation: Aimi & Georgiopoulou) (117). *Rictor* knockout induction possibly keeps FoxO1/3a in an active form hampering NO production, proliferation, migration and tube formation (198) contributing to our *in vivo* phenotype related with capillary diameter and neovascularization.

Neovascularization of the FGF2 Matrigel plugs was impaired by the absence of endothelial mTORC2 (**Figure 28**). Similar findings were observed in Sirolimus treated rat model of hepatocellular carcinoma (199) It was shown that Sirolimus treatment resulted in reduced vascularization of the carcinoma and decreased capillary diameter (200) a similar finding with ours. Many other studies in tumor growth and vascularization have shown that dual inhibition of both mTOR complexes induces a greater inhibition, than inhibiting mTORC1 alone (153,157,158).

The *in vivo* data collected during this project showed for the first time the involvement of endothelial mTORC2 in cellular processes under extreme angiogenic conditions. Only when high doses of FGF2 were administered, mTORC2 regulated the capillary diameter, the architecture of the remodeled vasculature, and neo-angiogenesis. Collectively all the *in vivo* data suggest for the first time a critical role of endothelial mTORC2 in FGF2 induced angiogenesis and vascular remodeling.

Inducible Cre-ER^{T2} mediated recombinase *in vivo*: Caveats and technical considerations

The mouse used in this project was the offspring of breeding a mouse with Ve-cadherin promoter driving Cre-ER^{T2} recombinase expression (kind donation from Prof. Iruella-Arispe, UCLA, California/USA) (168, 170, 182) and a mouse with loxed *Rictor* exons 4 and 5 (168). Cre-ER^{T2} is a Cre recombinase fused with the Estrogen Receptor α that specifically binds Tamoxifen and it is constitutively expressed under the transcriptional control of Ve-Cadherin promoter (170).

Rictor knockout was induced at the age of 4 weeks with Tamoxifen injections following the protocol of Movoinsin et al. (170) (February 2011). The efficiency of knockout induction was assessed by quantifying the mRNA levels of Rictor and Cre-ER^{T2} in isolated aortic endothelium **(Figure 1**). The expression levels of Cre-ER^{T2} in the animals

were very variable from high to low, however exons 4 and 5 were efficiently excised (**Figure 1).** The animals used for this experiment were 27-week-old (after the end of the weight gain study). We monitored the efficiency of *Rictor* knockout in rather old mice (28 week) to make sure that endothelial cells that potentially did not recombine, did not accumulate during adolescence and adulthood (182). The data of these experiment suggested that the recombination and excision of *Rictor* exons occurred efficiently and allowed assessment of the aims of this project on the role of endothelial *Rictor* in angiogenesis *in vivo*, beginning 1 of March 2011. All the *in vivo* data described in Results part B were obtained from March 2011 until July 2012. Furthermore, Cre-ER^{T2} is a fused protein with the Estrogen Receptor α: immunohistological staining of this receptor can monitor Cre-ER^{T2} expression. Skin muscle sections from the animals included in the dorsal skinfold chamber experiments were positively stained for Estrogen Receptor α (**Figure 25**) indicating the active transcription and presence of Cre-ER^{T2} recombinase (189-191).

One and a half years after the acquisition of the data discussed in the second part of the result section, the question about the efficiency or endothelial *Rictor* knockout induction in different tissues of interest that are the subject of investigation arose. Optimization of multiple techniques for endothelial cells isolation from lungs was achieved (Results Part A).The main goal was the isolation of pure enough endothelial cells, in order to have a clear result regarding the efficiency of *Rictor* knockout induction. The scraping of the aortic endothelium showed limitations in reproducibility to show *Rictor* knockout induction (**Figure 1/3**). However: pure populations of lung endothelial cells revealed that the induction of the knockout was not taking place (**Figures 8/10/11**).

Cre-ER^{T2} recombinase that is specifically expressed in the endothelium driven by Ve-Cadherin promoter should follow similar transcription patterns with the native Ve-Cadherin. Ve-cadherin is constitutively expressed in the endothelium beginning in E6.5 (202). It has also been demonstrated that Ve-cadherin mRNA is strongly induced under angiogenic conditions (193) and shows increased endogenous protein expression in lung

endothelium (193). The lung endothelial cells that were isolated with MACS and cultured in growth factor enriched medium showed up-regulation of Ve-Cadherin transcription as expected, however this was not matched by the transcription of Cre-ER^{T2} **(Figure 29/26**). These results indicate that the promoter regulating Cre-ER^{T2} expression is not properly transcribing the recombinase and thus *Rictor* knockout is not induced in the endothelium.

All the above results regarding the induction of *Rictor* knockout in the endothelium and the defective transcription of Cre-ER^{T2} urged us to reconsider the transgene model. We thoroughly discussed our troubleshooting processes and results with the generators of the VE-Cadherin Cre-ER^{T2} mice (Prof. Luisa Iruella-Arispe, UCLA), and learned that similar issues from several other research groups had been reported. The exact reason for this instability is not known. However, genomic insertion always bears a random risk of the transgene being silenced due to chromosomal position effects (216).

In order to reinstall a properly working inducible and endothelium-specific Cre-recombinase model, we followed the advice of Prof. Arispe and are now breeding a different VE-Cadherin promoter based Cre-ER^{T2} mouse strain from the Laboratory of Ralph Adams (Cdh5(PAC)-CreERT2) (203). This promoter mouse bears a different site of transgene insertion. It is reported to have stable Cre recombinase expression and a better penetrance particularly in brain tissue. This mouse is currently used by several researchers exploring effects of endothelium specific gene deletions (203, 204). Additionally a fluorescent reporter mouse (B6.Cg-Gt (ROSA)26Sor<tm9(CAG-tdTomato)Hze>/J) (204) is currently being crossed with Cdh5(PAC)-Cre-ER^{T2}; Rictor$^{lox/lox}$ mice. The robust native fluorescence of this reporter enables direct visualization of Cre-ER^{T2} activity in the vasculature during all steps of development and adolescence. Isolation of endothelial cells with the above mentioned techniques, preferably magnetic sorting, however is still required in order to prove that Cre-ER^{T2} removes the *Rictor* exons. The combined usage of these two approaches would provide solid information about the efficiency of Rictor knockout in the endothelium for the future experiments

Outlook

Gene expression and proteomic analysis of *Rictor* knockout endothelial cells will possibly reveal important molecules that are regulated by mTORC2 and it will be able to propose a molecular mechanism for the observed phenotype. A micro-array in *Rictor* knockout endothelial cells is currently conducted in the laboratory in order to investigate the molecular mechanism of our phenotype (Micro-array conducted by Fabio Aimi and Christian Schaer. Manuscript in preparation Aimi & Georgiopoulou)

There is a variety of genetic and acquired pathologies that are characterized by extensive and uncontrolled angiogenesis such as atherosclerosis, vascular malformations and transplantation induced arteriopathy, retinopathies, psoriasis, arthritis, obesity and inflammatory diseases (205, 206). Last but not least cancer is a disease that is dependent on angiogenesis for its growth and metastasis (206)

Management and ceasing angiogenesis is an attractive therapeutic target. Anti-angiogenesis therapies have been designed targeting fundamental signaling pathways of angiogenesis, such as VEGF/VEGFR2, PDGF/PDGFR and general inhibitors Tyrosine Kinase Receptors. Targeted anti-angiogenesis treatments are mainly used for cancer treatment (207). The main drawbacks of targeted anti-angiogenesis treatments is that fact that tumors acquire resistance in these therapies by activating alternative pathways to sustain their vascularization (7,70,73,77,78) and that provoke serious side effects such as hemorrhagic episodes and thrombosis which are difficult to manage (208).

mTOR inhibitors gained attention in the last years due to the anti-proliferative and anti-angiogenic capacity (7,157). Dissecting the specific role of mTORC2 in physiological and pathological angiogenesis could provide additional therapeutic targets.

The use of mTOR inhibitors has been approved for Renal Cell Carcinoma and prolonged the overall survival of the patients. Inhibition of mTORC1 and C2 can re-sensitize the resistant tumors to the treatment by blocking the PI3K/mTOR pathway (211). However in both pre-clinical and clinical studies it is shown that inhibition of these

pathways is cytostatic and not cytotoxic leading to stabilization of the disease rather than regression (212). The use of Rapamycin and analogues inhibits mainly mTORC1 and can provoke resistance due to feedback activation loops and activation of mTORC2 which in turn boosts Akt phosphorylation (212). From all the above pre-clinical and clinical studies it can be seen that mTOR inhibitors should and are used in combination with other anti-angiogenesis treatments, standard chemotherapy or radiotherapy (212,213).

The results acquired from our laboratory show that mTORC2 regulates capillary dilation and the remodeling architecture of FGF2 stimulated vasculature. The ablation of mTORC2 resulted in a less aberrant vasculature. Visually the overview of the FGF2 stimulated vasculature resembles a more physiological state. This could provide indirect evidence that the ablation of mTORC2 contributes to vascular normalization (209,210). On the other hand FGF2 loaded Matrigel plugs showed that the ablation of mTORC2 hampers neo-angiogenesis. Thus, inhibition of mTORC2 is an appealing therapeutic target, especially for cancer malignancies. However, further investigation is needed in order to understand how endothelial mTORC2 inhibition could affect the tumor environment. On the other hand data are needed to identify the specific growth factors that signal through mTORC2, since not all cancer types are dependent on the same growth factors. If the contribution of mTORC2 in vascular normalization can be proven, targeting endothelial mTORC2 could open a time window where the vasculature is more functional and radiation- and chemotherapy could be more efficient (209).

References

1. Dawson, T. H. (2001) Similitude in the cardiovascular system of mammals. *The Journal of experimental biology* **204**, 395-407

2. Wagenseil, J. E., and Mecham, R. P. (2009) Vascular extracellular matrix and arterial mechanics. *Physiological reviews* **89**, 957-989

3. Udan, R. S., Culver, J. C., and Dickinson, M. E. (2013) Understanding vascular development. *Wiley Interdiscip Rev Dev Biol* **2**, 327-346

4. Chappell, J. C., Wiley, D. M., and Bautch, V. L. (2011) Regulation of blood vessel sprouting. *Semin Cell Dev Biol* **22**, 1005-1011

5. Eilken, H. M., and Adams, R. H. (2010) Dynamics of endothelial cell behavior in sprouting angiogenesis. *Curr Opin Cell Biol* **22**, 617-625

6. Teixeira, V., Arede, N., Gardner, R., Rodriguez-Leon, J., and Tavares, A. T. (2011) Targeting the hemangioblast with a novel cell type-specific enhancer. *BMC developmental biology* **11**, 76

7. Folkman, J. (2007) Angiogenesis: an organizing principle for drug discovery? *Nat Rev Drug Discov* **6**, 273-286

8. Carmeliet, P., De Smet, F., Loges, S., and Mazzone, M. (2009) Branching morphogenesis and antiangiogenesis candidates: tip cells lead the way. *Nat Rev Clin Oncol* **6**, 315-326

9. Welti, J., Loges, S., Dimmeler, S., and Carmeliet, P. (2013) Recent molecular discoveries in angiogenesis and antiangiogenic therapies in cancer. *The Journal of clinical investigation* **123**, 3190-3200

10. Singh, S., Wu, B. M., and Dunn, J. C. (2011) The enhancement of VEGF-mediated angiogenesis by polycaprolactone scaffolds with surface cross-linked heparin. *Biomaterials* **32**, 2059-2069

11. Ennett, A. B., Kaigler, D., and Mooney, D. J. (2006) Temporally regulated delivery of VEGF in vitro and in vivo. *Journal of biomedical materials research. Part A* **79**, 176-184

12. Carmeliet, P. (2000) Mechanisms of angiogenesis and arteriogenesis. *Nature medicine* **6**, 389-395

13. MacLauchlan, S., Yu, J., Parrish, M., Asoulin, T. A., Schleicher, M., Krady, M. M., Zeng, J., Huang, P. L., Sessa, W. C., and Kyriakides, T. R. (2011) Endothelial nitric oxide synthase controls the expression of the angiogenesis inhibitor thrombospondin 2. *Proceedings of the National Academy of Sciences of the United States of America* **108**, E1137-1145

14. Gerhardt, H., Golding, M., Fruttiger, M., Ruhrberg, C., Lundkvist, A., Abramsson, A., Jeltsch, M., Mitchell, C., Alitalo, K., Shima, D., and

Betsholtz, C. (2003) VEGF guides angiogenic sprouting utilizing endothelial tip cell filopodia. *The Journal of cell biology* **161**, 1163-1177

15. Ferrara, N. (1999) Vascular endothelial growth factor: molecular and biological aspects. *Current topics in microbiology and immunology* **237**, 1-30

16. Ruhrberg, C., Gerhardt, H., Golding, M., Watson, R., Ioannidou, S., Fujisawa, H., Betsholtz, C., and Shima, D. T. (2002) Spatially restricted patterning cues provided by heparin-binding VEGF-A control blood vessel branching morphogenesis. *Genes Dev* **16**, 2684-2698

17. Gerhardt, H. (2008) VEGF and endothelial guidance in angiogenic sprouting. *Organogenesis* **4**, 241-246

18. Chen, T. T., Luque, A., Lee, S., Anderson, S. M., Segura, T., and Iruela-Arispe, M. L. (2010) Anchorage of VEGF to the extracellular matrix conveys differential signaling responses to endothelial cells. *The Journal of cell biology* **188**, 595-609

19. Hellstrom, M., Phng, L. K., Hofmann, J. J., Wallgard, E., Coultas, L., Lindblom, P., Alva, J., Nilsson, A. K., Karlsson, L., Gaiano, N., Yoon, K., Rossant, J., Iruela-Arispe, M. L., Kalen, M., Gerhardt, H., and Betsholtz, C. (2007) Dll4 signalling through Notch1 regulates formation of tip cells during angiogenesis. *Nature* **445**, 776-780

20. Tung, J. J., Tattersall, I. W., and Kitajewski, J. (2012) Tips, stalks, tubes: notch-mediated cell fate determination and mechanisms of tubulogenesis during angiogenesis. *Cold Spring Harb Perspect Med* **2**, a006601

21. Lobov, I. B., Renard, R. A., Papadopoulos, N., Gale, N. W., Thurston, G., Yancopoulos, G. D., and Wiegand, S. J. (2007) Delta-like ligand 4 (Dll4) is induced by VEGF as a negative regulator of angiogenic sprouting. *Proceedings of the National Academy of Sciences of the United States of America* **104**, 3219-3224

22. Leslie, J. D., Ariza-McNaughton, L., Bermange, A. L., McAdow, R., Johnson, S. L., and Lewis, J. (2007) Endothelial signalling by the Notch ligand Delta-like 4 restricts angiogenesis. *Development* **134**, 839-844

23. Liu, Z. J., Shirakawa, T., Li, Y., Soma, A., Oka, M., Dotto, G. P., Fairman, R. M., Velazquez, O. C., and Herlyn, M. (2003) Regulation of Notch1 and Dll4 by vascular endothelial growth factor in arterial endothelial cells: implications for modulating arteriogenesis and angiogenesis. *Mol Cell Biol* **23**, 14-25

24. Bentley, K., Gerhardt, H., and Bates, P. A. (2008) Agent-based simulation of notch-mediated tip cell selection in angiogenic sprout initialisation. *J Theor Biol* **250**, 25-36

25. Benedito, R., Trindade, A., Hirashima, M., Henrique, D., da Costa, L. L., Rossant, J., Gill, P. S., and Duarte, A. (2008) Loss of Notch signalling induced by Dll4 causes arterial calibre reduction by increasing endothelial cell response to angiogenic stimuli. *BMC developmental biology* **8**, 117

26. Boscolo, E., Mulliken, J. B., and Bischoff, J. (2011) VEGFR-1 mediates endothelial differentiation and formation of blood vessels in a murine model of infantile hemangioma. *Am J Pathol* **179**, 2266-2277

27. Fischer, C., Mazzone, M., Jonckx, B., and Carmeliet, P. (2008) FLT1 and its ligands VEGFB and PlGF: drug targets for anti-angiogenic therapy? *Nat Rev Cancer* **8**, 942-956

28. Siekmann, A. F., and Lawson, N. D. (2007) Notch signalling limits angiogenic cell behaviour in developing zebrafish arteries. *Nature* **445**, 781-784

29. Shibuya, M. (2006) Differential roles of vascular endothelial growth factor receptor-1 and receptor-2 in angiogenesis. *J Biochem Mol Biol* **39**, 469-478

30. Kappas, N. C., Zeng, G., Chappell, J. C., Kearney, J. B., Hazarika, S., Kallianos, K. G., Patterson, C., Annex, B. H., and Bautch, V. L. (2008) The VEGF receptor Flt-1 spatially modulates Flk-1 signaling and blood vessel branching. *The Journal of cell biology* **181**, 847-858

31. Chappell, J. C., Taylor, S. M., Ferrara, N., and Bautch, V. L. (2009) Local guidance of emerging vessel sprouts requires soluble Flt-1. *Developmental cell* **17**, 377-386

32. Krueger, J., Liu, D., Scholz, K., Zimmer, A., Shi, Y., Klein, C., Siekmann, A., Schulte-Merker, S., Cudmore, M., Ahmed, A., and le Noble, F. (2011) Flt1 acts as a negative regulator of tip cell formation and branching morphogenesis in the zebrafish embryo. *Development* **138**, 2111-2120

33. Jakobsson, L., Franco, C. A., Bentley, K., Collins, R. T., Ponsioen, B., Aspalter, I. M., Rosewell, I., Busse, M., Thurston, G., Medvinsky, A., Schulte-Merker, S., and Gerhardt, H. (2010) Endothelial cells dynamically compete for the tip cell position during angiogenic sprouting. *Nat Cell Biol* **12**, 943-953

34. Skobe, M., Hawighorst, T., Jackson, D. G., Prevo, R., Janes, L., Velasco, P., Riccardi, L., Alitalo, K., Claffey, K., and Detmar, M. (2001) Induction of tumor lymphangiogenesis by VEGF-C promotes breast cancer metastasis. *Nature medicine* **7**, 192-198

35. Tammela, T., Zarkada, G., Wallgard, E., Murtomaki, A., Suchting, S., Wirzenius, M., Waltari, M., Hellstrom, M., Schomber, T., Peltonen, R., Freitas, C., Duarte, A., Isoniemi, H., Laakkonen, P., Christofori, G., Yla-Herttuala, S., Shibuya, M., Pytowski, B., Eichmann, A., Betsholtz, C., and Alitalo, K. (2008) Blocking VEGFR-3 suppresses angiogenic sprouting and vascular network formation. *Nature* **454**, 656-660

36. Tammela, T., Zarkada, G., Nurmi, H., Jakobsson, L., Heinolainen, K., Tvorogov, D., Zheng, W., Franco, C. A., Murtomaki, A., Aranda, E., Miura, N., Yla-Herttuala, S., Fruttiger, M., Makinen, T., Eichmann, A., Pollard, J. W., Gerhardt, H., and Alitalo, K. (2011) VEGFR-3 controls tip to stalk conversion at vessel fusion sites by reinforcing Notch signalling. *Nat Cell Biol* **13**, 1202-1213

37. Fantin, A., Vieira, J. M., Gestri, G., Denti, L., Schwarz, Q., Prykhozhij, S., Peri, F., Wilson, S. W., and Ruhrberg, C. (2010) Tissue macrophages act as cellular chaperones for vascular anastomosis downstream of VEGF-mediated endothelial tip cell induction. *Blood* **116**, 829-840

38. Benedito, R., Rocha, S. F., Woeste, M., Zamykal, M., Radtke, F., Casanovas, O., Duarte, A., Pytowski, B., and Adams, R. H. (2012) Notch-dependent VEGFR3 upregulation allows angiogenesis without VEGF-VEGFR2 signalling. *Nature* **484**, 110-114

39. Shawber, C. J., Funahashi, Y., Francisco, E., Vorontchikhina, M., Kitamura, Y., Stowell, S. A., Borisenko, V., Feirt, N., Podgrabinska, S., Shiraishi, K., Chawengsaksophak, K., Rossant, J., Accili, D., Skobe, M., and Kitajewski, J. (2007) Notch alters VEGF responsiveness in human and murine endothelial cells by direct regulation of VEGFR-3 expression. *The Journal of clinical investigation* **117**, 3369-3382

40. Jain, R. K. (2003) Molecular regulation of vessel maturation. *Nature medicine* **9**, 685-693

41. Armulik, A., Abramsson, A., and Betsholtz, C. (2005) Endothelial/pericyte interactions. *Circulation research* **97**, 512-523

42. Stratman, A. N., and Davis, G. E. (2012) Endothelial cell-pericyte interactions stimulate basement membrane matrix assembly: influence on vascular tube remodeling, maturation, and stabilization. *Microsc Microanal* **18**, 68-80

43. Abramsson, A., Lindblom, P., and Betsholtz, C. (2003) Endothelial and nonendothelial sources of PDGF-B regulate pericyte recruitment and influence vascular pattern formation in tumors. *The Journal of clinical investigation* **112**, 1142-1151

44. Bjarnegard, M., Enge, M., Norlin, J., Gustafsdottir, S., Fredriksson, S., Abramsson, A., Takemoto, M., Gustafsson, E., Fassler, R., and Betsholtz, C. (2004) Endothelium-specific ablation of PDGFB leads to pericyte loss and glomerular, cardiac and placental abnormalities. *Development* **131**, 1847-1857

45. Lindblom, P., Gerhardt, H., Liebner, S., Abramsson, A., Enge, M., Hellstrom, M., Backstrom, G., Fredriksson, S., Landegren, U., Nystrom, H. C., Bergstrom, G., Dejana, E., Ostman, A., Lindahl, P., and Betsholtz, C. (2003) Endothelial PDGF-B retention is required for proper investment of pericytes in the microvessel wall. *Genes Dev* **17**, 1835-1840

46. Benjamin, L. E., Hemo, I., and Keshet, E. (1998) A plasticity window for blood vessel remodelling is defined by pericyte coverage of the preformed endothelial network and is regulated by PDGF-B and VEGF. *Development* **125**, 1591-1598

47. Eklund, L., and Saharinen, P. (2013) Angiopoietin signaling in the vasculature. *Exp Cell Res* **319**, 1271-1280

48. Suri, C., Jones, P. F., Patan, S., Bartunkova, S., Maisonpierre, P. C., Davis, S., Sato, T. N., and Yancopoulos, G. D. (1996) Requisite role of angiopoietin-1, a ligand for the TIE2 receptor, during embryonic angiogenesis. *Cell* **87**, 1171-1180

49. Sundberg, C., Kowanetz, M., Brown, L. F., Detmar, M., and Dvorak, H. F. (2002) Stable expression of angiopoietin-1 and other markers by cultured pericytes: phenotypic similarities to a subpopulation of cells in maturing vessels during later stages of angiogenesis in vivo. *Lab Invest* **82**, 387-401

50. Sato, T. N., Tozawa, Y., Deutsch, U., Wolburg-Buchholz, K., Fujiwara, Y., Gendron-Maguire, M., Gridley, T., Wolburg, H., Risau, W., and Qin, Y. (1995) Distinct roles of the receptor tyrosine kinases Tie-1 and Tie-2 in blood vessel formation. *Nature* **376**, 70-74

51. Dumont, D. J., Gradwohl, G., Fong, G. H., Puri, M. C., Gertsenstein, M., Auerbach, A., and Breitman, M. L. (1994) Dominant-negative and targeted null mutations in the endothelial receptor tyrosine kinase, tek, reveal a critical role in vasculogenesis of the embryo. *Genes Dev* **8**, 1897-1909

52. Iivanainen, E., Nelimarkka, L., Elenius, V., Heikkinen, S. M., Junttila, T. T., Sihombing, L., Sundvall, M., Maatta, J. A., Laine, V. J., Yla-Herttuala, S., Higashiyama, S., Alitalo, K., and Elenius, K. (2003) Angiopoietin-regulated recruitment of vascular smooth muscle cells by endothelial-derived heparin binding EGF-like growth factor. *FASEB J* **17**, 1609-1621

53. Mammoto, T., Parikh, S. M., Mammoto, A., Gallagher, D., Chan, B., Mostoslavsky, G., Ingber, D. E., and Sukhatme, V. P. (2007) Angiopoietin-1 requires p190 RhoGAP to protect against vascular leakage in vivo. *The Journal of biological chemistry* **282**, 23910-23918

54. Gavard, J., Patel, V., and Gutkind, J. S. (2008) Angiopoietin-1 prevents VEGF-induced endothelial permeability by sequestering Src through mDia. *Developmental cell* **14**, 25-36

55. Stratman, A. N., Malotte, K. M., Mahan, R. D., Davis, M. J., and Davis, G. E. (2009) Pericyte recruitment during vasculogenic tube assembly stimulates endothelial basement membrane matrix formation. *Blood* **114**, 5091-5101

56. Stratman, A. N., Schwindt, A. E., Malotte, K. M., and Davis, G. E. (2010) Endothelial-derived PDGF-BB and HB-EGF coordinately regulate pericyte recruitment during vasculogenic tube assembly and stabilization. *Blood* **116**, 4720-4730

57. Stratman, A. N., Saunders, W. B., Sacharidou, A., Koh, W., Fisher, K. E., Zawieja, D. C., Davis, M. J., and Davis, G. E. (2009) Endothelial cell lumen and vascular guidance tunnel formation requires MT1-MMP-dependent proteolysis in 3-dimensional collagen matrices. *Blood* **114**, 237-247

58. Saunders, W. B., Bohnsack, B. L., Faske, J. B., Anthis, N. J., Bayless, K. J., Hirschi, K. K., and Davis, G. E. (2006) Coregulation of

vascular tube stabilization by endothelial cell TIMP-2 and pericyte TIMP-3. *The Journal of cell biology* **175**, 179-191

59. Sacharidou, A., Koh, W., Stratman, A. N., Mayo, A. M., Fisher, K. E., and Davis, G. E. (2010) Endothelial lumen signaling complexes control 3D matrix-specific tubulogenesis through interdependent Cdc42- and MT1-MMP-mediated events. *Blood* **115**, 5259-5269

60. Lafleur, M. A., Handsley, M. M., Knauper, V., Murphy, G., and Edwards, D. R. (2002) Endothelial tubulogenesis within fibrin gels specifically requires the activity of membrane-type-matrix metalloproteinases (MT-MMPs). *J Cell Sci* **115**, 3427-3438

61. Styp-Rekowska, B., Hlushchuk, R., Pries, A. R., and Djonov, V. (2011) Intussusceptive angiogenesis: pillars against the blood flow. *Acta Physiol (Oxf)* **202**, 213-223

62. Caduff, J. H., Fischer, L. C., and Burri, P. H. (1986) Scanning electron microscope study of the developing microvasculature in the postnatal rat lung. *Anat Rec* **216**, 154-164

63. Djonov, V., Baum, O., and Burri, P. H. (2003) Vascular remodeling by intussusceptive angiogenesis. *Cell Tissue Res* **314**, 107-117

64. Burri, P. H., Hlushchuk, R., and Djonov, V. (2004) Intussusceptive angiogenesis: its emergence, its characteristics, and its significance. *Developmental dynamics : an official publication of the American Association of Anatomists* **231**, 474-488

65. Djonov, V. G., Galli, A. B., and Burri, P. H. (2000) Intussusceptive arborization contributes to vascular tree formation in the chick chorio-allantoic membrane. *Anat Embryol (Berl)* **202**, 347-357

66. Gambino, L. S., Wreford, N. G., Bertram, J. F., Dockery, P., Lederman, F., and Rogers, P. A. (2002) Angiogenesis occurs by vessel elongation in proliferative phase human endometrium. *Hum Reprod* **17**, 1199-1206.

67. Makanya, A. N., Hlushchuk, R., and Djonov, V. G. (2009) Intussusceptive angiogenesis and its role in vascular morphogenesis, patterning, and remodeling. *Angiogenesis* **12**, 113-123

68. Neufeld, G., and Kessler, O. (2008) The semaphorins: versatile regulators of tumour progression and tumour angiogenesis. *Nat Rev Cancer* **8**, 632-645

69. Folkman, J. (1971) Tumor angiogenesis: therapeutic implications. *N Engl J Med* **285**, 1182-1186

70. Kerbel, R. S. (2008) Tumor angiogenesis. *N Engl J Med* **358**, 2039-2049

71. Quintieri, L., Selmy, M., and Indraccolo, S. (2014) Metabolic effects of antiangiogenic drugs in tumors: therapeutic implications. *Biochem Pharmacol* **89**, 162-170

72. Hlushchuk, R., Riesterer, O., Baum, O., Wood, J., Gruber, G., Pruschy, M., and Djonov, V. (2008) Tumor recovery by angiogenic switch from sprouting to intussusceptive angiogenesis after treatment with PTK787/ZK222584 or ionizing radiation. *Am J Pathol* **173**, 1173-1185

73. Loges, S., Schmidt, T., and Carmeliet, P. (2010) Mechanisms of resistance to anti-angiogenic therapy and development of third-generation anti-angiogenic drug candidates. *Genes Cancer* **1**, 12-25

74. Bergers, G., and Hanahan, D. (2008) Modes of resistance to anti-angiogenic therapy. *Nat Rev Cancer* **8**, 592-603

75. Zern, B. J., Chu, H., and Wang, Y. (2010) Control growth factor release using a self-assembled [polycation:heparin] complex. *PloS one* **5**, e11017

76. Dimova, I., Popivanov, G., and Djonov, V. (2014) Angiogenesis in cancer - general pathways and their therapeutic implications. *J BUON* **19**, 15-21

77. Mittal, K., Ebos, J., and Rini, B. (2014) Angiogenesis and the tumor microenvironment: vascular endothelial growth factor and beyond. *Semin Oncol* **41**, 235-251

78. Benazzi, C., Al-Dissi, A., Chau, C. H., Figg, W. D., Sarli, G., de Oliveira, J. T., and Gartner, F. (2014) Angiogenesis in spontaneous tumors and implications for comparative tumor biology. *ScientificWorldJournal* **2014**, 919570

79. Gospodarowicz, D. (1974) Localisation of a fibroblast growth factor and its effect alone and with hydrocortisone on 3T3 cell growth. *Nature* **249**, 123-127

80. Murakami, M., and Simons, M. (2008) Fibroblast growth factor regulation of neovascularization. *Curr Opin Hematol* **15**, 215-220

81. Alessi, P., Leali, D., Camozzi, M., Cantelmo, A., Albini, A., and Presta, M. (2009) Anti-FGF2 approaches as a strategy to compensate resistance to anti-VEGF therapy: long-pentraxin 3 as a novel antiangiogenic FGF2-antagonist. *Eur Cytokine Netw* **20**, 225-234

82. Lieu, C., Heymach, J., Overman, M., Tran, H., and Kopetz, S. (2011) Beyond VEGF: inhibition of the fibroblast growth factor pathway and antiangiogenesis. *Clin Cancer Res* **17**, 6130-6139

83. Mignatti, P., Morimoto, T., and Rifkin, D. B. (1992) Basic fibroblast growth factor, a protein devoid of secretory signal sequence, is released by cells via a pathway independent of the endoplasmic reticulum-Golgi complex. *J Cell Physiol* **151**, 81-93

84. Tassi, E., Al-Attar, A., Aigner, A., Swift, M. R., McDonnell, K., Karavanov, A., and Wellstein, A. (2001) Enhancement of fibroblast growth factor (FGF) activity by an FGF-binding protein. *The Journal of biological chemistry* **276**, 40247-40253

85. Aigner, A., Butscheid, M., Kunkel, P., Krause, E., Lamszus, K., Wellstein, A., and Czubayko, F. (2001) An FGF-binding protein (FGF-BP) exerts its biological function by parallel paracrine stimulation of tumor cell and endothelial cell proliferation through FGF-2 release. *Int J Cancer* **92**, 510-517

86. Presta, M., Dell'Era, P., Mitola, S., Moroni, E., Ronca, R., and Rusnati, M. (2005) Fibroblast growth factor/fibroblast growth factor receptor system in angiogenesis. *Cytokine Growth Factor Rev* **16**, 159-178

87. Seghezzi, G., Patel, S., Ren, C. J., Gualandris, A., Pintucci, G., Robbins, E. S., Shapiro, R. L., Galloway, A. C., Rifkin, D. B., and Mignatti, P. (1998) Fibroblast growth factor-2 (FGF-2) induces vascular endothelial growth factor (VEGF) expression in the endothelial cells of forming capillaries: an autocrine mechanism contributing to angiogenesis. *J Cell Biol* **141**, 1659-1673

88. Rogers, M. S., Rohan, R. M., Birsner, A. E., and D'Amato, R. J. (2004) Genetic loci that control the angiogenic response to basic fibroblast growth factor. *FASEB J* **18**, 1050-1059

89. Claffey, K. P., Abrams, K., Shih, S. C., Brown, L. F., Mullen, A., and Keough, M. (2001) Fibroblast growth factor 2 activation of stromal cell vascular endothelial growth factor expression and angiogenesis. *Lab Invest* **81**, 61-75

90. Tsunoda, S., Nakamura, T., Sakurai, H., and Saiki, I. (2007) Fibroblast growth factor-2-induced host stroma reaction during initial tumor growth promotes progression of mouse melanoma via vascular endothelial growth factor A-dependent neovascularization. *Cancer Sci* **98**, 541-548

91. Magnusson, P., Rolny, C., Jakobsson, L., Wikner, C., Wu, Y., Hicklin, D. J., and Claesson-Welsh, L. (2004) Deregulation of Flk-1/vascular endothelial growth factor receptor-2 in fibroblast growth factor receptor-1-deficient vascular stem cell development. *J Cell Sci* **117**, 1513-1523

92. Shi, Y. H., Bingle, L., Gong, L. H., Wang, Y. X., Corke, K. P., and Fang, W. G. (2007) Basic FGF augments hypoxia induced HIF-1-alpha expression and VEGF release in T47D breast cancer cells. *Pathology* **39**, 396-400

93. Tille, J. C., Wood, J., Mandriota, S. J., Schnell, C., Ferrari, S., Mestan, J., Zhu, Z., Witte, L., and Pepper, M. S. (2001) Vascular endothelial growth factor (VEGF) receptor-2 antagonists inhibit VEGF- and basic fibroblast growth factor-induced angiogenesis in vivo and in vitro. *J Pharmacol Exp Ther* **299**, 1073-1085

94. Giavazzi, R., Sennino, B., Coltrini, D., Garofalo, A., Dossi, R., Ronca, R., Tosatti, M. P., and Presta, M. (2003) Distinct role of fibroblast growth factor-2 and vascular endothelial growth factor on tumor growth and angiogenesis. *Am J Pathol* **162**, 1913-19263

95. Jih, Y. J., Lien, W. H., Tsai, W. C., Yang, G. W., Li, C., and Wu, L. W. (2001) Distinct regulation of genes by bFGF and VEGF-A in endothelial cells. *Angiogenesis* **4**, 313-321

96. Kano, M. R., Morishita, Y., Iwata, C., Iwasaka, S., Watabe, T., Ouchi, Y., Miyazono, K., and Miyazawa, K. (2005) VEGF-A and FGF-2 synergistically promote neoangiogenesis through enhancement of endogenous PDGF-B-PDGFRbeta signaling. *J Cell Sci* **118**, 3759-3768

97. Cao, R., Eriksson, A., Kubo, H., Alitalo, K., Cao, Y., and Thyberg, J. (2004) Comparative evaluation of FGF-2-, VEGF-A-, and VEGF-C-induced angiogenesis, lymphangiogenesis, vascular fenestrations, and permeability. *Circulation research* **94**, 664-670

98. Nissen, L. J., Cao, R., Hedlund, E. M., Wang, Z., Zhao, X., Wetterskog, D., Funa, K., Brakenhielm, E., and Cao, Y. (2007) Angiogenic factors FGF2 and PDGF-BB synergistically promote murine tumor neovascularization and metastasis. *The Journal of clinical investigation* **117**, 2766-2777

99. Cao, R., Brakenhielm, E., Pawliuk, R., Wariaro, D., Post, M. J., Wahlberg, E., Leboulch, P., and Cao, Y. (2003) Angiogenic synergism, vascular stability and improvement of hind-limb ischemia by a combination of PDGF-BB and FGF-2. *Nature medicine* **9**, 604-613

100. Pickering, J. G., Uniyal, S., Ford, C. M., Chau, T., Laurin, M. A., Chow, L. H., Ellis, C. G., Fish, J., and Chan, B. M. (1997) Fibroblast growth factor-2 potentiates vascular smooth muscle cell migration to platelet-derived growth factor: upregulation of alpha2beta1 integrin and disassembly of actin filaments. *Circulation research* **80**, 627-637

101. Laplante, M., and Sabatini, D. M. (2009) mTOR signaling at a glance. *J Cell Sci* **122**, 3589-3594

102. Laplante, M., and Sabatini, D. M. (2012) mTOR signaling in growth control and disease. *Cell* **149**, 274-293

103. Oh, W. J., and Jacinto, E. (2011) mTOR complex 2 signaling and functions. *Cell cycle* **10**, 2305-2316

104. Jacinto, E., Loewith, R., Schmidt, A., Lin, S., Ruegg, M. A., Hall, A., and Hall, M. N. (2004) Mammalian TOR complex 2 controls the actin cytoskeleton and is rapamycin insensitive. *Nat Cell Biol* **6**, 1122-1128

105. Kim, D. H., Sarbassov, D. D., Ali, S. M., Latek, R. R., Guntur, K. V., Erdjument-Bromage, H., Tempst, P., and Sabatini, D. M. (2003) GbetaL, a positive regulator of the rapamycin-sensitive pathway required for the nutrient-sensitive interaction between raptor and mTOR. *Molecular cell* **11**, 895-904

106. Peterson, T. R., Laplante, M., Thoreen, C. C., Sancak, Y., Kang, S. A., Kuehl, W. M., Gray, N. S., and Sabatini, D. M. (2009) DEPTOR is an mTOR inhibitor frequently overexpressed in multiple myeloma cells and required for their survival. *Cell* **137**, 873-886

107. Hara, K., Maruki, Y., Long, X., Yoshino, K., Oshiro, N., Hidayat, S., Tokunaga, C., Avruch, J., and Yonezawa, K. (2002) Raptor, a binding

partner of target of rapamycin (TOR), mediates TOR action. *Cell* **110**, 177-189

108. Kim, D. H., Sarbassov, D. D., Ali, S. M., King, J. E., Latek, R. R., Erdjument-Bromage, H., Tempst, P., and Sabatini, D. M. (2002) mTOR interacts with raptor to form a nutrient-sensitive complex that signals to the cell growth machinery. *Cell* **110**, 163-175

109. Wang, L., Harris, T. E., Roth, R. A., and Lawrence, J. C., Jr. (2007) PRAS40 regulates mTORC1 kinase activity by functioning as a direct inhibitor of substrate binding. *The Journal of biological chemistry* **282**, 20036-20044

110. Sancak, Y., Thoreen, C. C., Peterson, T. R., Lindquist, R. A., Kang, S. A., Spooner, E., Carr, S. A., and Sabatini, D. M. (2007) PRAS40 is an insulin-regulated inhibitor of the mTORC1 protein kinase. *Molecular cell* **25**, 903-915

111. Jacinto, E., Facchinetti, V., Liu, D., Soto, N., Wei, S., Jung, S. Y., Huang, Q., Qin, J., and Su, B. (2006) SIN1/MIP1 maintains rictor-mTOR complex integrity and regulates Akt phosphorylation and substrate specificity. *Cell* **127**, 125-137

112. Sarbassov, D. D., Ali, S. M., Kim, D. H., Guertin, D. A., Latek, R. R., Erdjument-Bromage, H., Tempst, P., and Sabatini, D. M. (2004) Rictor, a novel binding partner of mTOR, defines a rapamycin-insensitive and raptor-independent pathway that regulates the cytoskeleton. *Current biology : CB* **14**, 1296-1302

113. Pearce, L. R., Huang, X., Boudeau, J., Pawlowski, R., Wullschleger, S., Deak, M., Ibrahim, A. F., Gourlay, R., Magnuson, M. A., and Alessi, D. R. (2007) Identification of Protor as a novel Rictor-binding component of mTOR complex-2. *The Biochemical journal* **405**, 513-522

114. Woo, S. Y., Kim, D. H., Jun, C. B., Kim, Y. M., Haar, E. V., Lee, S. I., Hegg, J. W., Bandhakavi, S., Griffin, T. J., and Kim, D. H. (2007) PRR5, a novel component of mTOR complex 2, regulates platelet-derived growth factor receptor beta expression and signaling. *The Journal of biological chemistry* **282**, 25604-25612

115. Frias, M. A., Thoreen, C. C., Jaffe, J. D., Schroder, W., Sculley, T., Carr, S. A., and Sabatini, D. M. (2006) mSin1 is necessary for Akt/PKB phosphorylation, and its isoforms define three distinct mTORC2s. *Current biology : CB* **16**, 1865-1870

116. Yang, Q., Inoki, K., Ikenoue, T., and Guan, K. L. (2006) Identification of Sin1 as an essential TORC2 component required for complex formation and kinase activity. *Genes & development* **20**, 2820-2832

117. Guertin, D. A., Stevens, D. M., Thoreen, C. C., Burds, A. A., Kalaany, N. Y., Moffat, J., Brown, M., Fitzgerald, K. J., and Sabatini, D. M. (2006) Ablation in mice of the mTORC components raptor, rictor, or mLST8 reveals that mTORC2 is required for signaling to Akt-FOXO and PKCalpha, but not S6K1. *Developmental cell* **11**, 859-871

118. Brown, E. J., Albers, M. W., Shin, T. B., Ichikawa, K., Keith, C. T., Lane, W. S., and Schreiber, S. L. (1994) A mammalian protein targeted by G1-arresting rapamycin-receptor complex. *Nature* **369**, 756-758

119. Brown, E. J., Beal, P. A., Keith, C. T., Chen, J., Shin, T. B., and Schreiber, S. L. (1995) Control of p70 s6 kinase by kinase activity of FRAP in vivo. *Nature* **377**, 441-446

120. Brunn, G. J., Hudson, C. C., Sekulic, A., Williams, J. M., Hosoi, H., Houghton, P. J., Lawrence, J. C., Jr., and Abraham, R. T. (1997) Phosphorylation of the translational repressor PHAS-I by the mammalian target of rapamycin. *Science* **277**, 99-101

121. Burnett, P. E., Barrow, R. K., Cohen, N. A., Snyder, S. H., and Sabatini, D. M. (1998) RAFT1 phosphorylation of the translational regulators p70 S6 kinase and 4E-BP1. *Proceedings of the National Academy of Sciences of the United States of America* **95**, 1432-1437

122. Phung, T. L., Ziv, K., Dabydeen, D., Eyiah-Mensah, G., Riveros, M., Perruzzi, C., Sun, J., Monahan-Earley, R. A., Shiojima, I., Nagy, J. A., Lin, M. I., Walsh, K., Dvorak, A. M., Briscoe, D. M., Neeman, M., Sessa, W. C., Dvorak, H. F., and Benjamin, L. E. (2006) Pathological angiogenesis is induced by sustained Akt signaling and inhibited by rapamycin. *Cancer cell* **10**, 159-170

123. Sarbassov, D. D., Ali, S. M., Sengupta, S., Sheen, J. H., Hsu, P. P., Bagley, A. F., Markhard, A. L., and Sabatini, D. M. (2006) Prolonged rapamycin treatment inhibits mTORC2 assembly and Akt/PKB. *Mol Cell* **22**, 159-168

124. Inoki, K., Li, Y., Zhu, T., Wu, J., and Guan, K. L. (2002) TSC2 is phosphorylated and inhibited by Akt and suppresses mTOR signalling. *Nature cell biology* **4**, 648-657

125. Ma, L., Chen, Z., Erdjument-Bromage, H., Tempst, P., and Pandolfi, P. P. (2005) Phosphorylation and functional inactivation of TSC2 by Erk implications for tuberous sclerosis and cancer pathogenesis. *Cell* **121**, 179-193

126. Manning, B. D., Tee, A. R., Logsdon, M. N., Blenis, J., and Cantley, L. C. (2002) Identification of the tuberous sclerosis complex-2 tumor suppressor gene product tuberin as a target of the phosphoinositide 3-kinase/akt pathway. *Molecular cell* **10**, 151-162

127. Potter, C. J., Pedraza, L. G., and Xu, T. (2002) Akt regulates growth by directly phosphorylating Tsc2. *Nature cell biology* **4**, 658-665

128. Roux, P. P., Ballif, B. A., Anjum, R., Gygi, S. P., and Blenis, J. (2004) Tumor-promoting phorbol esters and activated Ras inactivate the tuberous sclerosis tumor suppressor complex via p90 ribosomal S6 kinase. *Proceedings of the National Academy of Sciences of the United States of America* **101**, 13489-13494

129. Tee, A. R., Manning, B. D., Roux, P. P., Cantley, L. C., and Blenis, J. (2003) Tuberous sclerosis complex gene products, Tuberin and

Hamartin, control mTOR signaling by acting as a GTPase-activating protein complex toward Rheb. *Current biology : CB* **13**, 1259-1268

130. Inoki, K., Ouyang, H., Zhu, T., Lindvall, C., Wang, Y., Zhang, X., Yang, Q., Bennett, C., Harada, Y., Stankunas, K., Wang, C. Y., He, X., MacDougald, O. A., You, M., Williams, B. O., and Guan, K. L. (2006) TSC2 integrates Wnt and energy signals via a coordinated phosphorylation by AMPK and GSK3 to regulate cell growth. *Cell* **126**, 955-968

131. Inoki, K., Li, Y., Xu, T., and Guan, K. L. (2003) Rheb GTPase is a direct target of TSC2 GAP activity and regulates mTOR signaling. *Genes & development* **17**, 1829-1834

132. Brugarolas, J., Lei, K., Hurley, R. L., Manning, B. D., Reiling, J. H., Hafen, E., Witters, L. A., Ellisen, L. W., and Kaelin, W. G., Jr. (2004) Regulation of mTOR function in response to hypoxia by REDD1 and the TSC1/TSC2 tumor suppressor complex. *Genes & development* **18**, 2893-2904

133. Duvel, K., Yecies, J. L., Menon, S., Raman, P., Lipovsky, A. I., Souza, A. L., Triantafellow, E., Ma, Q., Gorski, R., Cleaver, S., Vander Heiden, M. G., MacKeigan, J. P., Finan, P. M., Clish, C. B., Murphy, L. O., and Manning, B. D. (2010) Activation of a metabolic gene regulatory network downstream of mTOR complex 1. *Molecular cell* **39**, 171-183

134. Hudson, C. C., Liu, M., Chiang, G. G., Otterness, D. M., Loomis, D. C., Kaper, F., Giaccia, A. J., and Abraham, R. T. (2002) Regulation of hypoxia-inducible factor 1alpha expression and function by the mammalian target of rapamycin. *Molecular and cellular biology* **22**, 7004-7014

135. Ikenoue, T., Inoki, K., Yang, Q., Zhou, X., and Guan, K. L. (2008) Essential function of TORC2 in PKC and Akt turn motif phosphorylation, maturation and signalling. *The EMBO journal* **27**, 1919-1931

136. Partovian, C., Ju, R., Zhuang, Z. W., Martin, K. A., and Simons, M. (2008) Syndecan-4 regulates subcellular localization of mTOR Complex2 and Akt activation in a PKCalpha-dependent manner in endothelial cells. *Molecular cell* **32**, 140-149

137. Sarbassov, D. D., Guertin, D. A., Ali, S. M., and Sabatini, D. M. (2005) Phosphorylation and regulation of Akt/PKB by the rictor-mTOR complex. *Science* **307**, 1098-1101

138. Facchinetti, V., Ouyang, W., Wei, H., Soto, N., Lazorchak, A., Gould, C., Lowry, C., Newton, A. C., Mao, Y., Miao, R. Q., Sessa, W. C., Qin, J., Zhang, P., Su, B., and Jacinto, E. (2008) The mammalian target of rapamycin complex 2 controls folding and stability of Akt and protein kinase C. *The EMBO journal* **27**, 1932-1943

139. Hauge, C., Antal, T. L., Hirschberg, D., Doehn, U., Thorup, K., Idrissova, L., Hansen, K., Jensen, O. N., Jorgensen, T. J., Biondi, R. M., and Frodin, M. (2007) Mechanism for activation of the growth factor-activated AGC kinases by turn motif phosphorylation. *The EMBO journal* **26**, 2251-2261

140. Lee, K., Gudapati, P., Dragovic, S., Spencer, C., Joyce, S., Killeen, N., Magnuson, M. A., and Boothby, M. (2010) Mammalian target of rapamycin protein complex 2 regulates differentiation of Th1 and Th2 cell subsets via distinct signaling pathways. *Immunity* **32**, 743-753

141. Gould, C. M., Kannan, N., Taylor, S. S., and Newton, A. C. (2009) The chaperones Hsp90 and Cdc37 mediate the maturation and stabilization of protein kinase C through a conserved PXXP motif in the C-terminal tail. *The Journal of biological chemistry* **284**, 4921-4935

142. Lang, F., Bohmer, C., Palmada, M., Seebohm, G., Strutz-Seebohm, N., and Vallon, V. (2006) (Patho)physiological significance of the serum- and glucocorticoid-inducible kinase isoforms. *Physiological reviews* **86**, 1151-1178

143. Garcia-Martinez, J. M., and Alessi, D. R. (2008) mTOR complex 2 (mTORC2) controls hydrophobic motif phosphorylation and activation of serum- and glucocorticoid-induced protein kinase 1 (SGK1). *The Biochemical journal* **416**, 375-385

144. Marzec, M., Kasprzycka, M., Liu, X., El-Salem, M., Halasa, K., Raghunath, P. N., Bucki, R., Wlodarski, P., and Wasik, M. A. (2007) Oncogenic tyrosine kinase NPM/ALK induces activation of the rapamycin-sensitive mTOR signaling pathway. *Oncogene* **26**, 5606-5614

145. Drenan, R. M., Liu, X., Bertram, P. G., and Zheng, X. F. (2004) FKBP12-rapamycin-associated protein or mammalian target of rapamycin (FRAP/mTOR) localization in the endoplasmic reticulum and the Golgi apparatus. *The Journal of biological chemistry* **279**, 772-778

146. Del Bufalo, D., Ciuffreda, L., Trisciuoglio, D., Desideri, M., Cognetti, F., Zupi, G., and Milella, M. (2006) Antiangiogenic potential of the Mammalian target of rapamycin inhibitor temsirolimus. *Cancer research* **66**, 5549-5554

147. Roy, D., Sin, S. H., Lucas, A., Venkataramanan, R., Wang, L., Eason, A., Chavakula, V., Hilton, I. B., Tamburro, K. M., Damania, B., and Dittmer, D. P. (2013) mTOR inhibitors block Kaposi sarcoma growth by inhibiting essential autocrine growth factors and tumor angiogenesis. *Cancer research* **73**, 2235-2246

148. Du, W., Gerald, D., Perruzzi, C. A., Rodriguez-Waitkus, P., Enayati, L., Krishnan, B., Edmonds, J., Hochman, M. L., Lev, D. C., and Phung, T. L. (2013) Vascular tumors have increased p70 S6-kinase activation and are inhibited by topical rapamycin. *Laboratory investigation; a journal of technical methods and pathology* **93**, 1115-1127

149. Frost, P., Berlanger, E., Mysore, V., Hoang, B., Shi, Y., Gera, J., and Lichtenstein, A. (2013) Mammalian target of rapamycin inhibitors induce tumor cell apoptosis in vivo primarily by inhibiting VEGF expression and angiogenesis. *Journal of oncology* **2013**, 897025

150. Frost, P., Shi, Y., Hoang, B., and Lichtenstein, A. (2007) AKT activity ability of mTOR inhibitors to prevent angiogenesis and VEGF expression in multiple myeloma cells. *Oncogene* **26**, 2255-2262

151. Ishikawa, D., Takeuchi, S., Nakagawa, T., Sano, T., Nakade, J., Nanjo, S., Yamada, T., Ebi, H., Zhao, L., Yasumoto, K., Nakamura, T., Matsumoto, K., Kagamu, H., Yoshizawa, H., and Yano, S. (2013) mTOR inhibitors control the growth of EGFR mutant lung cancer even after acquiring resistance by HGF. *PloS one* **8**, e62104

152. Guba, M., von Breitenbuch, P., Steinbauer, M., Koehl, G., Flegel, S., Hornung, M., Bruns, C. J., Zuelke, C., Farkas, S., Anthuber, M., Jauch, K. W., and Geissler, E. K. (2002) Rapamycin inhibits primary and metastatic tumor growth by antiangiogenesis: involvement of vascular endothelial growth factor. *Nature medicine* **8**, 128-135

153. Falcon, B. L., Barr, S., Gokhale, P. C., Chou, J., Fogarty, J., Depeille, P., Miglarese, M., Epstein, D. M., and McDonald, D. M. (2011) Reduced VEGF production, angiogenesis, and vascular regrowth contribute to the antitumor properties of dual mTORC1/mTORC2 inhibitors. *Cancer research* **71**, 1573-1583

154. Pignochino, Y., Dell'Aglio, C., Basirico, M., Capozzi, F., Soster, M., Marchio, S., Bruno, S., Gammaitoni, L., Sangiolo, D., Torchiaro, E., D'Ambrosio, L., Fagioli, F., Ferrari, S., Alberghini, M., Picci, P., Aglietta, M., and Grignani, G. (2013) The Combination of Sorafenib and Everolimus Abrogates mTORC1 and mTORC2 upregulation in osteosarcoma preclinical models. *Clinical cancer research : an official journal of the American Association for Cancer Research* **19**, 2117-2131

155. Xue, Q., Hopkins, B., Perruzzi, C., Udayakumar, D., Sherris, D., and Benjamin, L. E. (2008) Palomid 529, a novel small-molecule drug, is a TORC1/TORC2 inhibitor that reduces tumor growth, tumor angiogenesis, and vascular permeability. *Cancer research* **68**, 9551-9557

156. Xu, S., Li, S., Guo, Z., Luo, J., Ellis, M. J., and Ma, C. X. (2013) Combined targeting of mTOR and AKT is an effective strategy for basal-like breast cancer in patient-derived xenograft models. *Molecular cancer therapeutics* **12**, 1665-1675

157. Fokas, E., Im, J. H., Hill, S., Yameen, S., Stratford, M., Beech, J., Hackl, W., Maira, S. M., Bernhard, E. J., McKenna, W. G., and Muschel, R. J. (2012) Dual inhibition of the PI3K/mTOR pathway increases tumor radiosensitivity by normalizing tumor vasculature. *Cancer research* **72**, 239-248

158. Fokas, E., Yoshimura, M., Prevo, R., Higgins, G., Hackl, W., Maira, S. M., Bernhard, E. J., McKenna, W. G., and Muschel, R. J. (2012) NVP-BEZ235 and NVP-BGT226, dual phosphatidylinositol 3-kinase/mammalian target of rapamycin inhibitors, enhance tumor and endothelial cell radiosensitivity. *Radiation oncology (London, England)* **7**, 48

159. Bernardi, R., Guernah, I., Jin, D., Grisendi, S., Alimonti, A., Teruya-Feldstein, J., Cordon-Cardo, C., Simon, M. C., Rafii, S., and Pandolfi, P. P. (2006) PML inhibits HIF-1alpha translation and neoangiogenesis through repression of mTOR. *Nature* **442**, 779-785

160. Dodd, K. M., Yang, J., Shen, M. H., Sampson, J. R., and Tee, A. R. (2014) mTORC1 drives HIF-1alpha and VEGF-A signalling via multiple mechanisms involving 4E-BP1, S6K1 and STAT3. *Oncogene*

161. Nayak, B. K., Feliers, D., Sudarshan, S., Friedrichs, W. E., Day, R. T., New, D. D., Fitzgerald, J. P., Eid, A., Denapoli, T., Parekh, D. J., Gorin, Y., and Block, K. (2013) Stabilization of HIF-2alpha through redox regulation of mTORC2 activation and initiation of mRNA translation. *Oncogene* **32**, 3147-3155

162. Li, W., Petrimpol, M., Molle, K. D., Hall, M. N., Battegay, E. J., and Humar, R. (2007) Hypoxia-induced endothelial proliferation requires both mTORC1 and mTORC2. *Circulation research* **100**, 79-87

163. Humar, R., Kiefer, F. N., Berns, H., Resink, T. J., and Battegay, E. J. (2002) Hypoxia enhances vascular cell proliferation and angiogenesis in vitro via rapamycin (mTOR)-dependent signaling. *FASEB J* **16**, 771-780

164. Liegl, R., Koenig, S., Siedlecki, J., Haritoglou, C., Kampik, A., and Kernt, M. (2014) Temsirolimus inhibits proliferation and migration in retinal pigment epithelial and endothelial cells via mTOR inhibition and decreases VEGF and PDGF expression. *PloS one* **9**, e88203

165. Dormond, O., Madsen, J. C., and Briscoe, D. M. (2007) The effects of mTOR-Akt interactions on anti-apoptotic signaling in vascular endothelial cells. *The Journal of biological chemistry* **282**, 23679-23686

166. Dada, S., Demartines, N., and Dormond, O. (2008) mTORC2 regulates PGE2-mediated endothelial cell survival and migration. *Biochemical and biophysical research communications* **372**, 875-879

167. Zhuang, G., Yu, K., Jiang, Z., Chung, A., Yao, J., Ha, C., Toy, K., Soriano, R., Haley, B., Blackwood, E., Sampath, D., Bais, C., Lill, J. R., and Ferrara, N. (2013) Phosphoproteomic analysis implicates the mTORC2-FoxO1 axis in VEGF signaling and feedback activation of receptor tyrosine kinases. *Sci Signal* **6**, ra25

168. Bentzinger, C. F., Romanino, K., Cloetta, D., Lin, S., Mascarenhas, J. B., Oliveri, F., Xia, J., Casanova, E., Costa, C. F., Brink, M., Zorzato, F., Hall, M. N., and Ruegg, M. A. (2008) Skeletal muscle-specific ablation of raptor, but not of rictor, causes metabolic changes and results in muscle dystrophy. *Cell Metab* **8**, 411-424

169. Polak, P., Cybulski, N., Feige, J. N., Auwerx, J., Ruegg, M. A., and Hall, M. N. (2008) Adipose-specific knockout of raptor results in lean mice with enhanced mitochondrial respiration. *Cell Metab* **8**, 399-410

170. Monvoisin, A., Alva, J. A., Hofmann, J. J., Zovein, A. C., Lane, T. F., and Iruela-Arispe, M. L. (2006) VE-cadherin-CreERT2 transgenic mouse: a model for inducible recombination in the endothelium. *Developmental dynamics : an official publication of the American Association of Anatomists* **235**, 3413-3422

171. Kanda, S., Tomasini-Johansson, B., Klint, P., Dixelius, J., Rubin, K., and Claesson-Welsh, L. (1999) Signaling via fibroblast growth factor

receptor-1 is dependent on extracellular matrix in capillary endothelial cell differentiation. *Exp Cell Res* **248**, 203-213

172. Smedsrod, B., and Pertoft, H. (1985) Preparation of pure hepatocytes and reticuloendothelial cells in high yield from a single rat liver by means of Percoll centrifugation and selective adherence. *Journal of leukocyte biology* **38**, 213-230

173. Peier, M., Walpen, T., Christofori, G., Battegay, E., and Humar, R. (2013) Sprouty2 expression controls endothelial monolayer integrity and quiescence. *Angiogenesis* **16**, 455-468

174. Lindenblatt, N., Calcagni, M., Contaldo, C., Menger, M. D., Giovanoli, P., and Vollmar, B. (2008) A new model for studying the revascularization of skin grafts in vivo: the role of angiogenesis. *Plastic and reconstructive surgery* **122**, 1669-1680

175. Rando, T. A., and Blau, H. M. (1994) Primary mouse myoblast purification, characterization, and transplantation for cell-mediated gene therapy. *The Journal of cell biology* **125**, 1275-1287

176. Springer, M. L., and Blau, H. M. (1997) High-efficiency retroviral infection of primary myoblasts. *Somatic cell and molecular genetics* **23**, 203-209

177. Akhtar, N., Dickerson, E. B., and Auerbach, R. (2002) The sponge/Matrigel angiogenesis assay. *Angiogenesis* **5**, 75-80

178. Baumann, C. I., Bailey, A. S., Li, W., Ferkowicz, M. J., Yoder, M. C., and Fleming, W. H. (2004) PECAM-1 is expressed on hematopoietic stem cells throughout ontogeny and identifies a population of erythroid progenitors. *Blood* **104**, 1010-1016

179. Bhattacharya, I., Dragert, K., Albert, V., Contassot, E., Damjanovic, M., Hagiwara, A., Zimmerli, L., Humar, R., Hall, M. N., Battegay, E. J., and Haas, E. (2013) Rictor in perivascular adipose tissue controls vascular function by regulating inflammatory molecule expression. *Arteriosclerosis, thrombosis, and vascular biology* **33**, 2105-2111

180. Fehrenbach, M. L., Cao, G., Williams, J. T., Finklestein, J. M., and Delisser, H. M. (2009) Isolation of murine lung endothelial cells. *American journal of physiology. Lung cellular and molecular physiology* **296**, L1096-1103

181. Marelli-Berg, F. M., Peek, E., Lidington, E. A., Stauss, H. J., and Lechler, R. I. (2000) Isolation of endothelial cells from murine tissue. *Journal of immunological methods* **244**, 205-215

182. Alva, J. A., Zovein, A. C., Monvoisin, A., Murphy, T., Salazar, A., Harvey, N. L., Carmeliet, P., and Iruela-Arispe, M. L. (2006) VE-Cadherin-Cre-recombinase transgenic mouse: a tool for lineage analysis and gene deletion in endothelial cells. *Developmental dynamics : an official publication of the American Association of Anatomists* **235**, 759-767

183. Paredes-Gamero, E. J., Medeiros, V. P., Farias, E. H., Justo, G. Z., Trindade, E. S., Andrade-Lopes, A. L., Godinho, R. O., de Miranda, A.,

Ferreira, A. T., Tersariol, I. L., and Nader, H. B. (2010) Heparin induces rat aorta relaxation via integrin-dependent activation of muscarinic M3 receptors. *Hypertension* **56**, 713-721

184. Springer, M. L., Chen, A. S., Kraft, P. E., Bednarski, M., and Blau, H. M. (1998) VEGF gene delivery to muscle: potential role for vasculogenesis in adults. *Molecular cell* **2**, 549-558

185. Danielian, P. S., White, R., Hoare, S. A., Fawell, S. E., and Parker, M. G. (1993) Identification of residues in the estrogen receptor that confer differential sensitivity to estrogen and hydroxytamoxifen. *Molecular endocrinology* **7**, 232-240

186. Feil, R., Wagner, J., Metzger, D., and Chambon, P. (1997) Regulation of Cre recombinase activity by mutated estrogen receptor ligand-binding domains. *Biochemical and biophysical research communications* **237**, 752-757

187. Leone, D. P., Genoud, S., Atanasoski, S., Grausenburger, R., Berger, P., Metzger, D., Macklin, W. B., Chambon, P., and Suter, U. (2003) Tamoxifen-inducible glia-specific Cre mice for somatic mutagenesis in oligodendrocytes and Schwann cells. *Molecular and cellular neurosciences* **22**, 430-440

188. Jackson, K. A., Snyder, D. S., and Goodell, M. A. (2004) Skeletal muscle fiber-specific green autofluorescence: potential for stem cell engraftment artifacts. *Stem cells* **22**, 180-187

189. Red-Horse, K., Crawford, Y., Shojaei, F., and Ferrara, N. (2007) Endothelium-microenvironment interactions in the developing embryo and in the adult. *Developmental cell* **12**, 181-194

190. Lymboussaki, A., Olofsson, B., Eriksson, U., and Alitalo, K. (1999) Vascular endothelial growth factor (VEGF) and VEGF-C show overlapping binding sites in embryonic endothelia and distinct sites in differentiated adult endothelia. *Circulation research* **85**, 992-999

191. Barilli, A., Visigalli, R., Sala, R., Gazzola, G. C., Parolari, A., Tremoli, E., Bonomini, S., Simon, A., Closs, E. I., Dall'Asta, V., and Bussolati, O. (2008) In human endothelial cells rapamycin causes mTORC2 inhibition and impairs cell viability and function. *Cardiovascular research* **78**, 563-571

192. Kim, J. A., Jang, H. J., Martinez-Lemus, L. A., and Sowers, J. R. (2012) Activation of mTOR/p70S6 kinase by ANG II inhibits insulin-stimulated endothelial nitric oxide synthase and vasodilation. *American journal of physiology. Endocrinology and metabolism* **302**, E201-208

194. Hilker, M., Buerke, M., Guckenbiehl, M., Schwertz, H., Buhler, J., Moersig, W., Hake, U., and Oelert, H. (2003) Rapamycin reduces neointima formation during vascular injury. *VASA. Zeitschrift fur Gefasskrankheiten* **32**, 10-13

195. Hofmann, J. J., and Iruela-Arispe, M. L. (2007) Notch signaling in blood vessels: who is talking to whom about what? *Circulation research* **100**, 1556-1568

196. Scehnet, J. S., Jiang, W., Kumar, S. R., Krasnoperov, V., Trindade, A., Benedito, R., Djokovic, D., Borges, C., Ley, E. J., Duarte, A., and Gill, P. S. (2007) Inhibition of Dll4-mediated signaling induces proliferation of immature vessels and results in poor tissue perfusion. *Blood* **109**, 4753-4760

197. Skuli, N., Majmundar, A. J., Krock, B. L., Mesquita, R. C., Mathew, L. K., Quinn, Z. L., Runge, A., Liu, L., Kim, M. N., Liang, J., Schenkel, S., Yodh, A. G., Keith, B., and Simon, M. C. (2012) Endothelial HIF-2alpha regulates murine pathological angiogenesis and revascularization processes. *The Journal of clinical investigation* **122**, 1427-1443

198. Toschi, A., Lee, E., Gadir, N., Ohh, M., and Foster, D. A. (2008) Differential dependence of hypoxia-inducible factors 1 alpha and 2 alpha on mTORC1 and mTORC2. *The Journal of biological chemistry* **283**, 34495-34499

199. Potente, M., Urbich, C., Sasaki, K., Hofmann, W. K., Heeschen, C., Aicher, A., Kollipara, R., DePinho, R. A., Zeiher, A. M., and Dimmeler, S. (2005) Involvement of Foxo transcription factors in angiogenesis and postnatal neovascularization. *The Journal of clinical investigation* **115**, 2382-2392

200. Semela, D., Piguet, A. C., Kolev, M., Schmitter, K., Hlushchuk, R., Djonov, V., Stoupis, C., and Dufour, J. F. (2007) Vascular remodeling and antitumoral effects of mTOR inhibition in a rat model of hepatocellular carcinoma. *Journal of hepatology* **46**, 840-848

201. Cross, M. J., and Claesson-Welsh, L. (2001) FGF and VEGF function in angiogenesis: signalling pathways, biological responses and therapeutic inhibition. *Trends Pharmacol Sci* **22**, 201-207

202. Lambeng, N., Wallez, Y., Rampon, C., Cand, F., Christe, G., Gulino-Debrac, D., Vilgrain, I., and Huber, P. (2005) Vascular endothelial-cadherin tyrosine phosphorylation in angiogenic and quiescent adult tissues. *Circulation research* **96**, 384-391

203. Wang, Y., Nakayama, M., Pitulescu, M. E., Schmidt, T. S., Bochenek, M. L., Sakakibara, A., Adams, S., Davy, A., Deutsch, U., Luthi, U., Barberis, A., Benjamin, L. E., Makinen, T., Nobes, C. D., and Adams, R. H. (2010) Ephrin-B2 controls VEGF-induced angiogenesis and lymphangiogenesis. *Nature* **465**, 483-486

204. Madisen, L., Zwingman, T. A., Sunkin, S. M., Oh, S. W., Zariwala, H. A., Gu, H., Ng, L. L., Palmiter, R. D., Hawrylycz, M. J., Jones, A. R., Lein, E. S., and Zeng, H. (2010) A robust and high-throughput Cre reporting and characterization system for the whole mouse brain. *Nature neuroscience* **13**, 133-140

205. Timar, J., Dome, B., Fazekas, K., Janovics, A., and Paku, S. (2001) Angiogenesis-dependent diseases and angiogenesis therapy. *Pathology oncology research : POR* **7**, 85-94

206. Carmeliet, P., Moons, L., Luttun, A., Vincenti, V., Compernolle, V., De Mol, M., Wu, Y., Bono, F., Devy, L., Beck, H., Scholz, D., Acker, T., DiPalma, T., Dewerchin, M., Noel, A., Stalmans, I., Barra, A., Blacher, S., VandenDriessche, T., Ponten, A., Eriksson, U., Plate, K. H., Foidart, J. M., Schaper, W., Charnock-Jones, D. S., Hicklin, D. J., Herbert, J. M., Collen, D., and Persico, M. G. (2001) Synergism between vascular endothelial growth factor and placental growth factor contributes to angiogenesis and plasma extravasation in pathological conditions. *Nature medicine* **7**, 575-583

207. Bellou, S., Pentheroudakis, G., Murphy, C., and Fotsis, T. (2013) Anti-angiogenesis in cancer therapy: Hercules and hydra. *Cancer letters* **338**, 219-228

208. Elice, F., and Rodeghiero, F. (2012) Hematologic malignancies and thrombosis. *Thrombosis research* **129**, 360-366

209. Jain, R. K. (2013) Normalizing tumor microenvironment to treat cancer: bench to bedside to biomarkers. *Journal of clinical oncology : official journal of the American Society of Clinical Oncology* **31**, 2205-2218

210. Huang, Y., Goel, S., Duda, D. G., Fukumura, D., and Jain, R. K. (2013) Vascular normalization as an emerging strategy to enhance cancer immunotherapy. *Cancer research* **73**, 2943-2948

211. Fruman, D. A., and Rommel, C. (2014) PI3K and cancer: lessons, challenges and opportunities. *Nat Rev Drug Discov* **13**, 140-156

212. Wander, S. A., Hennessy, B. T., and Slingerland, J. M. (2011) Next-generation mTOR inhibitors in clinical oncology: how pathway complexity informs therapeutic strategy. *The Journal of clinical investigation* **121**, 1231-1241

213. Husseinzadeh, N., and Husseinzadeh, H. D. (2014) mTOR inhibitors and their clinical application in cervical, endometrial and ovarian cancers: a critical review. *Gynecologic oncology* **133**, 375-381

214. Dreaden, E. C., Austin, L. A., Mackey, M. A., and El-Sayed, M. A. (2012) Size matters: gold nanoparticles in targeted cancer drug delivery. *Therapeutic delivery* **3**, 457-478

215. Pallet, N., and Legendre, C. (2013) Adverse events associated with mTOR inhibitors. *Expert opinion on drug safety* **12**, 177-186

216. Oleg E. Tolmachov, Tatiana Subkhankulova and Tanya Tolmachova (2013). Silencing of Transgene Expression: A Gene Therapy Perspective, Gene Therapy - Tools and Potential Applications, Dr. Francisco Martin (Ed.), ISBN: 978-953-51-1014-9, InTech, DOI: 10.5772/53379. Available from: http://www.intechopen.com/books/gene-therapy-tools-and-potential-applications/silencing-of-transgene-expression-a-gene-therapy-perspective